SYNTHESIS, CHARACTERISATION AND BIOLOGICAL EVALUATION OF PHOSPHINEGOLD(I) THIOLATES

YEO CHIEN ING

FACULTY OF SCIENCE
UNIVERSITY OF MALAYA
KUALA LUMPUR

2016

SYNTHESIS, CHARACTERISATION AND BIOLOGICAL EVALUATION OF PHOSPHINEGOLD(I) THIOLATES

YEO CHIEN ING

THESIS SUBMITTED IN FULFILMENT OF THE REQUIREMENTS FOR THE DEGREE OF DOCTOR OF PHILOSOPHY

FACULTY OF SCIENCE
UNIVERSITY OF MALAYA
KUALA LUMPUR

2016

UNIVERSITY OF MALAYA

ORIGINAL LITERARY WORK DECLARATION

Name of Candidate: YEO CHIEN ING

Registration/Matric No: SHC 110071

Name of Degree: DOCTOR OF PHILOSOPHY (EXCEPT MATHEMATICS & SCIENCE PHILOSOPHY)

Title of Project Paper/Research Report/Dissertation/Thesis ("this Work"):

SYNTHESIS, CHARACTERISATION AND BIOLOGICAL EVALUATION OF PHOSPHINEGOLD(I) THIOLATES

Field of Study: INORGANIC CHEMISTRY

I do solemnly and sincerely declare that:

(1) I am the sole author/writer of this Work;
(2) This Work is original;
(3) Any use of any work in which copyright exists was done by way of fair dealing and for permitted purposes and any excerpt or extract from, or reference to or reproduction of any copyright work has been disclosed expressly and sufficiently and the title of the Work and its authorship have been acknowledged in this Work;
(4) I do not have any actual knowledge nor do I ought reasonably to know that the making of this work constitutes an infringement of any copyright work;
(5) I hereby assign all and every rights in the copyright to this Work to the University of Malaya ("UM"), who henceforth shall be owner of the copyright in this Work and that any reproduction or use in any form or by any means whatsoever is prohibited without the written consent of UM having been first had and obtained;
(6) I am fully aware that if in the course of making this Work I have infringed any copyright whether intentionally or otherwise, I may be subject to legal action or any other action as may be determined by UM.

Candidate's Signature Date:

Subscribed and solemnly declared before,

Witness's Signature Date:

Name:

Designation:

ABSTRACT

A series of mononuclear phosphanegold(I) thiocarbamides, $Ph_3PAu\{SC(OR)=NC_6H_4X\text{-}4\}$ for R = alkyl, X = H, CH_3, Cl and NO_2, and dinuclear $(Ph_2P\text{-}Fc\text{-}PPh_2)\{AuSC(OiPr)=NC_6H_4X\text{-}4\}_2$ and $(R_3PAu)_2\{1,4\text{-}[SC(OMe)=N]_2C_6H_4\}$ with X = H, CH_3, Cl and *i*Pr, R = Et, Ph and Cy, were prepared from the reaction of the respective phosphanegold(I) precursor with thiolate ligands in the presence of base. The complexes were characterised by IR spectroscopy, (multi)NMR spectroscopy, elemental analyses, thermogravimetric analyses, UV/Vis spectroscopy, photoluminescent study, powder X-Ray diffraction (PXRD) analyses and single-crystal X-ray diffraction studies. The crystal structures of the compounds featured essentially linear gold atom coordination geometries defined by phosphane-P and thiolate-S atoms. Both parent phosphanegold(I) complexes and the N-bound *p*-tolyl derivatives showed promising cytotoxicity against the HT-29 cancer cell line, and the N-bound *p*-tolyl series were found to exhibit specific antibacterial activity against Gram-positive bacteria. Dinuclear compounds, $(Ph_2P\text{-}Fc\text{-}PPh_2)\{AuSC(OiPr)=NC_6H_4X\text{-}4\}_2$, possessed better cytotoxicity against HEK-293 embryonic kidney cells as compared to the mononuclear analogues and less toxic against MCF-7 breast cancer cell lines. $(R_3PAu)_2\{1,4\text{-}[SC(OMe)=N]_2C_6H_4\}$ displayed unexpected Au…π interactions which are more stable by at least 12 kcal mol^{-1}. The disk diffusion results for this series demonstrated that the Et_3P analogue exhibited a broad spectrum of anti-bacterial activity toward 24 strains of Gram-positive and Gram-negative bacteria while the Ph_3P and Cy_3P analogues were limited to Gram-positive bacteria. Contemplating the study on phosphanegold(I) complexes, exploration studies conducted on $(Ph_3P)_2Cu[ROC(=S)N(H)Ph]Cl$ with R = Me, Et and *i*Pr revealed interesting interactions, i.e. C–H···π(quasichelate ring) where a six-membered quasi-chelate ring is closed by an N–H···Cl hydrogen bond. Calculations suggest that the energy of attraction provided by such interactions approximates 3.5 kcal mol^{-1}.

ABSTRAK

Satu siri sebatian emas(I)fosfana tiokarbamat, $Ph_3PAu\{SC(OR)=NC_6H_4X\text{-}4\}$, $(Ph_2P\text{-}Fc\text{-}PPh_2)\{AuSC(OiPr)=NC_6H_4X\text{-}4\}_2$ [R = alkil, X = H, CH_3, Cl dan NO_2] dan $(R_3PAu)_2\{1,4\text{-}[SC(OMe)=N]_2C_6H_4\}$ [R = Et, Ph dan Cy] telah disediakan daripada tindak balas bahan pemula emas(I)fosfana dengan tiokarbamat. Sebatian yang telah disediakan telah dicirikan dengan pelbagai spektroskopi NMR (^1H, ^{13}C dan ^{31}P), IR, UV/Vis, fotoluminasi, analisis unsur, analisis gravimetric, pembelauan X-ray serbuk (PXRD) dan pembelauan X-ray hablur tunggal (SCXRD). Daripada struktur hablur yang diperolehi, sebatian emas(I) telah memaparkan geometri lurus; daripada penyelarasan atom emas, fosforus dan sulfur atom pada ligan. Semua sebatian emas(I)fosfana tiokarbamat menunjukkan kesan sitotoksik terhadap sel kanser HT-29 dan siri *p*-tolyl menunjukkan aktiviti terhad terhadap bakteria Gram-negatif. Sementara itu, sebatian dinuklear emas(I) $(Ph_2P\text{-}Fc\text{-}PPh_2)\{AuSC(OiPr)=NC_6H_4X\text{-}4\}_2$, menunjukkan kesan sitotoksik yang lebih baik terhadap HEK-293, iaitu sel kanser buah pinggang berbanding dengan analog mononuklear dan kurang toksik terhadap sel kanser payudara; MCF-7. $(R_3PAu)_2\{1,4\text{-}[SC(OMe)=N]_2C_6H_4\}$ menunjukkan iteraksi Au...π yang tidak dijangkakan dan lebih stabil dengan sekurang-kurangnya 12 kcal mol^{-1}. Keputusan resapan cakera menunjukkan bahawa analog Et_3P mempamerkan aktiviti anti-bakteria yang luas terhadap 24 jenis bakteria Gram-positif dan Gram-negatif. Sebaliknya, aktiviti anti-bakteria oleh analog Ph_3P dan Cy_3P adalah terhad kepada bakteria Gram-positif. Siri $(Ph_3P)_2Cu[ROC(=S)N(H)Ph]Cl$ dengan R = Me, Et dan *i*Pr juga dikajikan dan mendedahkan interaksi yang menarik, iaitu C-H···π (bulatan kuasi kelat) di mana enam ahli dalam bulatan kuasi kelat dihubungkan melalui ikatan hidrogen N-H···Cl. Pengiraan menunjukkan bahawa tenaga tarikan yang ditunjukkan oleh interaksi tersebut adalah lebih kurang 3.5 kcal mol^{-1}.

ACKNOWLEDGEMENTS

First and foremost, I would like to express my heartfelt gratitude to my supervisors, Professor Dr Edward Richard Tom Tiekink and Dr Siti Nadiah Abdul Halim, for their support and guidance throughout the entire Ph.D. program. I would never be at where I am today, without their companion as a friend, advisor and mentor. I appreciate the encouragement given whenever I was drowning in despair during my thesis preparation. One could never imagine how grateful I am with their presence in my life.

I would like to take this opportunity to thank Dr Seng Hoi Ling, who has been a good mentor and friend that lead me through thick and thin. Also, I am grateful to the collaborators from University Putra Malaysia (UPM), Dr Cheah Yoke Kqueen, Dr Suzanne Khoo, Dr Alberto Otero-de-la-Roza, Professor Julio Zukerman-Schpector and Professor Marco Antonio Barbosa Ferreira for their contributions and efforts. My sincere thanks also go to Tan Yee Seng and Professor Ng Soon, for providing continuous support and ideas for my research.

I am thankful for the financial support from Trans Disiplinary Research Grant (TRGS) Malaysia, High Impact Research (HIR) and Brightspark Scheme from University of Malaya. Last but not least, I wish to thank my family for their mental support. They brighten up my days when I was in grief and sorrow. Also, not to be neglected, my laboratory mates who have made their presence a great impact to my life. A truthful thank to everyone who has made an effort to participate to shape me into a better person.

TABLE OF CONTENTS

LIST OF FIGURES

LIST OF TABLES

LIST OF SYMBOLS AND ABREVIATIONS

DNA	Deoxyribonucleic Acid
HIV	Human Immunodeficiency Virus
NNRTIs	Non-Nucleoside Reverse Transcriptase Inhibitors
SAR	Specific Absorption Rate
LMCT	Ligand-Metal Charge Transfer
MLCT	Metal-Ligand Charge Transfer
HOMO	Highest Occupied Molecular Orbitals
LUMO	Lowest Unoccupied Molecular Orbitals
HT-29	Human Colorectal Adenocarcinoma Cell Line
RNA	Ribonucleic Acid
AO/PI	Acridine Orange/Propidium Iodide
dppm	bis(dimethylphosphino)methane
NOE	Nuclear Overhauser Effect

CHAPTER 1:INTRODUCTION

1.1 Cancer and Medicinal Chemistry

Cancer remains as a main health issue owing to its impediments to successful treatment and recovery. Cancer is a form of disease that erupts from abnormal cell growth and is often lethal. It happens when the DNA of a cell is changed or damaged, and causes unwanted effect on cell growth where, damaged cells replicate in an uncontrolled manner, forming lumps or masses of tissue that is known as a tumour. There are numerous types of cancer, including the top leading killers: breast cancer, colorectal cancer and lung cancer, to name a few. Amongst these cancers, colorectal cancer brings to the second highest mortality rate in the developed countries (Jemal *et al.*, 2011).

Owing to the above, medicinal chemistry has always attracted noteworthy attention due to its importance and impact in tackling human disease, including cancer and tumour malignancies that afflict communities owing its life-threatening nature not to mention chronic pain caused by the disease itself and that related to its treatment. In the realm of medicinal chemistry, designing and developing effective bio-active molecules is often constrained by poor understanding of the underlying mechanism of action. This, however, does not limit exploration of new chemistry; enormous efforts are underway to delineate and discover potential pharmaceutical agents. In the area of metal-based drugs, gold formulations have received extensive attention with exploration of their medicinal properties dating since ancient times; Indian, Chinese and Arabian physicians employed gold in their prescriptions for the treatment of various ailments (Kean *et al.*, 1985). The use of gold compounds in modern for medicinal purposes was first initiated by Robert Koch in his discovery of the anti-tubercular activity of gold cyanide in 1890. Despite gold cyanide was proven to be ineffective against tuberculosis in the 1920s. The above later

lead to the discovery of gold drugs, *e.g.* auranofin, which serves as an important agent to halt the progression of rheumatoid arthritis.

1.2 Chrysotherapy and Gold Drugs

The Chinese used gold as a medicinal agent dated back to as early as 2500 BCE (Merchant, 1998). Triethylphosphanegold(I) tetraacetylatedthioglucosate, commonly known as auranofin, is a phosphinegold(I) thiolate derivative, and a key example of the potential anti-proliferative gold complexes. Studies of auranofin on cultured tumour cells were conducted in 1985 to delineate its mechanism of action (Mirabelli *et al.*, 1985), thus laid the foundation for the development of other gold drug analogues. Complementing studies of molecular gold compounds, the use of gold nanoparticles as new agents for drug or gene delivery open up new paradigms in drug-related therapies (Pissuwan *et al.*, 2011).

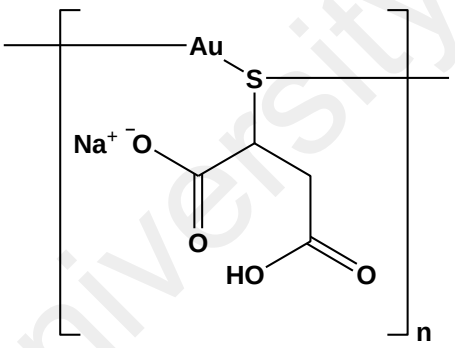

Myocrisin

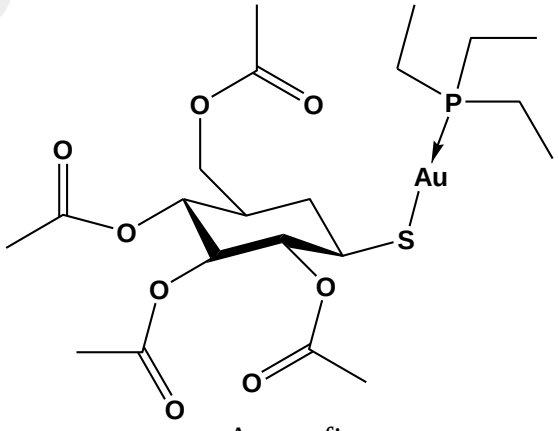

Auranofin

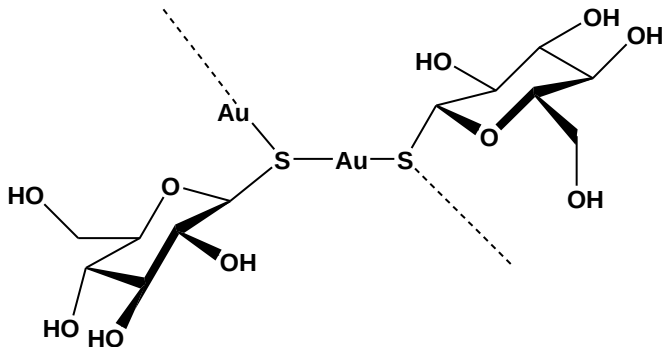

Aurothioglucose

Figure 1.1: Chemical structure of Class I (myocrisin and aurothioglucose) and Class II (Auranofin) gold drugs.

Chrysotherapy, the use of gold compounds in medicine, often refers to the treatment of rheumatoid arthritis (Gielen *et al.*, 2005; Sadler *et al.*, 1998; Shaw, 1999). In general, there are two classes of gold drugs used in this context: Class I, being polymeric, charged and water soluble, as in myocrisin and aurothioglucose. Class II, represented by auranofin, is monomeric, neutral and hydrophobic, as depicted in Figure 1.1. Auranofin was first approved for clinical use in 1985 (Sutton, 1986; Sutton *et al.*, 1972), and it showed comparable efficacy during treatment. However, administration of gold drugs results in inevitable side effects, *e.g.* nausea, weakness, rashes and the most common adverse effect, diarrhea (Giannini *et al.*, 1990). Auranofin has now been rarely used clinically as there are more anti-rheumatic agents become available. Myocrisin and aurothioglucose, on the other hand, are injectable gold drugs. Unfortunately, the typical side effects associated with chrysotherapy still being the main limitation of the treatment, let alone the poor response of some patients towards treatment using gold drugs. Despite there are tremendous efforts dedicated to the development of gold drugs, their mechanism of action still remains poorly understood. Some of the side effects of chrysotherapy may relate to the generation of gold(III). When gold(I) dismutase to gold(III) ions and metallic gold(0), the gold(III) species denature proteins and nucleic acids, which are believed to be responsible for the toxicity of the administered gold(I) drugs (Brown *et al.*, 2007; De Wall *et al.*, 2006; Shaw, 1999).

1.3 Thiocarbamide

Thiocarbamide, with the general formula of ROC(=S)NR'R", is a type of thione molecule (Vallejos *et al.*, 2009) as illustrated in Figure 1.2. This molecule, when deprotonated, becomes a thiolate and it forms the focus of current research. Thiocarbamide comprises a potential coordinating sulphur atom and thus it is classified as a soft base, which usually forms strong bonding with soft acids and monovalent Group 11 cations (Aslanidis *et al.*, 2005; Sigel *et al.*, 1979).

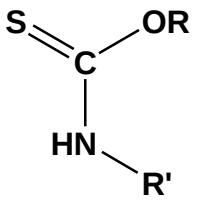

R, R' = alkyl and/or aryl group

Figure 1.2: General chemical structure of thiocarbamide.

Characteristically, thiocarbamide binds to a metal centre *via* the thione sulphur. Examples of the neutral thiocarbamide connect as a monodentate thione are seen in the complexes of *trans*-Pd[S=C(OEt)N(H)Me]$_2$(SCN)$_2$ (Bardi *et al.*, 1981) and [Au(S=C(OEt)N(H)Me]$_2$Cl (Casellato *et al.*, 1990). In the contrary, thiocarbamide functions as a thiolate ligand upon deprotonation as in gold(I) compounds, *e.g.* Ph$_3$PAu[SC(OMe)N=Ph] and other related structures as described in the literature (Ho *et al.*, 2007; Kuan *et al.*, 2008). Alternatively, chelating modes are adopted *via* the S and N atoms in palladium(II) (Tarantelli *et al.*, 1971) complexes. In rare occasions, the ligand coordinates *via* both anionic S- ligand mode and a N-,S-chelate in the same molecule of [Pd{PhNC(OMe)S}$_2$(PPh$_3$)] (Furlani *et al.*, 1971). Despite both S and N atoms are available for bond formation, it is possible that with cyclic thiocarbamide molecule, such coordination is not observed as the electron lone pairs are involved in conjugation (Tsukamoto *et al.*, 1980; Varma *et al.*, 1968).

1.3.1 Preparation of Thiocarbamides

Thiocarbamate glycosides that embodies a -OC(S)N(H)- moiety was first found in the leaves of *Moringa oleifera*, by Faizi et al. (Faizi *et al.*, 1992; Faizi *et al.*, 1994), who discovered the first thiocarbamide moiety in natural product. Later, synthesis of thiocarbamides has been developed as discussed below.

The preparation of thiocarbamide mainly involves alcohol and molecules containing S=C=N to serve as the starting materials. In 1994, Sekiyama and colleagues discovered that allyl isothiocyanate reacted more rapidly in the presence of alcohol even

when no mechanical stirring was applied, and the reactivity increased at higher temperature (Sekiyama *et al.*, 1994). This study reveals that reaction between alcohol and isothiocyanate is facile, and the reaction mechanism is as illustrated in Figure 1.3.

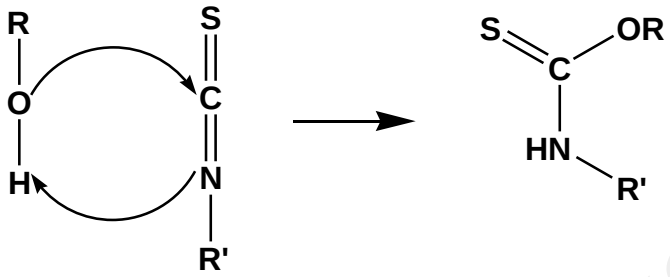

Figure 1.3: Facile reaction of alcohol and isothiocyanate, where R, R' = alkyl/aryl groups.

It is common to prepare thiocarbamides from the heating of isothiocyanate and alcohol, (Gomes *et al.*, 2009; Gomes *et al.*, 2011; Kutschy *et al.*, 2002; Kutschy *et al.*, 2001; Ribeiro da Silva *et al.*, 2007; Zhou *et al.*, 2009) or by reflux method (Breme *et al.*, 2007; El-Adasy, 2007; Elderfield *et al.*, 1953; Ellis *et al.*, 2009; Ghorab *et al.*, 2008). Deprotonating agents such as alkali metal (*e.g.* Na) (Bost *et al.*, 1943; Dixit *et al.*, 2005), sodium hydride (NaH) (Alajarin *et al.*, 2009; Arora *et al.*, 2004; Cesarini *et al.*, 2008; Dixit *et al.*, 2005; Du *et al.*, 2003; Gais *et al.*, 2002; Lee *et al.*, 2004; Min *et al.*, 2010; Rudra *et al.*, 2007; Spallarossa *et al.*, 2009; Tamaru *et al.*, 1987; Tokuyama *et al.*, 2001; Yoon *et al.*, 2003), potassium hydride (KH) (Yamashita *et al.*, 2011; Yamashita *et al.*, 2009), base (*e.g.* NaOH, KOH) (Ho *et al.*, 2005; Jian *et al.*, 2006; Kuan *et al.*, 2007) and Bronsted base (*e.g.* Et_3N) (Stanetty *et al.*, 1996) are also employed in the preparation of thiocarbamides to afford alkoxides with higher reactivity. The reactions are later completed by addition of acid (*e.g.* HCl, TFA) (Ho *et al.*, 2005; Jian *et al.*, 2006; Kuan *et al.*, 2007; Lee *et al.*, 2004; Tokuyama *et al.*, 2001), or Bronsted acid (*e.g.* NH_4Cl, $NaHCO_3$) (Cesarini *et al.*, 2008; Gais *et al.*, 2002; Spallarossa *et al.*, 2009; Yamashita *et al.*, 2011). The use of aryl/acyl chloride, thiocyanate salt and alcohol (Arslan *et al.*, 2007; Montiel-Ortega *et al.*, 2004; Plutín *et al.*, 2010; Plutín *et al.*, 2005; Skinner *et al.*, 1955)

on the other hand paved the synthesis of new and novel thiocarbamide ligands. Alternatively, chlorothionoformate (Taguchi *et al.*, 2003; Zhang, 2008) or thiophosgene (Selvakumar *et al.*, 2003; Selvakumar *et al.*, 2006; Takhi *et al.*, 2008) are reacted with amine to produce thiocarbamides.

1.3.2 Chemical Properties and Their Applications

Thiocarbamide, when protonated, features a N-H bond stretching mode around 3200 cm^{-1} in the IR spectra (Arslan *et al.*, 2007; Ho *et al.*, 2006; Kuan *et al.*, 2007; Vallejos *et al.*, 2009). This characteristic N-H stretch forms a significant indication for successful coordination of thiocarbamide as a thiolate ligand to the metal centre. In such case, the nitrogen atom is deprotonated and the respective N-H stretching is no longer observed in the IR spectra of metal complexes (Ho *et al.*, 2006; Kuan *et al.*, 2008). Likewise, thiocarbamide exhibits a characteristic N-H resonance around 8.6 ppm in the ^{1}H NMR spectra, which disappears upon successful complexation (Cesarini *et al.*, 2008; Dixit *et al.*, 2005).

Theoretical studies, *e.g.* DFT- B3LYP method (Al-Omary *et al.*, 2014; Arslan *et al.*, 2007; Jian *et al.*, 2006; Vallejos *et al.*, 2009), were performed to delineate the characteristic electronic resonance of thiocarbamide molecules (Kaur *et al.*, 2005). Molecular packing of $ROC(S)N(H)C(O)OCH_3$ (R = CH_3– and CH_3CH_2–), were found stabilised by intermolecular N-H···S=C hydrogen bonding, in addition to the *trans* orientation of sulphur and oxygen atoms within the -(S)N(H)C(O)- moiety, as reported by Vallejos *et al.* in 2009. Analogous intermolecular hydrogen bondings were also observed in the structure of O-ethyl benzoylthiocarbamate (Arslan *et al.*, 2007). Such interactions are thought to be responsible for the discrepancy of the calculated and experimental frequencies of the N-H stretching vibration mode, with an approximate difference of 195 cm^{-1}.

Crystallographic studies however revealed that {…H–N–C=S}$_2$ synthon does not predominate in the crystal structures of thiocarbamide, and the substance may form *E*- and *Z*- conformations about the central C–N bond. The study performed on O-methyl-N-arylthiocarbamides concluded that both *E*- and *Z*- conformations coexist in the solution state while in the solid state, the *E*-conformation has higher stability by approximate 5 kJ mol^{-1} due to the formations of hydrogen bonding (Ho *et al.*, 2005).

Thiocarbamide provides opportunities for its applications as catalysts, owing to the stability of N-H bonding over thiourea towards high moisture content in bromolactonisation reactions. This higher tolerance to moisture leads to the development of thiocarbamides as effective chiral catalyst for asymmetric bromolactonisation (Tan *et al.*, 2011) as well as for highly region- and enantioselective synthesis of lactones (Tan *et al.*, 2012). Over and above, due to the strong affinity toward selective ions and related chelating ability, thiocarbamide functions as a sequestering substance of heavy metal ions (Quas *et al.*, 2000; Ribeiro Da Silva *et al.*, 2004; Schroder *et al.*, 1995; Shagun *et al.*, 2006); (Harris *et al.*, 1954; Seryakova *et al.*, 1975).

Biological activities of thiocarbamides are also accessed and they have been used widely as herbicides (Mizuno *et al.*, 2003; Zhou *et al.*, 2009; Zhu *et al.*, 2007), bactericides (Goel *et al.*, 2002; Ryder *et al.*, 1986) and pesticides (Breiter *et al.*, 1998; Lee *et al.*, 2004). Remarkably, thiocarbamides are also identified as HIV-1 non-nucleoside reverse transcriptase inhibitors (NNRTIs) (Cesarini *et al.*, 2008; Ranise *et al.*, 2005). The pharmacological activity of thiocarbamides may correspond to the molecular flexibility of the conjugated C-N linkages which is dictated by the restricted rotation around the chemical bonds (Beers *et al.*, 1970). Incorporation of a thiocarbamide group in the linezolid, a synthetic antibiotic used for treatments of infections caused by Gram-positive bacteria, found to improve the biological activities (Selvakumar *et al.*, 2003) (Dixit *et al.*, 2005; Selvakumar *et al.*, 2006), let alone the promising fungicidal activity

possessed by thiocarbamides (Albores-Velasco *et al.*, 1995; Soung *et al.*, 2010). In short, understanding of the structural/stability/reactivity relations remains as a key factor for the design of thiocarbamide molecules with higher effectiveness regardless of the specific application.

1.4 Phosphinegold(I) Compounds

While thiocarbamide molecules possess promising biological activity, in addition to its facile preparation and potential structural modification, research on the bioactivity of their gold (I) species are however limited. The biological potential demonstrated by auranofin prompted efforts to study related phosphinegold(I) thiolate species.

Gold(I), the soft Lewis acid, forms stable compounds with soft donor ligands. Conversely, coordination of gold(I) with hard ligands may induce disproportionation to gold(III) and gold(0). While gold(III) species are postulated to cause toxicity as well as to contribute to protein and nucleic acids denaturation, stable gold(I) species may eliminate such negative effects. In view of the above, complexation of thiocarbamides and phosphinegold(I) precursors is thought worthwhile for the preparation of highly potent gold species.

1.4.1 Phosphinegold(I) Precursors

Gold(I), with an oxidation state of +1, favours the complexation with soft donor ligands such as thiolates, cyanide and phosphine to form stable compounds. Gold(I) usually adopts linear geometry, but trigonal and tetrahedral geometries are also possible with multidentate ligands. Other than promoting stability, phosphine ligands essentially enhance the biological activity of related gold(I) species (Fortman *et al.*, 2010; Glisic *et al.*, 2014; Hashmi *et al.*, 2010; Partyka *et al.*, 2007; Perez-Galan *et al.*, 2010). This is further substantiated when gold thiolates (Berners-Price *et al.*, 1988; Mirabelli *et al.*, 1986;

Snyder *et al.*, 1986) and gold chlorides without phosphorus donors were found to have reduced potency (Tiekink, 2002). The selection of appropriate phosphine ligand is therefore crucial, as suggested from the work of Glisic and Djuran (Glisic *et al.*, 2014), which demonstrated that replacement of phenyl groups with less bulky methyl groups on the phosphorous atom in dinuclear complexes resulted in significant reduction of anti-microbial activity. In contrast, the gold(I) compounds that bear comparable small phosphine group, triethylphosphine (PEt_3), exhibited high activity against selected strains of bacteria and fungi.

A wide range of phoshinegold(I) halide precursors can be sourced commercially, or prepared from the reduction of gold(III) salts, *e.g.* $KAuCl_4$, by incorporating reducing agents such as thiodiglycol (Batsanov *et al.*, 2009), phosphine (Santini *et al.*, 2011) and sodium sulphite (Xiong *et al.*, 2014). Reactions involved in the reduction of gold(III) to gold(I) using sodium sulphite are shown as below (Romankiw *et al.*, 2000):

$$[Au(SO_3)_2]^{3-} \rightarrow [Au(SO_3)]^{-} + SO_3^{2-} \quad (1)$$

$$[Au(SO_3)]^{-} \rightarrow Au^{+} + SO_3^{2-} \quad (2)$$

$$Au^{+} + e^{-} \rightarrow Au \quad (3)$$

As the reduction of gold(III) to gold(0) is unfavourable, the control over the rate of reaction is therefore crucial to optimise the production of desired gold(I) species. This can be achieved by monitoring the reaction temperature, *e.g.* 0 °C from ice/salt combination, and/or, by fine-tuning the solvent system polarity *e.g.* mixture of acetone/water, so that the reduction is carried out at a controllable pace. Indication of successful gold(III) reduction to gold(I) is observed from the changes of colour from yellow to colourless.

1.4.2 Phosphinegold(I) Thiolate Compounds

Preparation of phosphinegold(I) thiolate compounds from the respective phosphinegold(I) chloride and thiocarbamide is often aided with base, *e.g.* NaOH. Successful complexation is indicated from the absence of broad resonance around δ 8 ppm corresponding to thiocarbamide N-H in the ^{1}H NMR spectrum of the phosphinegold(I) compound. The upfield shift of the resonance in the $^{13}C\{^{1}H\}$ NMR due to the quaternary carbon may be observed as a consequence of reorganisation of π-electron density in the ligand upon deprotonation and subsequent C=N bond formation (Ho *et al.*, 2006). Coordination of thiocarbamide as a thiolate ligand is also observed in the IR spectra of the respective phosphinegold(I) compounds due to the absence of the characteristic N-H stretching band absorption at ~ 3200 cm^{-1}.

1.4.2.1 Chemical Properties and Their Applications

One of the motivating factors behind the interest in gold(I) compounds, often relates to their characteristic luminescent properties (Chao *et al.*, 2002; Elbjeirami *et al.*, 2007; Lee *et al.*, 2003; Lee *et al.*, 2002; Stott *et al.*, 2005; Tzeng *et al.*, 2004; Yun *et al.*, 2006; Zhang *et al.*, 2001). The above leads to the development of gold(I) compounds function as molecular sensors, energy storage devices as well as for the detection of alkali ions, *e.g.* K^{+}. The macrocyclic residues carried by functionalised dinuclear phosphinegold(I) thiolates sandwich the cation and promote Au…Au interactions that cause a luminescent event (Li *et al.*, 2005; Li *et al.*, 2004; Yam *et al.*, 2001; Yam *et al.*, 1998).

The frontier orbitals of gold(I) species with electron configuration d^{10} are the filled 5*d* orbitals followed by empty 6*s* and 6*p* orbitals. Arising from the oxidising as well as reducing abilities of gold(I), both the LMCT and MLCT occur with comparable probability depending on the ligand coordinated, and these transitions are thought to be responsible for the luminescence properties. In addition to intraligand, metal-centered,

LMCT and MLCT transitions, aurophilic interactions are speculated to influence the luminescence properties, as a result of lower energy gap and higher transition probability (Tiekink *et al.*, 2009; van Zyl *et al.*, 2000). Au…Au interactions are found leading to a σ overlap of 5*d* and 6*p* orbitals in polynuclear gold(I) compounds, thereby introduces stabilisation of the gold(I) 6*p* orbitals and thus the HOMO and LUMO are σ_d^* and σ_p^b orbitals respectively (Vogler *et al.*, 2001). Such phenomena resulted in the corresponding metal centred *dp* absorption as observed in $[Au_2(dppm)_2]^{2+}$ species at λ_{max} = 292 nm, and the phosphorescence from such *dp* triplets at λ_{max} in the range of 565 – 593 nm was reported (Che *et al.*, 1990; Che *et al.*, 1989; King *et al.*, 1989; Yam *et al.*, 1990). The bulky phosphine ligand in mononuclear phosphinegold(I) precursors, *e.g.* Ph_3PAuCl, restrains the formation of Au…Au interactions, however. When the compound was excited in the UV region, two emission bands were observed in the 350 - 500 and 420 - 600 nm regions, respectively (Larson *et al.*, 1995), correspond to phosphorescence phenomena. From the SCF-Xα-SW calculations performed, the HOMO of this molecule is mainly of phenyl-π character while the LUMO centred on gold, phosphorous and chloride atoms (Tiekink *et al.*, 2009).

The luminescence properties of the phosphinegold(I) thiolate compounds are mainly governed by the nature of the ligand employed. The optical process occurs predominantly due to the excitation of sulphur with subsequent charge transfer to gold, despite the fact that chromophore are often present in the phosphine ligand. A series of mononuclear $[R_3PAu\{SC(OMe)=NC_6H_4NO_2\text{-}4\}]$, for R = Et, Cy, and Ph, and binuclear $[(Ph_2P(CH_2)_nPPh_2)\ \{Au\{SC(OMe)=NC_6H_4NO_2\text{-}4\}_2]$, for *n* = 1–4 were found to display shoulders at ~260-262 nm in the absorption spectra arisen from the thiocarbamide ligand-centered π-π* transition which were also observed in the ligand itself at ~256 nm. Meanwhile, the intraligand transitions due to the phenyl rings of the phosphine ligands were observed at ~266 - 270 nm. When these compounds were examined for their

luminescence properties, the results indicated that the nature of the ancillary phosphines, presence of Au…Au either intra- or inter-molecular, did not induce a significant influence on the luminescence properties (Ho *et al.*, 2006). This is further supported by the work of Jones *et al.* and Narayanaswamy *et al.* (Jones *et al.*, 1995; Narayanaswamy *et al.*, 1993), in which, the photophysical data of dinuclear diphosphinegold(I) thiolate compounds with phosphine ligand of various spacer proved that there is no correlation between the Au…Au interactions and luminescence properties. The observed luminescence originates from the charge transfer of sulphur to gold atom, with low energy absorption bands observed below 300 nm assigned to LMCT (S→Au) and the emission maxima appeared in the 485-510 nm region.

1.4.2.2 Crystallography and Related Interactions

Gold(I) compounds generally feature linear geometry, as in the structures of related phosphinegold(I) thiocarbamide compounds, where the gold atom is connected to a sulphur and a phosphorous donor atom, with the angle of P-Au-S close to linearity (Ho *et al.*, 2006; Ho *et al.*, 2007; Kuan *et al.*, 2008). The crystal packing of the molecules may be influenced by the nature of the thiolate ligand, in addition to other forces arising from possible intramolecular Au…Au, Au…O, Au…π and intermolecular Au…X (X = halide) interactions. While the additional interactions occur mainly around the gold(I) centre as a consequence of the relativistic effect, this has paved the possibilities for crystal engineers to utilise such interactions to design gold(I) compounds of desired properties for respective applications.

Aurophilic interactions are often observed when gold(I) atoms are connected by a multidentate ligand that holds them in close proximity, which arise from the overlap of filled 5*d* orbitals and 6*p* orbitals due to relativistic effect. Such interaction is perceived to afford comparable stabilisation energy to that of a hydrogen bonding (Pyykko *et al.*, 1997;

Schmidbaur, 2001). The influence of aurophilic interactions upon supramolecular aggregation patterns is well described in the literature (Ahrland *et al.*, 1985; Coker *et al.*, 2004; Jones *et al.*, 1998; Schmidbaur *et al.*, 1990) where, the reported structures resembles a rod or cone in the absence of aurophilic interactions. When the gold(I) atoms in these structures are connected to each other, the structural dimensionality is increased to a 1-D chain. Hence, harnessing aurophilicity aids in designing gold(I) compounds with different architectures, *e.g.* simple dimers, infinite bands or sheets and complex 3-D arrays in some cases (Katz *et al.*, 2008). (*p*-Tolyl)$_3$PAuCl is an example of gold(I) compounds that appears in polymorphic forms, where the presence of Au…Au contact is detected in one of the forms while the other is not, governed by the crystallisation modes (Bott *et al.*, 2004; Cookson *et al.*, 1994). The well-established aurophilic interactions in gold(I) compounds are of great interest for their specific influences on the physical properties, which can be employed for applications such as photocatalysts, vapochromic or solvatochromic sensors and light-emitting diodes (Schmidbaur *et al.*, 2012).

Intramolecular Au…O interactions commonly feature in R$_3$PAu[SC(OMe)=NR′], where R, R′ = aryl and alkyl (Ho *et al.*, 2006; Kuan *et al.*, 2008). Tiekink and colleagues discovered that substituting the P-bound phenyl rings with electron rich *p*-tolyl ring promoted formation of Au…π(arene) interactions while insertion of a nitro group to the thiolate-arene ring was sufficient to restore the Au…O interactions. The above implies that varying the N- and P-bound groups influence the formation of Au…O or Au…π(arene) interactions. Au…π(arene) interactions receive less attention as compared to aurophilicity. A delocalised Au…π interaction is recognised at the distance of gold atom and the ring centroid less than 4.0 Å (Tiekink *et al.*, 2009). In fact, the energy of stabilisation imparted by these two interactions are of similar strength, as in the two polymorphic forms of (Ph$_2$PCH$_2$PPh$_2$)(AuCl)$_2$, bis(diphenylphosphino)methane-di[chloridogold(I)] where Au…π(arene) interactions were found to stabilise one

polymorphic form while the other featured Au…Au contacts (Healy, 2003; Schmidbaur *et al.*, 1977). In short, these interactions play a crucial role in the overall molecular structures of gold(I) compounds and each of the interactions imparts considerable impact.

1.4.3 Stability of Gold(I) Compounds under Biological Condition

The use of gold species for the treatment of cancer (Tiekink, 2002) and HIV (Okada *et al.*, 1993) is another driving force for extensive studies of their pharmacological properties. Buckley and his colleagues (Buckley *et al.*, 1996) first reported some organogold(III) complexes endowed with significant cytotoxic and anticancer properties. However, a number of gold(III) complexes are found to exhibit poor stability under physiological condition owing to their high reduction potential and fast hydrolysis rate, thus only limited gold(III) complexes are found demonstrating anticancer activity (Berners-Price *et al.*, 2011; Nobili *et al.*, 2010). During the past decade, various gold(III) complexes of sufficient stability in the physiological environment have been synthesized and evaluated for *in vitro* anti-cancer properties (Casini *et al.*, 2006). In view of the above, focus is directed to prepare related gold(I) compounds with acceptable stability. Recently, mono- and bis-phosphinegold(I) species, including thiolate derivatives, are found to demonstrate promising anti-tumour activities, as discussed in recent bibliographic reviews (McKeage *et al.*, 2002; Ott, 2009; Tiekink, 2003).

Notwithstanding a broad range of linear two coordinate gold(I) compounds display promising in vitro cytotoxicity, the characteristic feature of these compounds to undergo facile ligand exchange reactions limit their application as anti-cancer agents. The sensitivity of gold(I) compounds rely on the structural rigidity induced by the attached ligands. Therefore, the interactions of gold(I) compounds with proteins and enzymes comprising cysteine or selenocysteine residues active sites have received much attention as these sites are suggested to be the major targets for gold(I) compounds (Bhabak *et al.*,

2011). Langdon-Jones and colleague (Langdon-Jones *et al.*, 2014) suggested higher lipophilicity in four coordinate gold(I) compounds induce less reactivity to thiols. The incorporation of chelating phosphine ligand was later aimed to increase the structural stability of gold(I) compounds so as to reduce their high thiol activity. Unfortunately, enhanced lipophilicity resulted in severe toxicity in the mitochondria of both normal and tumorigenic cells (Berners-Price *et al.*, 1986). Gold(I) compounds with triethylphosphine, however, were found to impart considerable lipophilicity and exhibit several pharmacokinetic advantages (Bhabak *et al.*, 2011). Research on gold(I) compounds with promising biological activity require a long term effort as the delineation of the structural/stability/reactivity relations still remains elusive.

1.5 Related Copper(I) Thiolate Compounds

Thiocarbamides, with both nitrogen and sulphur to function as potential donating atoms, also form strong bonding with monovalent copper cation which appears at the top of Group 11 in periodic table, above silver and gold. Efforts are devoted to study the related copper(I) thiocarbamide compounds owing to the rich coordination chemistry displayed (Aslanidis *et al.*, 2004; Aslanidis *et al.*, 2002; Divanidis *et al.*, 2005; Hadjikakou *et al.*, 1991; Karagiannidis *et al.*, 1990). Copper(I) compounds generally present linear (regular and irregular), trigonal and tetrahedral coordination geometries due to the highly labile and easily distorted d^{10} coordination sphere (Greenwood *et al.*, 2012). The coordination of copper(I) with sulphur containing ligand yielded rich variety of structures of mononuclear trigonal planar and tetrahedral compounds as in the literature (Aslanidis *et al.*, 2004), with the copper(I) centre coordinated to the sulphur atom via terminal and/or μ_2-S bridging modes. Interest is also directed to develop diverse coordination networks from copper(I) and soft bases which may exhibit conducting, catalytic and magnetic exchange properties (Carlucci *et al.*, 2000; Lobana *et al.*, 2006). The interesting structures of 1D polymers, $\{Cu_6(\mu_3\text{-}SC_3H_6N_2)_4(\mu\text{-}SC_3H_6N_2)_2(\mu\text{-}I)_2I_4\}$,

$\{Cu_6(\mu_3\text{-}SC_3H_6N_2)_2(\mu\text{-}SC_3H_6N_2)_4(\mu\text{-}Br)_4Br_2\}_n$ and 3D polymer $\{Cu_2(\mu\text{-}SC_3H_6N_2)_2(\mu\text{-}SCN)_2\}_n$, were reported containing 20-membered metallacyclic rings in their preparation of coordination networks (Carlucci *et al.*, 2000; Lobana *et al.*, 2006). In addition to the non-biological applications, copper(I) is an essential trace element for living organism (Linder, 1991). The remarkable feature of cancer cells and tissues to accumulate copper lead to the development of potential strategy in cancer chemotherapy; in the presence of copper, sulphur containing molecules become active proteasome inhibitors and breast cancer killers (Daniel *et al.*, 2005). Owing to the above, copper complexes of sulphur containing ligands have been paid enormous attention including their cytotoxicity and anti-proliferative activity toward various types of tumours (Rodríguez-Argüelles *et al.*, 2009) and nuclease activity (Krishna *et al.*, 2009).

1.6 Aims of Study

(i) To prepare highly potent gold-based therapeutic agents, the phosphinegold(I) thiolate compounds.

(ii) To employ various characterisation techniques in the delineation of the chemistry, *e.g.* infrared (IR) spectroscopy, multi-nuclear magnetic resonance (multi-NMR) spectroscopy, thermogravimetric analyses, elemental analyses, powder X-ray diffraction and single crystal X-ray diffraction.

(iii) To review the synthesised compounds for their biological activities against HT-29 colon cancer cell line, MCF-7 breast cancer cell line and HEK-293 embryonic kidney cell line as well a broad panel of Gram-positive and Gram negative bacteria for exploration of structure/activity relationships.

(iv) To explore the chemistry and structural study of related phosphinecopper(I) compounds to contemplate the study on gold(I) derivatives.

CHAPTER 2:METHODOLOGY

2.1 Materials

Water, sodium hydroxide (Merck), hydrochloric acid fuming 37% (Merck), methanol, for analysis EMSURE® grade (Merck), ethanol, for analysis EMSURE® grade (Merck), isopropranol, for analysis EMSURE® grade (Merck), chloroform, for analysis EMSURE® grade (Merck), dichloromethane, for analysis EMSURE® grade (Merck), acetone, for analysis EMPARTA® grade, acetonitrile, for analysis EMSURE® grade (Merck), triethylphosphine solution,1.0 M in THF (Merck), triphenylphosphine (Sigma-Aldrich), tricyclohexylphosphine 98% (Sigma-Aldrich), 1,1′-Bis(diphenylphosphino)ferrocene 97% (Sigma-Aldrich), phenyl isothiocyanate 98% (Merck), *p*-tolyl isothiocyanate (Merck), 4-chlorophenyl isothiocyanate (Sigma-Aldrich), 4-nitrophenyl isothiocyanate (Acros Organic), *p*-phenylene diisothiocyanate 98% (Sigma-Aldrich), potassium tetrachloroaurate(III) 98% (Sigma-Adrich), sodium sulfite ≥ 98% (Merck), copper(I) chloride (Merck). All chemicals and solvents were sourced commercially and used as received.

2.2 Synthesis

2.2.1 Thiocarbamide

All reactions were carried out under ambient conditions. The methods employed for the preparation of thiocarbamide ligands were similar, so that the preparation of the parent thiocarbamide is described in detail as a representative example.

$MeOC(=S)N(H)C_6H_5$ was prepared in quantitative yields by adding phenyl isothiocyanate (1.0 mmol) to a stirred solution of NaOH (1.0 mmol) in methanol (50 mL). The resulting mixture was stirred at room temperature for 2 h, followed by addition of excess HCl (5 M) and stirred for another 1 h. The final product was later extracted from the aqueous solution with chloroform and left for slow evaporation at room temperature.

Bi-functional thiocarbamide was prepared in similar manner as described above where *p*-phenylene diisothiocyanate (1 mmol) was reacted in methanol (100 ml) in the presence of two mole equivalents of NaOH.

MeOC(=S)N(H)Ph (L1)

mp 93.0 – 94.0 °C. *Anal*. Calc. for C_8H_9NOS: C, 57.46; H, 5.42; N, 8.38. Found: C, 57.48; H, 5.25; N, 8.33 %. IR (cm^{-1}): 3184 (*br*) ν(N–H), 1448 (*s*) ν(C–N), 1207 (*s*) ν (C=S), 1059 (*s*) ν(C–O). ^{1}H NMR ($CDCl_3$): δ 8.67 [*s*, br, 1H, NH], 7.33 [*t*, 2H, *m*-aryl-H, J = 7.72 Hz], 7.27 [br, 2H, *o*-aryl-H, overlapped with solvent resonance], 7.19 [*t*, 2H, *p*-aryl-H, J = 7.14 Hz], 4.14 [*s*, 3H, OCH_3] ppm. $^{13}C\{^1H\}$ NMR ($CDCl_3$): δ 188.7 [C_q], 137.0 [C_{ipso}], 129.1 [C_{meta}], 125.6 [C_{para}], 121.8 [C_{ortho}], 58.8 [OCH_3] ppm.

EtOC(=S)N(H)Ph (L2)

mp 66.0 – 68.0 °C. *Anal*. Calc. for $C_9H_{11}NOS$: C, 59.64; H, 6.12; N, 7.73. Found: C, 59.49; H, 6.09; N, 7.73 %. IR (cm^{-1}): 3214 (*br*) ν(N–H), 1446 (*s*) ν(C–N), 1199 (*s*) ν (C=S), 1038 (*s*) ν(C–O). ^{1}H NMR ($CDCl_3$): δ 8.68 [*s*, br, 1H, NH], 7.34 [*t*, 2H, *m*-aryl-H, J = 7.70 Hz], 7.27 [br, 2H, *o*-aryl-H, overlapped with solvent resonance], 7.17 [*t*, 2H, *p*-aryl-H, J = 7.10 Hz], 4.63 [*s*, br, 2H, OCH_2], 1.41 [*t*, 3H, CH_3, J = 7.10 Hz] ppm. $^{13}C\{^1H\}$ NMR ($CDCl_3$): δ 188.7 [C_q], 137.2 [C_{ipso}], 129.0 [C_{meta}], 125.4 [C_{para}], 121.6 [C_{ortho}], 68.8 [OCH_2], 14.1 [CH_3] ppm.

***i*PrOC(=S)N(H)Ph (L3)**

mp 75.0 – 77.0 °C. *Anal*. Calc. for $C_{10}H_{13}NOS$: C, 61.50; H, 6.71; N, 7.17. Found: C, 61.89; H, 6.83; N, 7.28 %. IR (cm^{-1}): 3169 (*br*) ν(N–H), 1450 (*s*) ν(C–N), 1206 (*s*) ν (C=S), 1090 (*s*) ν(C–O). ^{1}H NMR ($CDCl_3$): δ 8.68 [*s*, br, 1H, NH], 7.33 [*t*, 2H, *m*-aryl-H, J = 7.66 Hz], 7.27 [br, 2H, *o*-aryl-H, overlapped with solvent resonance], 7.15 [*t*, 2H, *p*-aryl-H, J = 7.06 Hz], 5.66 [*sept*, 1H, OCH, J = 6.23 Hz], 1.41 [*d*, 6H, CH_3, J = 6.24 Hz]

ppm. $^{13}C\{^{1}H\}$ NMR ($CDCl_3$): δ 188.0 [C_q], 137.2 [C_{ipso}], 129.0 [C_{meta}], 125.3 [C_{para}], 121.1 [C_{ortho}], unobserved [OCH], 21.7 [CH_3] ppm.

MeOC(=S)N(H)C_6H_4Me-4 (L4)

mp 78.0 – 80.0 °C. *Anal*. Calc. for $C_9H_{11}NOS$: C, 59.64; H, 6.17; N, 7.73. Found: C, 59.26; H, 6.29; N, 7.74 %. IR (cm^{-1}): 3234 (*br*) ν(N–H), 1451 (*s*) ν(C–N), 1204 (*s*) ν (C=S), 1061 (*s*) ν(C–O). ^{1}H NMR ($CDCl_3$): δ 8.70 [*s*, br, 1H, NH], 7.13 [*s*, br, 4H, aryl-H], 4.11 [*s*, 3H, OCH_3], 2.32 [*s*, 3H, aryl-CH_3] ppm. $^{13}C\{^{1}H\}$ NMR ($CDCl_3$): δ 189.6 [C_q], 135.5 [C_{ipso}], 134.4 [C_{para}], 129.6 [C_{meta}], 122.0 [C_{ortho}], 58.8 [OCH_3], 21.0 [aryl-CH_3] ppm.

EtOC(=S)N(H)C_6H_4Me-4 (L5)

mp 64.0 – 67.0 °C. *Anal*. Calc. for $C_{10}H_{13}NOS$: C, 61.50; H, 6.71; N, 7.23. Found: C, 61.30; H, 6.82; N, 7.23 %. IR (cm^{-1}): 3236 (*br*) ν(N–H), 1450 (*s*) ν(C–N), 1202 (*s*) ν (C=S), 1042 (*s*) ν(C–O). ^{1}H NMR ($CDCl_3$): δ 8.68 [*s*, br, 1H, NH], 7.13 [*s*, br, 4H, aryl-H], 4.62 [*s*, br, 2H, OCH_2], 2.32 [*s*, 3H, aryl-CH_3], 1.39 [*t*, 3H, CH_3, J = 7.10 Hz] ppm. $^{13}C\{^{1}H\}$ NMR ($CDCl_3$): δ 188.6 [C_q], 135.2 [C_{ipso}], 134.6 [C_{para}], 129.6 [C_{meta}], 121.6 [C_{ortho}], 68.7 [OCH_2], 20.9 [aryl-CH_3], 14.1 [CH_3], ppm.

***i*PrOC(=S)N(H)C_6H_4Me-4 (L6)**

mp 91.0 – 92.0 °C. *Anal*. Calc. for $C_{11}H_{15}NOS$: C, 63.12; H, 7.22; N, 6.69. Found: C, 63.35; H, 7.33; N, 6.70 %. IR (cm^{-1}): 3221 (*br*) ν(N–H), 1462 (*s*) ν(C–N), 1205 (*s*) ν (C=S), 1087 (*s*) ν(C–O). ^{1}H NMR ($CDCl_3$): δ 8.65 [*s*, br, 1H, NH], 7.13 [*s*, br, 4H, aryl-H], 5.65 [*sept*, 1H, OCH, J = 6.22 Hz], 2.32 [*s*, 3H, aryl-CH_3], 1.39 [*d*, 6H, CH_3, J = 6.20 Hz] ppm. $^{13}C\{^{1}H\}$ NMR ($CDCl_3$): δ 187.8 [C_q], 135.0 [C_{ipso}], 134.7 [C_{para}], 129.5 [C_{meta}], 121.5 [C_{ortho}], 73.7 [OCH], 21.7 [CH_3], 20.9 [aryl-CH_3] ppm.

_i_PrOC(=S)N(H)C$_6$H$_4$Cl-4 (L7)

mp 92.0 – 93.0 °C. *Anal*. Calc. for $C_{10}H_{12}ClNOS$: C, 52.28; H, 5.27; N, 6.10. Found: C, 52.27; H, 5.10; N, 6.10 %. IR (cm^{-1}): 3198 (*br*) ν(N–H), 1498 (*s*) ν(C–N), 1207 (*s*) ν (C=S), 1091 (*s*) ν(C–O). ^{1}H NMR ($CDCl_3$): δ 8.58 [*s*, br, 1H, NH], 7.30 [*d*, 2H, *m*-aryl-H, J = 8.52 Hz], 7.21 [*s*, br, 2H, *o*-aryl-H], 5.64 [*sept*, 1H, OCH, J = 6.23 Hz], 1.40 [*d*, 6H, CH_3, J = 6.20 Hz] ppm. ^{13}C{^{1}H} NMR ($CDCl_3$): δ 187.8 [C_q], 135.7 [C_{ipso}], 129.1 [C_{meta}], 126.6 [C_{para}], 122.7 [C_{ortho}], unobserved [OCH], 21.7 [CH_3] ppm.

_i_PrOC(=S)N(H)C$_6$H$_4$NO$_2$-_p_ (L8)

mp 119.0 – 121.5 °C. *Anal*. Calc. for $C_{10}H_{12}N_2O_3S$: C, 49.99; H, 5.03; N, 11.66. Found: C, 50.19; H, 5.02; N, 11.86 %. IR (cm^{-1}): 3240 (*br*) ν(N–H), 1495 (*s*) ν(C–N), 1209 (*s*) ν (C=S), 1084 (*s*) ν(C–O). ^{1}H NMR ($CDCl_3$): δ 8.60 [*s*, br, 1H, NH], 8.22 [*dt*, 2H, *m*-aryl-H, J = 9.12 Hz, J = 2.47 Hz], 7.54 [*s*, br, 2H, *o*-aryl-H], 5.68 [*sept*, 1H, OCH, J = 6.24 Hz], 1.46 [*d*, 6H, CH_3, J = 6.24 Hz] ppm. ^{13}C{^{1}H} NMR ($CDCl_3$): δ 187.5 [C_q], 143.9 [C_{ipso}], 142.7 [C_{para}], 125.1 [C_{meta}], 120.4 [C_{ortho}], unobserved [OCH], 21.6 [CH_3] ppm.

1,4-[MeOC(=S)N(H)]$_2$C$_6$H$_4$ (L9)

mp 209.0 – 210.0 °C. *Anal*. Calc. for $C_{10}H_{12}N_2O_2S_2$: C, 46.85; H, 4.72; N, 10.93. Found: C, 46.71; H, 4.64; N, 10.94 %. IR (cm^{-1}): 3219 (*br*) ν(N–H), 1454 (*s*) ν(C–N), 1140 (*s*) ν(C–O), 1046 (*s*) ν (C=S). ^{1}H NMR (DMSO-d_6): δ 11.10 [*s*, br, 2H, NH], 7.59 [*s*, br, 2H, aryl-H], 7.30 [*s*, br, 2H, aryl-H], 3.99 [*s*, 6H, OCH_3] ppm. ^{1}H NMR ($CDCl_3$): δ 8.32 [*s*, br, 2H, NH], 7.56 [*s*, br, 2H, aryl-H], 7.22 [*s*, br, 2H, aryl-H], 4.12 [*s*, 6H, OCH_3] ppm. ^{13}C{^{1}H} NMR (DMSO-d_6): δ 189.1, 188.4 [C_q], 135.8, 134.8 [C_{ipso}], 123.7 and 122.6 [C_{ortho}], 58.3, 56.8 [OCH_3] ppm.

2.2.2 Gold(I) Compounds

$Ph_3PAu\{SC(OR)=NC_6H_4X\text{-}4\}$ for R = Me, Et and *i*Pr, X = H, CH_3, Cl and NO_2 were obtained from the reaction of Ph_3PAuCl precursor (synthesized by the reduction of $KAuCl_4$ by sodium sulfite followed by the addition of Ph_3P) with one mole equivalent of ROC(=S)N(H)Ph in the presence of base. The preparation of $Ph_3PAu\{SC(OMe)=NC_6H_5\}$ is described as a representative example.

NaOH (0.50 mmol) in MeOH (5 mL) was added to a suspension of Ph_3PAuCl (0.50 mmol) in MeOH (20 mL), followed by the addition of $MeOC(=S)NHC_6H_5$ in MeOH (20 mL). The resulting mixture was stirred for 3 h at 50 °C. An equal volume of dichloromethane was added and the solution was left for slow evaporation at room temperature.

$Ph_3PAu[SC(OMe)=NC_6H_5]$ (1)

Colourless crystal. Yield: 0.288 g (91 %). mp 142.0-144.0 °C. *Anal*. Calc. for $C_{26}H_{23}AuNOPS$: C, 49.93; H, 3.71; N, 2.24. Found: C, 49.69; H, 3.45; N, 2.28 %. IR (cm^{-1}): 1435 (*s*) ν(C=N), 1145 (*s*) ν(C–O), 1099 (*s*) ν(C–S). ^1H NMR ($CDCl_3$): δ 7.53 – 7.42 [*m*, br, 15H, Ph_3P], 7.04 [*t*, 2H, *m*-aryl-H, J = 7.80 Hz]. 6.84 [*dd*, 2H, *o*-aryl-H, J = 8.34 Hz, J = 1.10 Hz], 6.71 [*t*, 1H, *p*-aryl-H, J = 7.36 Hz], 3.91 [*s*, 3H, OCH_3] ppm. $^{13}C\{^1H\}$ NMR ($CDCl_3$): δ 164.6 [C_q], 151.1 [aryl, C_{ipso}], 134.3 [*d*, *m*-Ph_3P, $^3J_{CP}$ = 13.84 Hz], 131.6 [*d*, *p*-Ph_3P, $^4J_{CP}$ = 2.29 Hz], 129.5 [*d*, *i*-Ph_3P, $^1J_{CP}$ = 56.62 Hz], 129.1 [*d*, *o*-Ph_3P, $^2J_{CP}$ = 11.49 Hz], 128.8 [aryl, C_{meta}], 122.5 [aryl, C_{para}], 121.9 [aryl, C_{ortho}], 55.3 [OCH_3] ppm. $^{31}P\{^1H\}$ NMR ($CDCl_3$): δ 38.0 ppm.

$Ph_3PAu[SC(OEt)=NC_6H_5]$ (2)

Colourless crystal. Yield: 0.284 g (88 %). mp 134.0-136.0 °C. *Anal*. Calc. for $C_{27}H_{25}AuNOPS$: C, 50.71; H, 3.94; N, 2.19. Found: C, 50.64; H, 3.75; N, 2.26 %. IR (cm^{-1}): 1438 (*s*) ν(C=N), 1131 (*s*) ν(C–O), 1100 (*s*) ν(C–S). ^1H NMR ($CDCl_3$): δ 7.54 – 7.44 [*m*, br, 15H, Ph_3P], 7.06 [*t*, 2H, *m*-aryl-H, J = 7.78 Hz]. 6.84 [*d*, 2H, *o*-aryl-H, J = 8.28 Hz], 6.73 [*t*, 1H, *p*-aryl-H, J = 7.36 Hz], 4.35 [*q*, 2H, OCH_2, J = 7.09 Hz], 1.34 [*t*, 3H, CH_3, J = 7.10 Hz] ppm. $^{13}C\{^1H\}$ NMR ($CDCl_3$): δ 164.0 [C_q], 151.2 [aryl, C_{ipso}], 134.3 [*d*, *m*-Ph_3P, $^3J_{CP}$ = 13.83 Hz], 131.6 [*d*, *p*-Ph_3P, $^4J_{CP}$ = 2.25 Hz], 129.5 [*d*, *i*-Ph_3P, $^1J_{CP}$ = 59.12 Hz], 129.1 [*d*, *o*-Ph_3P, $^2J_{CP}$ = 11.49 Hz], 128.7 [aryl, C_{meta}], 122.4 [aryl, C_{para}], 121.9 [aryl, C_{ortho}], 63.9 [OCH_2], 14.6 [CH_3] ppm. $^{31}P\{^1H\}$ NMR ($CDCl_3$): δ 37.8 ppm.

$Ph_3PAu[SC(O\mathit{i}Pr)=NC_6H_5]$ (3)

Colourless crystal. Yield: 0.297 g (90 %). mp 139.0-142.0 °C. *Anal*. Calc. for $C_{28}H_{27}AuNOPS$: C, 51.46; H, 4.16; N, 2.14. Found: C, 51.31; H, 3.84; N, 2.39 %. IR (cm^{-1}): 1436 (*s*) ν(C=N), 1148 (*s*) ν(C–O), 1099 (*s*) ν(C–S). ^1H NMR ($CDCl_3$): δ 7.54 – 7.44 [*m*, br, 15H, Ph_3P], 7.05 [*t*, 2H, *m*-aryl-H, J = 7.78 Hz]. 6.84 [*d*, 2H, *o*-aryl-H, J = 8.28 Hz], 6.71 [*t*, 1H, *p*-aryl-H, J = 7.36 Hz], 5.29 [*sept*, 1H, OCH, J = 6.19 Hz], 1.32 [*d*, 6H, CH_3, J = 6.20 Hz] ppm. $^{13}C\{^1H\}$ NMR ($CDCl_3$): δ 163.1 [C_q], 151.4 [aryl, C_{ipso}], 134.3 [*d*, *m*-Ph_3P, $^3J_{CP}$ = 13.85 Hz], 131.6 [*d*, *p*-Ph_3P, $^4J_{CP}$ = 2.23 Hz], 129.6 [*d*, *i*-Ph_3P, $^1J_{CP}$ = 56.74 Hz], 129.0 [*d*, *o*-Ph_3P, $^2J_{CP}$ = 11.48 Hz], 128.7 [aryl, C_{meta}], 122.2 [aryl, C_{para}], 121.9 [aryl, C_{ortho}], 70.4 [OCH], 22.1 [CH_3] ppm**.** $^{31}P\{^1H\}$ NMR ($CDCl_3$): δ 37.9 ppm.

$Ph_3PAu\{SC(OMe)=NC_6H_4Me\text{-}4\}$ (4)

Colourless crystal. Yield: 0.297 g (93 %). mp 143.0 – 145.0 °C. *Anal*. Calc. for $C_{27}H_{25}AuNOPS$: C, 50.71; H, 3.94; N, 2.19. Found: C, 50.93; H, 3.64; N, 2.18 %. IR (cm^{-1}): 1436 (*s*) ν(C=N), 1146 (*s*) ν(C–O), 1100 (*s*) ν(C–S). ^1H NMR ($CDCl_3$): δ 7.53 – 7.40

[*m*, br, 15H, Ph_3P], 6.82 [*d*, 2H, *m*-aryl-H, J = 8.04 Hz]. 6.73 [*dt*, 2H, *o*-aryl-H, J = 8.20 Hz, J = 1.95 Hz], 3.90 [*s*, 3H, OCH_3], 2.03 [*s*, 3H, aryl-CH_3] ppm. $^{13}C\{^1H\}$ NMR ($CDCl_3$): δ 164.4 [C_q], 148.6 [aryl, C_{ipso}], 134.3 [*d*, *m*-Ph_3P, $^3J_{CP}$ = 13.86 Hz], 131.6 [*d*, *p*-Ph_3P, $^4J_{CP}$ = 2.16 Hz], 131.5 [aryl, C_{para}], 129.5 [*d*, *i*-Ph_3P, $^1J_{CP}$ = 56.86 Hz], 129.6 [aryl, C_{meta}], 129.1 [*d*, *o*-Ph_3P, $^2J_{CP}$ = 11.49 Hz], 121.8 [aryl, C_{ortho}], 55.3 [OCH_3], 20.8 [aryl-CH_3] ppm. $^{31}P\{^1H\}$ NMR ($CDCl_3$): δ 38.0 ppm.

$Ph_3PAu\{SC(OEt)=NC_6H_4Me\text{-}4\}$ (5)

Colourless crystal. Yield: 0.278 g (85 %). mp 131.0 – 133.0 °C. *Anal*. Calc. for $C_{28}H_{27}AuNOPS$: C, 51.46; H, 4.16; N, 2.14. Found: C, 51.68; H, 3.91; N, 2.22 %. IR (cm^{-1}): 1431 (*s*) ν(C=N), 1118 (*s*) ν(C–O), 1101 (*s*) ν(C–S). ^1H NMR ($CDCl_3$): δ 7.53 – 7.40 [*m*, br, 15H, Ph_3P], 6.83 [*d*, 2H, *m*-aryl-H, J = 8.04 Hz]. 6.73 [*d*, 2H, *o*-aryl-H, J = 8.20 Hz], 4.34 [*q*, 2H, OCH_2, J = 7.12 Hz], 2.05 [*s*, 3H, aryl-CH_3], 1.33 [*t*, 3H, CH_3, J = 7.10 Hz] ppm. $^{13}C\{^1H\}$ NMR ($CDCl_3$): δ 163.8 [C_q], 148.7 [aryl, C_{ipso}], 134.3 [*d*, *m*-Ph_3P, $^3J_{CP}$ = 13.85 Hz], 131.6 [*d*, *p*-Ph_3P, $^4J_{CP}$ = 2.27 Hz], 131.4 [aryl, C_{para}], 129.5 [*d*, *i*-Ph_3P, $^1J_{CP}$ = 56.84 Hz], 129.5 [aryl, C_{meta}], 129.1 [*d*, *o*-Ph_3P, $^2J_{CP}$ = 11.44 Hz], 121.8 [aryl, C_{ortho}], 63.8 [OCH_2], 20.8 [aryl-CH_3], 14.7 [CH_3] ppm. $^{31}P\{^1H\}$ NMR ($CDCl_3$): δ 38.0 ppm.

$Ph_3PAu\{SC(O\mathit{i}Pr)=NC_6H_4Me\text{-}4\}$ (6)

Colourless crystal. Yield: 0.297 g (89 %). mp 148.0 – 151.0 °C. *Anal*. Calc. for $C_{29}H_{29}AuNOPS$: C, 52.18; H, 4.38; N, 2.10. Found: C, 52.15; H, 4.25; N, 2.15 %. IR (cm^{-1}): 1437 (*s*) ν(C=N), 1132 (*s*) ν(C–O), 1093 (*s*) ν(C–S). ^1H NMR ($CDCl_3$): δ 7.53 – 7.42 [*m*, br, 15H, Ph_3P], 6.83 [*d*, 2H, *m*-aryl-H, J = 8.04 Hz]. 6.72 [*d*, 2H, *o*-aryl-H, J = 8.16 Hz], 5.28 [*sept*, 1H, OCH, J = 6.20 Hz], 2.05 [*s*, 3H, aryl-CH_3], 1.32 [*d*, 6H, CH_3, J = 6.20 Hz] ppm. $^{13}C\{^1H\}$ NMR ($CDCl_3$): δ 162.9 [C_q], 148.9 [aryl, C_{ipso}], 134.3 [*d*, *m*-Ph_3P, $^3J_{CP}$ = 13.84 Hz], 131.6 [*d*, *p*-Ph_3P, $^4J_{CP}$ = 2.30 Hz], 131.2 [aryl, C_{para}], 129.6 [*d*, *i*-Ph_3P, $^1J_{CP}$

= 56.73 Hz], 129.5 [aryl, C_{meta}], 129.0 [*d*, *o*-Ph_3P, $^2J_{CP}$ = 11.40 Hz], 121.7 [aryl, C_{ortho}], 70.3 [OCH], 22.1 [CH_3], 20.8 [aryl-CH_3] ppm. $^{31}P\{^1H\}$ NMR ($CDCl_3$): δ 38.0 ppm.

$Ph_3PAu\{SC(OiPr)=NC_6H_4Cl\text{-}4\}$ (7)

Colourless crystal. Yield: 0.313 g (91 %). mp 163.0 – 166.0 °C. *Anal*. Calc. for $C_{28}H_{26}AuClNOPS$: C, 48.88; H, 3.81; N, 2.04. Found: C, 49.06; H, 3.69; N, 2.06 %. IR (cm^{-1}): 1436 (*s*) ν(C=N), 1138 (*s*) ν(C–O), 1094 (*s*) ν(C–S). ^1H NMR ($CDCl_3$): δ 7.54 – 7.42 [*m*, br, 15H, Ph_3P], 6.97 [*dt*, 2H, *m*-aryl-H, J = 8.60 Hz, J = 2.46 Hz], 6.75 [*dt*, 2H, *o*-aryl-H, J = 8.56 Hz, J = 2.45 Hz], 5.26 [*sept*, 1H, OCH, J = 6.20 Hz], 1.32 [*d*, 6H, CH_3, J = 6.20 Hz] ppm. $^{13}C\{^1H\}$ NMR ($CDCl_3$): δ 163.8 [C_q], 150.0 [aryl, C_{ipso}], 134.2 [*d*, *m*-Ph_3P, $^3J_{CP}$ = 13.81 Hz], 131.7 [*d*, *p*-Ph_3P, $^4J_{CP}$ = 2.34 Hz], 129.4 [*d*, *i*-Ph_3P, $^1J_{CP}$ = 57.25 Hz], 129.1 [*d*, *o*-Ph_3P, $^2J_{CP}$ = 11.50 Hz], 128.8 [aryl, C_{meta}], 127.3 [aryl, C_{para}], 123.4 [aryl, C_{ortho}], 70.6 [OCH], 22.1 [CH_3] ppm. $^{31}P\{^1H\}$ NMR ($CDCl_3$): δ 38.1 ppm.

$Ph_3PAu\{SC(iPr)=NC_6H_4NO_2\text{-}p\}$ (8)

Yellowish crystal. Yield: 0.314 g (90 %). mp 166.0 – 167.5 °C. *Anal*. Calc. for $C_{28}H_{26}AuN_2O_3PS$: C, 48.15; H, 3.75; N, 4.01. Found: C, 47.78; H, 3.47; N, 3.76 %. IR (cm^{-1}): 1435 (*s*) ν(C=N), 1149 (*s*) ν(C–O), 1097 (*s*) ν(C–S). ^1H NMR ($CDCl_3$): δ 7.93 [*dt*, 2H, *m*-aryl-H, J = 8.92 Hz, J = 2.42 Hz], 7.56 – 7.39 [*m*, br, 15H, Ph_3P], 6.89 [*dt*, 2H, *o*-aryl-H, J = 8.92 Hz, J = 2.42 Hz], 5.25 [*sept*, 1H, OCH, J = 6.20 Hz], 1.33 [*d*, 6H, CH_3, J = 6.20 Hz] ppm. $^{13}C\{^1H\}$ NMR ($CDCl_3$): δ 164.7 [C_q], 157.6 [aryl, C_{ipso}], 142.6 [aryl, C_{para}], 134.1 [*d*, *m*-Ph_3P, $^3J_{CP}$ = 13.79 Hz], 131.8 [*d*, *p*-Ph_3P, $^4J_{CP}$ = 2.36 Hz], 129.2 [*d*, *o*-Ph_3P, $^2J_{CP}$ = 11.55 Hz], 129.1 [*d*, *i*-Ph_3P, $^1J_{CP}$ = 57.52 Hz], 124.9 [aryl, C_{meta}], 122.5 [aryl, C_{ortho}], 71.5 [OCH], 22.0 [CH_3] ppm. $^{31}P\{^1H\}$ NMR ($CDCl_3$): δ 37.9 ppm.

DPPFeAu$_2${SC(OR)=NC$_6$H$_4$X-4}$_2$ for R = Me, Et and *i*Pr, X = H, CH$_3$, Cl and NO$_2$ were prepared in a similar manner as mono-functional analogues and the preparation of DPPFeAu$_2${SC(OMe)=NC$_6$H$_5$}$_2$ is described as a representative example.

NaOH (0.50 mmol) in water (5 mL) was added to a suspension of DPPFeAu$_2$Cl$_2$ (0.25 mmol) in acetonitrile (20 mL), followed by addition of MeOC(=S)N(H)C$_6$H$_5$ (0.50 mmol) in 20 mL acetonitrile and the resulting mixture was stirred for 3 h at 50 °C. The solution mixture was extracted with chloroform and left for slow evaporation at room temperature.

DPPFeAu$_2${SC(O*i*Pr)=NC$_6$H$_5$}$_2$ (9)

Orange crystal. Yield: 0.231 g (69 %). mp 209.0 – 210.0 °C. *Anal*. Calc. for C$_{54}$H$_{52}$Au$_2$FeN$_2$O$_2$P$_2$S$_2$: C, 48.52; H, 3.92; N, 2.10. Found: C, 48.49; H, 3.59; N, 2.06 %. IR (cm^{-1}): 1435 (*s*) ν(C=N), 1139 (*s*) ν(C–O), 1086 (*s*) ν(C–S). ^{1}H NMR (CDCl$_3$): δ 7.48 – 7.39 [*m*, br, 20H, Ph$_3$P], 7.11 [*t*, 4H, *m*-aryl-H, J = 7.68 Hz], 6.85 [*d*, 4H, *o*-aryl-H, J = 7.60 Hz], 6.79 [*t*, 4H, *p*-aryl-H, J = 7.34 Hz], 5.33 [*sept*, 2H, OCH, J = 6.16 Hz], 4.65 [*s*, br, 4H$_a$, PC$_5$H$_4$], 4.19 [*s*, br, 4H$_b$, PC$_5$H$_4$], 1.35 [*d*, 12H, CH$_3$, J = 6.16 Hz] ppm. ^{13}C{^{1}H} NMR (CDCl$_3$): δ 162.9 [C$_q$], 151.2 [aryl, C$_{ipso}$], 133.6 [*d*, *m*-PC$_6$H$_5$, ^{3}J$_{CP}$ = 14.00 Hz], 131.6 [*d*, *p*-PC$_6$H$_5$, ^{4}J$_{CP}$ = 2.18 Hz], 130.9 [*d*, *i*-PC$_6$H$_5$, ^{1}J$_{CP}$ = 58.31 Hz], 128.9 [*d*, *o*-PC$_6$H$_5$, ^{2}J$_{CP}$ = 11.51 Hz], 128.8 [aryl, C$_{meta}$], 122.4 [aryl, C$_{para}$], 121.8 [aryl, C$_{ortho}$], 75.2 [*d*, *o*-PC$_5$H$_4$, ^{2}J$_{CP}$ = 8.27 Hz], 74.7 [*d*, *m*-PC$_5$H$_4$, ^{3}J$_{CP}$ = 13.33 Hz], 71.7 [*d*, *i*-PC$_5$H$_4$, ^{1}J$_{CP}$ = 65.54 Hz], 70.4 [OCH], 22.2 [CH$_3$] ppm. ^{31}P{^{1}H}NMR (CDCl$_3$): δ 32.7 ppm.

DPPFeAu$_2${SC(O*i*Pr)=NC$_6$H$_4$Me-4}$_2$ (10)

Orange crystal. Yield: 0.283 g (83 %). mp 192.0 – 193.0 °C. *Anal*. Calc. for C$_{56}$H$_{56}$Au$_2$FeN$_2$O$_2$P$_2$S$_2$: C, 49.28; H, 4.14; N, 2.05. Found: C, 48.90; H, 4.05; N, 1.88 %. IR (cm^{-1}): 1435 (*s*) ν(C=N), 1137 (*s*) ν(C–O), 1092 (*s*) ν(C–S). ^{1}H NMR (CDCl$_3$): δ 7.49

– 7.41 [*m*, br, 20H, Ph_3P], 6.91 [*d*, 4H, *m*-aryl-H, J = 7.80 Hz], 6.75 [*d*, 4H, *o*-aryl-H, J = 7.88 Hz], 5.32 [*sept*, 2H, OCH, J = 6.14 Hz], 4.66 [*s*, br, $4H_a$, PC_5H_4], 4.16 [*s*, br, $4H_b$, PC_5H_4], 2.13 [*s*, 6H, aryl-CH_3], 1.34 [*d*, 12H, CH_3, J = 6.12 Hz] ppm. $^{13}C\{^1H\}$ NMR ($CDCl_3$): δ 162.7 [C_q], 148.7 [aryl, C_{ipso}], 133.6 [*d*, *m*-PC_6H_5, $^3J_{CP}$ = 14.04 Hz], 131.6 [*d*, *p*-PC_6H_5, $^4J_{CP}$ = 2.20 Hz], 131.4 [aryl, C_{para}], 131.0 (*d*, *i*-PC_6H_5, J_{CP} = 58.33 Hz), 129.5 [aryl, C_{meta}], 128.9 (*d*, *o*-PC_6H_5, $^2J_{CP}$ = 11.49 Hz), 121.6 [aryl, C_{ortho}], 75.2 [*d*, *o*-PC_5H_4, $^2J_{CP}$ = 8.38 Hz], 74.6 [*d*, *m*-PC_5H_4, $^3J_{CP}$ = 13.19 Hz], 71.7 [*d*, *i*-PC_5H_4, $^1J_{CP}$ = 65.65 Hz], 70.2 [OCH], 22.2 [CH_3], 20.9 [aryl-CH_3] ppm. $^{31}P\{^1H\}$NMR ($CDCl_3$): δ 32.5 ppm.

$DPPFeAu_2\{SC(OiPr)=NC_6H_4Cl\text{-}4\}_2$ (11)

Orange crystal. Yield: 0.278 g (79 %). mp 200.0 – 201.0 °C. *Anal*. Calc. for $C_{54}H_{50}Au_2Cl_2FeN_2O_2P_2S_2$: C, 46.14; H, 3.59; N, 1.99. Found: C, 46.03; H, 3.28; N, 1.86 %. IR (cm^{-1}): 1435 (*s*) ν(C=N), 1140 (*s*) ν(C–O), 1091 (*s*) ν(C–S). ^1H NMR ($CDCl_3$): δ 7.50 – 7.40 [*m*, br, 20H, Ph_3P], 7.07 [*d*, 4H, *m*-aryl-H, J = 8.52 Hz], 6.79 [*d*, 4H, *o*-aryl-H, J = 8.48 Hz], 5.29 [*sept*, 2H, OCH, J = 6.17 Hz], 4.64 [*s*, br, $4H_a$, PC_5H_4], 4.21 [*s*, br, $4H_a$, PC_5H_4], 1.33 [*d*, 12H, CH_3, J = 6.20 Hz] ppm. $^{13}C\{^1H\}$ NMR ($CDCl_3$): δ 163.6 [C_q], 149.8 [aryl, C_{ipso}], 133.6 [*d*, *m*-PC_6H_5, $^3J_{CP}$ = 14.02 Hz], 131.7 [*d*, *p*-PC_6H_5, $^4J_{CP}$ = 2.25 Hz], 130.8 [*d*, *i*-PC_6H_5, $^1J_{CP}$ = 58.57 Hz], 129.0 [*d*, *o*-PC_6H_5, $^2J_{CP}$ = 11.52 Hz], 128.7 [aryl, C_{meta}], 127.4 [aryl, C_{para}], 123.3 [aryl, C_{ortho}], 75.0 [*d*, *o*-PC_5H_4, $^2J_{CP}$ = 8.46 Hz], 74.8 [*d*, *m*-PC_5H_4, $^3J_{CP}$ = 13.15 Hz], 71.8 [*d*, *i*-PC_5H_4, $^1J_{CP}$ = 65.48 Hz], 70.6 [OCH], 22.2 [CH_3] ppm. $^{31}P\{^1H\}$NMR ($CDCl_3$): δ 32.6 ppm.

$DPPFeAu_2\{SC(OiPr)=NC_6H_4NO_2\text{-}4\}_2$ (12)

Orange crystal. Yield: 0.267 g (75 %). mp 190.0 – 191.5 °C. *Anal*. Calc. for $C_{54}H_{50}Au_2FeN_4O_6P_2S_2$: C, 45.46; H, 3.53; N, 3.93. Found: C, 45.68; H, 3.50; N, 3.88 %. IR (cm^{-1}): 1435 (*s*) ν(C=N), 1162 (*s*) ν(C–O), 1101 (*s*) ν(C–S). ^1H NMR ($CDCl_3$): δ 8.02 [*d*, 4H, *m*-aryl-H, J = 8.92 Hz], 7.53 – 7.41 [*m*, br, 20H, Ph_3P], 6.91 [*d*, 4H, *o*-aryl-H, J =

8.88 Hz], 5.26 [*sept*, 2H, OCH, J = 6.17 Hz], 4.60 [*s*, br, $4H_a$, PC_5H_4], 4.28 [*s*, br, $4H_b$, PC_5H_4], 1.32 [*d*, 12H, CH_3, J = 6.20 Hz] ppm. $^{13}C\{^1H\}$ NMR ($CDCl_3$): δ 164.5 [C_q], 157.5 [aryl, C_{ipso}], 142.7 [aryl, C_{para}], 133.5 [*d*, *m*-PC_6H_5, $^3J_{CP}$ = 14.04 Hz], 131.8 [*s*, br, *p*-PC_6H_5], 130.5 [*d*, *i*-PC_6H_5, $^1J_{CP}$ = 58.73 Hz], 129.1 [*d*, *o*-PC_6H_5, $^2J_{CP}$ = 11.59 Hz], 124.8 [aryl, C_{meta}], 122.5 [aryl, C_{ortho}], 75.1 [*d*, *m*-PC_5H_4, $^3J_{CP}$ = 13.0 Hz], 74.6 [*d*, *o*-PC_5H_4, $^2J_{CP}$ = 8.21 Hz], 72.0 [*d*, *i*-PC_5H_4, $^1J_{CP}$ = 65.87 Hz], 71.4 [OCH], 22.2 [CH_3] ppm. $^{31}P\{^1H\}$NMR ($CDCl_3$): δ 32.1 ppm.

The methods employed for the preparation of $(R_3PAu)_2L$ with R = Et, Ph and Cy, L = 1,4-$[MeOC(=S)N(H)]_2C_6H_4$ were similar, so that the preparation of the Et_3P derivative is described in detail as a representative example.

NaOH (0.50 mmol) in water (5 ml) was added to a suspension of Et_3PAuCl (0.50 mmol) in acetonitrile (20 ml) followed by addition of 1,4-$[MeOC(=S)N(H)]_2C_6H_4$ (0.25 mmol) in acetonitrile (20 ml). The resulting mixture was stirred for 3 h at 50 °C. Extraction followed with dichloromethane (100 mL) and an equivalent volume of acetonitrile added. The solution was left for slow evaporation at room temperature.

$(Et_3PAu)_2L$ (13)

Colourless crystals. Yield: 0.206 g (93 %). mp 174.0-176.0 °C. *Anal*. Calc. for $C_{22}H_{40}Au_2N_2O_2P_2S_2$: C, 29.87; H, 4.56; N, 3.17. Found: C, 29.92; H, 4.53; N, 3.04 %. IR (cm^{-1}): 1421 (*m*) ν(C=N), 1123 (*vs*) ν(C–O), 1094 (*s*) ν(C–S). ^1H NMR ($CDCl_3$): δ 6.72 [*s*, 4H, aryl-H], 3.81 [*s*, 6H, OCH_3], 1.70 [*dq*, 12H, CH_2P, J = 7.70 Hz, J = 9.82 Hz], 1.06 [*dt*, 18H, $C\underline{H}_3CH_2P$, J = 7.62 Hz, J = 18.32 Hz] ppm. $^{13}C\{^1H\}$ NMR ($CDCl_3$): δ 165.3 [C_q], 145.7 [aryl, C_{ipso}], 122.8 [aryl, C_{ortho}], 55.2 [OCH_3], 17.6 [*d*, CH_2P $^1J_{CP}$ = 33.3 Hz], 8.8 [*s*, $\underline{C}H_3CH_2P$] ppm. $^{31}P\{^1H\}$ NMR ($CDCl_3$): δ 35.6 ppm.

$(Ph_3PAu)_2L$ (14)

Colourless crystals. Yield: 0.255 g (87 %). mp 181.5-183.0 °C. *Anal*. Calc. for $C_{46}H_{40}Au_2N_2O_2P_2S_2$: C, 47.11; H, 3.44; N, 2.39. Found: C, 47.25; H, 3.31; N, 2.41 %. IR (cm^{-1}): 1434 (*s*) ν(C=N), 1143 (*s*) ν(C–O), 1101 (*s*) ν(C–S). ^{1}H NMR ($CDCl_3$): δ 7.49–7.41 [*m*, 30 H, Ph_3P], 6.41 [*s*, 4H, aryl-H], 3.73 [*s*, 6H, OCH_3] ppm. $^{13}C\{^1H\}$ NMR ($CDCl_3$): δ 163.2 [C_q], 145.7 [aryl, C_{ipso}], 134.4 [*d*, *o*-Ph_3P, $^3J_{CP}$ = 13.9 Hz], 131.4 [*d*, *p*-Ph_3P, $^5J_{CP}$ = 2.2 Hz], 129.6 [*d*, *i*-Ph_3P, J_{CP} = 57.04 Hz], 128.9 [*d*, *m*-Ph_3P, $^4J_{CP}$ = 11.47 Hz], 122.4 [aryl, C_{ortho}], 55.0 [OCH_3] ppm. $^{31}P\{^1H\}$NMR ($CDCl_3$): δ 38.1 ppm.

$(Cy_3PAu)_2L$ (15)

Colourless crystals. Yield: 0.275 g (91 %). mp 180.0-181.0 °C. *Anal*. Calc. for $C_{46}H_{76}Au_2N_2O_2P_2S_2$: C, 45.69; H, 6.34; N, 2.32. Found: C, 45.57; H, 6.40; N, 2.24 %. IR (cm^{-1}): 1444 (*s*) ν(C=N), 1130 (*s*) ν(C–O), 1093 (*m*) ν(C–S). ^{1}H NMR ($CDCl_3$): δ 6.84 [*s*, 4H, aryl-H], 3.82 [*s*, 6H, OCH_3], 1.98–1.20 [*m*, 66 H, Cy_3P] ppm. $^{13}C\{^1H\}$ NMR ($CDCl_3$): δ 163.9 [C_q], 145.4 [aryl, C_{ipso}], 122.4 [aryl, C_{ortho}], 54.8 [OCH_3], 33.3 [*d*, *i*-Cy_3P, J_{CP} = 27.8 Hz], 30.7 [*s*, *m*-Cy_3P], 27.0 [*d*, *o*-Cy_3P, $^3J_{CP}$ = 11.9 Hz], 25.9 [*s*, *p*-Cy_3P] ppm. $^{31}P\{^1H\}$NMR ($CDCl_3$): δ 56.5 ppm.

2.2.3 Copper(I) Compounds

Preparation of $(Ph_3P)_2CuCl\{ROC(=S)N(H)C_6H_5\}$ with R = Me, Et and *i*Pr are similar so that preparation of $(Ph_3P)_2CuCl\{MeOC(=S)N(H)C_6H_5\}$ is described in detail as a representative example.

CuCl (2.5 mmol) in acetonitrile (25 mL) was added equivalent molar of MeOC(=S)NHPh (2.5 mmol) in acetonitrile (25 mL), followed by addition of two mole equivalent triphenylphosphine (5.0 mmol) in acetonitrile (25 mL). The resulting mixture was stirred for 3 h at 50°C, giving white suspension. Equivolume (75 mL) of

dichloromethane was added to the suspension and the clear solution was left for slow evaporation at room temperature.

$(Ph_3P)_2CuCl\{MeOC(=S)N(H)C_6H_5\}$ (16)

Colourless crystals. Yield: 1.898 g (96 %). mp 160 – 161 °C. *Anal.* Calc. for $C_{44}H_{39}ClCuNOP_2S$: C, 66.83; H, 4.97; N, 1.77. Found: C, 66.92; H, 4.81; N, 1.77 %. IR (cm^{-1}): 3052 (*w*) ν(N-H), 1434(*s*) ν(C-N), 1219(*s*) ν(C=S), 1094(*s*) ν(C–O). ^1H NMR ($CDCl_3$): δ 11.86 [*s*, br, 1H, NH], 7.45 – 7.16 [*m*, br, 35H, Ph_3P, *o*-aryl-H, *m*-aryl-H], 7.12 [*t*, 1H, *p*-aryl-H, J = 7.40 Hz], 3.96 [*s*, 3H, OCH_3] ppm. $^{13}C\{^1H\}$ NMR ($CDCl_3$): δ 186.7 [C_q], 137.5 [aryl, C_{ipso}], 133.9 [*d*, *m*-PC_6H_5, J_{CP} = 14.66 Hz], 133.9 [*d*, *i*-PC_6H_5, J_{CP} = 24.85 Hz], 129.4 [s, *p*-PC_6H_5], 128.7 [aryl, C_{ortho}], 128.4 [*d*, *o*-PC_6H_5, J_{CP} = 8.96 Hz], 125.1 [aryl, C_{para}], 121.9 [aryl, C_{meta}], 58.2 [OCH_3] ppm. $^{31}P\{^1H\}$NMR ($CDCl_3$): δ -4.0 ppm.

$(Ph_3P)_2CuCl\{EtOC(=S)N(H)C_6H_5\}$ (17)

Colourless crystals. Yield: 1.891 g (94 %). mp 163 – 166 °C. *Anal.* Calc. for $C_{45}H_{41}ClCuNOP_2S$: C, 67.16; H, 5.14; N, 1.74. Found: C, 67.51; H, 5.01; N, 1.77 %. IR (cm^{-1}): 3054 (*w*) ν(N-H), 1433(*s*) ν(C-N), 1225(*s*) ν(C=S), 1093(*s*) ν(C–O). ^1H NMR ($CDCl_3$): δ 11.81 [*s*, br, 1H, NH], 7.48 [*d*, 2H, *o*-aryl-H, J = 7.88 Hz], 7.42 – 7.16 [*m*, br, 32H, Ph_3P, *m*-aryl-H], 7.11 [*t*, 1H, *p*-aryl-H, J = 7.38 Hz], 4.45 [*q*, 2H, OCH_2, J = 7.08 Hz], 1.29 [*t*, 3H, CH_3, J = 7.08 Hz] ppm. $^{13}C\{^1H\}$ NMR ($CDCl_3$): δ 185.7 [C_q], 137.7 [aryl, C_{ipso}], 133.9 [*d*, *m*-PC_6H_5, J_{CP} = 14.76 Hz], 133.9 [*d*, *i*-PC_6H_5, J_{CP} = 23.82 Hz], 129.3 [s, *p*-PC_6H_5], 128.7 [aryl, C_{ortho}], 128.3 [*d*, *o*-PC_6H_5, J_{CP} = 8.69 Hz], 124.9 [aryl, C_{para}], 121.8 [aryl, C_{meta}], 68.1 [OCH_2], 14.1 [CH_3] ppm. $^{31}P\{^1H\}$NMR ($CDCl_3$): δ -4.1 ppm.

$(Ph_3P)_2CuCl\{iPrOC(=S)N(H)C_6H_5\}$ (18)

Colourless crystals. Yield: 1.904 g (93 %). mp 169 – 173 °C. *Anal.* Calc. for $C_{45}H_{43}ClCuNOP_2S$: C, 67.48; H, 5.29; N, 1.71. Found: C, 67.79; H, 4.91; N, 1.84 %. IR (cm^{-1}): 3048 (*w*) ν(N-H), 1433(*s*) ν(C-N), 1225(*s*) ν(C=S), 1093(*s*) ν(C–O). ^1H NMR ($CDCl_3$): δ 11.86 [*s*, br, 1H, NH], 7.50 [*d*, 2H, *o*-aryl-H, J = 7.88 Hz], 7.41 – 7.15 [*m*, br, 32H, Ph_3P, *m*-aryl-H], 7.11 [*t*, 1H, *p*-aryl-H, J = 7.34 Hz], 5.46 [*sept*, 1H, OCH_3, J = 6.13 Hz], 1.24 [*d*, 6H, CH_3, J = 6.16 Hz] ppm. $^{13}C\{^1H\}$ NMR ($CDCl_3$): δ 184.8 [C_q], 137.8 [aryl, C_{ipso}], 133.9 [*d*, *m*-PC_6H_5, J_{CP} = 14.82 Hz], 133.9 [*d*, *i*-PC_6H_5, J_{CP} = 23.83 Hz], 129.3 [s, *p*-PC_6H_5], 128.7 [aryl, C_{ortho}], 128.3 [*d*, *o*-PC_6H_5, J_{CP} = 8.89 Hz], 124.8 [aryl, C_{para}], 121.8 [aryl, C_{meta}], 76.3 [OCH], 21.7 [CH_3] ppm. $^{31}P\{^1H\}$NMR ($CDCl_3$): δ -4.3 ppm.

2.3 Instrumentations

Elemental analyses were performed on a Perkin Elmer PE 2400 CHN Elemental Analyser. Melting points were determined on a Krüss KSP1N melting point meter. ^1H and $^{13}C\{^1H\}$ NMR spectra were recorded in respective deuterated solutions on a Bruker Avance 400 MHz NMR spectrometer with chemical shifts relative to tetramethylsilane. $^{31}P\{^1H\}$ NMR spectra were recorded in respective deuterated solution on the same instrument but with the chemical shifts recorded relative to 85% aqueous H_3PO_4 as the external reference; abbreviations for NMR assignments: *s*, singlet; *d*, doublet; *t*, triplet; *q*, quartet; sept, septet; *m*, multiplet; *dd*, doublet of doublets; *dt*, doublet of triplets; *dq*, dublet of quartet; *br*, broad. IR spectra were obtained on a Perkin Elmer Spectrum 400 FT Mid-IR/Far-IR spectrophotometer from 4000 to 400 cm^{-1}; abbreviations: *w*, weak; *s*, strong; *br*, broad. Powder X-ray diffraction (PXRD) data were recorded with a PANalytical Empyrean XRD system with Cu-Kα1 radiation (λ = 1.54056 Å) in the 2θ range 5 to 40°. The comparison between experimental and calculated (from CIF's) PXRD patterns were

performed with X'Pert HighScore Plus. Stock aqueous solutions of $Ph_3PAu\{SC(OR)=NC_6H_4X\text{-}4\}_2$, $DPPFeAu_2\{SC(O\textit{i}Pr)=NC_6H_4X\text{-}4\}_2$ and $(Ph_3P)_2CuCl\{ROC(=S)N(H)C_6H_5\}$ (1×10^{-3} M) and ligand $ROC(=S)N(H)C_6H_4X\text{-}4$ (1×10^{-2} M) for R = Me, Et and *i*Pr, X = H, CH_3, Cl and NO_2 were prepared in respective solvent system for photoluminescent study. The stock solutions were further diluted to concentration of 1×10^{-5} M and 1×10^{-4} M for metal(I) complexes and ligands respectively using the same solvent system for optical measurement. The optical absorption spectra were measured in the range 190-1100 nm on a single-beam Agilent Cary 60 UV-Vis spectrophotometer. Photoluminescence (PL) measurements were carried out on an Agilent Varian Cary Eclipse Fluorescence Spectrophotometer using a Xenon flash lamp as the excitation source at room temperature. Thermogravimetric analyses were performed on a Perkin Elmer TGA 4000 Thermogravimetric Analyzer in the range of 35 – 800 °C at the rate of 10 °C/min.

2.4 X-Ray Crystallography

Intensity measurements were made at 100 K on an Agilent Technologies SuperNova Dual CCD with an Atlas detector fitted with MoKα radiation (λ = 0.71073 Å) to θ_{max} = 27.5°. Data processing and absorption correction were accomplished with CrysAlis PRO (CrysAlisPro, 2010). The structures were solved by direct methods with SHELXS-97 (Sheldrick, 2008) and refinement (anisotropic displacement parameters, C-bound hydrogen atoms in the riding model approximation and a weighting scheme of the form $w = 1/[\sigma^2(F_o^2) + (aP)^2 + bP]$ for $P = (F_o^2 + 2F_c^2)/3$) was on F^2 by means of SHELXL-97 (Sheldrick, 2008). The molecular structure diagrams were drawn with ORTEP-3 for Windows (Farrugia, 2012) at the 70% probability level, the overlap diagram was drawn with QMol (Gans *et al.*, 2001) and the remaining crystallographic figures were drawn

with DIAMOND (Brandenburg, 2006) using arbitrary spheres. Data manipulation and interpretation were with WinGX (Farrugia, 2012) and PLATON (Spek, 2003).

2.5 NMR Relaxation Measurements

For the relaxation experiments, a solution of the compound (20 mg) was prepared in $CDCl_3$ (4.5 cm) in a 5 mm NMR tube (Wilmad). The solution was degassed through five freeze-pump-thaw cycles and sealed under vacuum. The NMR measurements were carried out on a JEOL ECX500 NMR spectrometer. The ^{13}C spin–lattice relaxation time (T_1) was obtained by using the two-pulse inversion–recovery (IR) method (Harris, 1986; Nelson, 2003). Initially, an approximate T_1 value was obtained before a more precise measurement was made using 10 IR intervals in a range up to $1.5T_1$. Subsequently, a final measurement was made to confirm the value T_1 = 0.69 s at 20 ºC. Then, the NOE measurements were made in two consecutive experiments: one with complete proton decoupling with relaxation delay of 6.0 s and acquisition time of 1.04 s, and the other experiment with gated-decoupling in which the NOE was suppressed with the other conditions the same as in the first experiment. The pulse angle was 90º. Good signal intensity was obtained with 1024 scans. The total integrated intensity of the signal was obtained with the spectrometer's data processing software. The ratio of the signal intensities in the two experiments gives the NOE value, usually given as NOE = 1 + η, where η is the NOE enhancement factor.

CHAPTER 3:RESULTS AND DISCUSSION

3.1 Triphenylphosphinegold(I) Thiocarbamides: Biological Activity Against HT-29 Colon Cancer Cells

3.1.1 Synthesis and Spectroscopic Characterisation

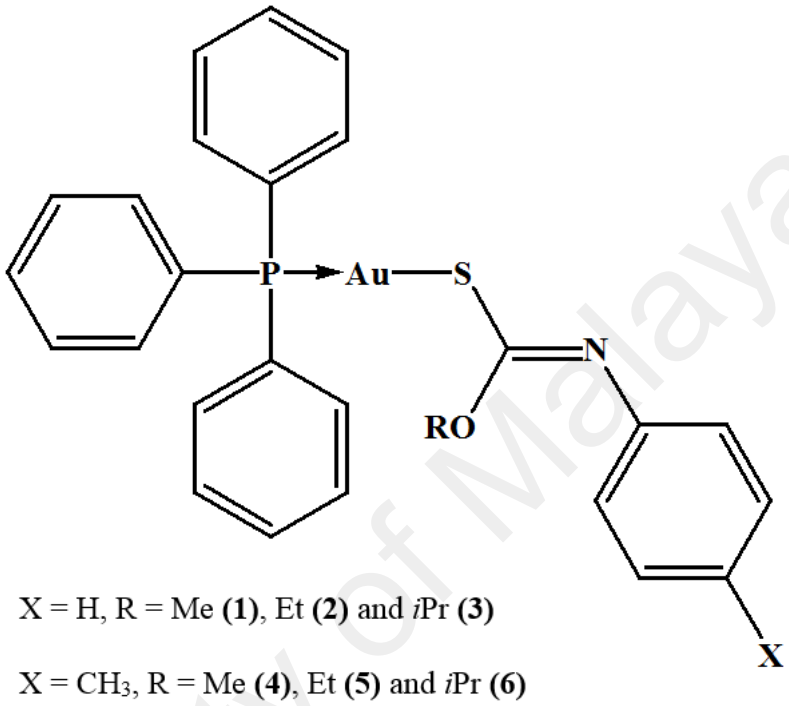

X = H, R = Me **(1)**, Et **(2)** and *i*Pr **(3)**

X = CH_3, R = Me **(4)**, Et **(5)** and *i*Pr **(6)**

Figure 3.1: Chemical Structures of $Ph_3PAu\{SC(OR)=NC_6H_4X\text{-}4\}$ with R = Me, Et and *i*Pr, X = H, CH_3.

A series of six mononuclear triphenylphosphinegold(I) thiocarbamides, $Ph_3PAu\{SC(OR)=NC_6H_4X\text{-}4\}$ with X = H, CH_3, R = Me, Et and *i*Pr was prepared to assess their anti-cancer properties against HT-29 colon cancer cells. The compounds were prepared from the metathetical reaction between Ph_3PAuCl and thiocarbamides, $ROC(=S)NHC_6H_4X\text{-}4$ with X = H, CH_3, R = Me, Et and *i*Pr in the presence of NaOH. They are air-, light- and moisture-stable and present as colourless crystalline solids, with good solubility in chlorinated organic solvents, *e.g.* chloroform and dichloromethane, partially soluble in acetonitrile and dimethylsulfoxide, sparingly soluble in alcohols and acetone, and insoluble in water. Compounds **1** – **6** were characterised using infrared

spectroscopy, multi-nuclear (^{1}H, $^{13}C\{^{1}H\}$ and $^{31}P\{^{1}H\}$) NMR and ultraviolet-visible (UV/Vis) spectroscopy.

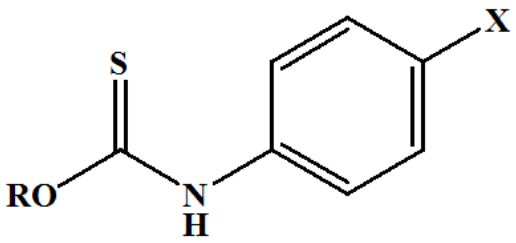

X = H, R = Me **(L1)**, Et **(L2)** and *i*Pr **(L3)**

X = CH_3, R = Me **(L4)**, Et **(L5)** and *i*Pr **(L6)**

Figure 3.2: Chemical Structures of thiocarbamides, $ROC(=S)NHC_6H_4X$-4 with R = Me, Et and *i*Pr, X = H, CH_3.

Each of the infrared spectrum of thiocarbamides displayed characteristic absorption bands at *ca.* 3200 cm^{-1}, 1450 cm^{-1}, 1200 cm^{-1} and 1050 cm^{-1} correspond to ν(N-H), ν(C–N), ν(C=S) and ν(C–O) respectively. Absence of ν(N-H) and reduction of C=S double bond character as indicated by the red shift of *ca.* 100 cm^{-1} to lower wavenumber in infrared spectra of **1** – **6** provide evidence that thiocarbamides functioned as thiolate ligands upon successful complexation.

Similarly, the presence of resonance attributed to N-H in thiocarbamides was observed at *a.* δ 8.7 ppm in their ^{1}H NMR spectra. This N-H resonance appeared as a broad resonance due to the rapid intermolecular proton exchange involving the N-H group (Ho *et al.*, 2005). The benzene ring of parent thiocarbamides **L1** – **L3** clearly resolved into three groups of protons; the triplets at *ca.* δ 7.33 and 7.17 ppm, respectively correspond to *meta* and *para* aromatic protons. The doublet resonance of *ortho* protons was poorly identified as it was overlapped with $CDCl_3$ solvent resonance at δ 7.26 ppm. In contrast, benzene ring of **L4** – **L6** which has $–CH_3$, a moderate electron donating group,

attached to the *para* position gave rise to a broad singlet resonance around δ 7.13 ppm as the aromatic protons are having nearly identical chemical shift despite the protons are not quite chemically equivalent. Each of **L1** – **L6** exhibited resonance around δ 4.10 – 5.70 ppm region due to the O-bound alkyl groups, i.e. –OC$\underline{H}_3$, –OC$\underline{H}_2CH_3$ and –OC$\underline{H}(CH_3)_2$, while more shielded alkyl protons appeared at the higher field region at *ca.* δ 1.40 ppm for –$OCH_2C\underline{H}_3$ and –$OCH(C\underline{H}_3)_2$. Another resonance occurred at ca δ 2.30 ppm in the spectra of **L4** – **L6** arisen from aryl-CH_3.

Complexation of thiocarbamides as thiolate anions exhibited similar characteristic resonances as in the ^{1}H spectra of compounds **1** – **6**, except the observed disappearance of N-H resonance due to the deprotonation of thiocarbamides. Overall, the resonances of thiolate anions experienced slight shifting to lower chemical shifts as a consequence of more shielded chemical environments upon coordination. Protons of triphenylphosphine for compounds **1** – **6** occurred in the range of *ca.* δ 7.40 – 7.50 ppm as a multiplet.

$^{13}C\{^1H\}$ spectra of thiocarbamides **L1** – **L6** and compounds **1** – **6** revealed the expected resonances. Compared to that of **L1** – **L6**, systematic shifts to lower, higher and lower chemical shifts are observed for resonances due to C_q, C_{ipso} and C_{para} in $^{13}C\{^1H\}$ spectra of compounds **1** – **6**, consistent with the mode of complexation of the thiolate anions. Notable the resonances correspond to benzene ring of triphenylphosphine split into doublets due to the heteronuclear coupling effect of P atom, with J-coupling values of *ca.* 56.60 Hz, 11.50 Hz, 13.80 Hz and 2.30 Hz for $C_{ipso,}$ $C_{ortho,}$ C_{meta} and C_{para}, respectively. A single resonance was observed for each of the compounds **1** – **6** in the $^{31}P\{^1H\}$ spectra at approximate 38.0 ppm, shifted to higher chemical shift in comparison with uncoordinated PPh_3 at -5.2 ppm.

Table 3.1: Absorption data for **L1 - L6** and compounds **1** – **6** measured in acetonitrile.

Compound	λ_{abs} (nm)	ε (L $cm^{-1}mol^{-1}$)	Band Assignments
L1	274	17,800	π-π* Transition
L2	275	18,270	
L3	276	18,450	
L4	275	17,270	
L5	276	18,260	
L6	277	17,190	
1	240	22,964	LMCT (S → Au)
	267	12,378	Intraligand Transition
	275	10,586	π-π* Transition
2	240	24,918	LMCT (S → Au)
	267	12,052	Intraligand Transition
	275	10.423	π-π* Transition
3	240	26,384	LMCT (S → Au)
	267	12,378	Intraligand Transition
	275	10,423	π-π* transition
4	240	34,390	LMCT (S → Au)
	267	14,671	Intraligand Transition
	275	11,865	π-π* Transition
5	240	31,219	LMCT (S → Au)
	267	14,320	Intraligand Transition
	275	11,962	π-π* Transition
6	240	27,700	LMCT (S → Au)
	267	13,500	Intraligand Transition
	275	12,400	π-π* Transition

Absorption spectra for thiocarbamides and the respective gold(I) compounds were evaluated in acetonitrile, each exhibited characteristic bands as listed in Table 3.1. Thiocarbamides **L1** – **L6** each showed a single band at *ca.* 276 nm ascribed to carbonimidothioate ligand-centered π-π* transition (Ho *et al.*, 2006). By comparison with

the absorption data for compounds **1** – **6**, additional two bands were observed at approximate 240 nm and 267 nm respectively. The observed band at 240 nm in compounds **1** – **6** is assigned to LMCT (S → Au) (Jones *et al.*, 1995; Narayanaswamy *et al.*, 1993) whilst the band at 267 nm is resulted from the phenyl groups of triphenylphosphine moiety (Ho *et al.*, 2006).

3.1.2 Molecular Structures

The coordination of thiocarbamides to gold(I) centre as thiolate ligands is further confirmed by the crystal structure determination of the respective gold(I) compounds. Molecular structures of two independent molecules comprising the crystallographic asymmetric unit in **3** and molecular structure of **6** are illustrated in Figure 3.3 and 3.4 respectively. The gold atom is linearly coordinated by phosphine-P and sulphur-S atoms in each structure.

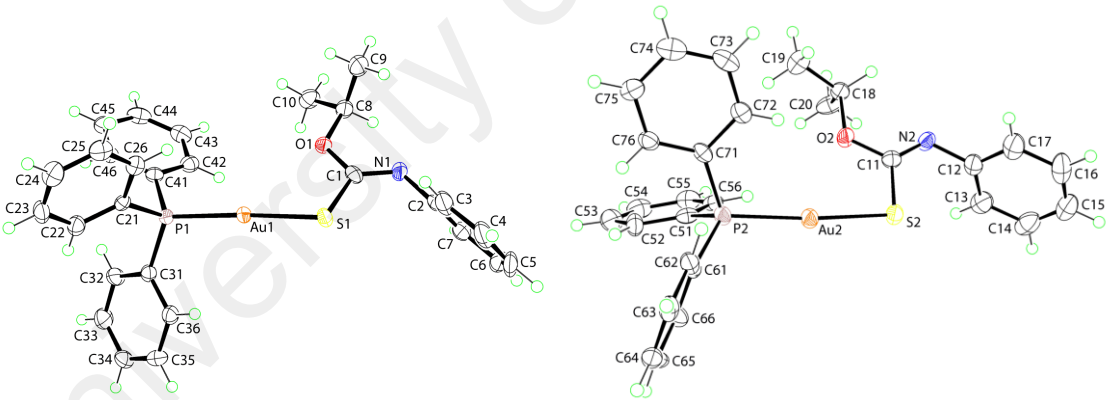

Figure 3.3: Molecular structures of the two independent molecules comprising the crystallographic asymmetric unit in $Ph_3PAu\{SC(OiPr)=NC_6H_5\}$ (**3**). Displacement ellipsoids are shown at the 50% probability level.

In comparison with crystal structures of thiocarbamides, elongation of C1 – S1 and shortening of C1 – N1 bond lengths are demonstrated, i.e. 1.7647 (53) and 1.2812 (65) for **3** respectively, as presented in Table 3.2. The above is consistent with thiocarbamides functioned as thiolate anions. Similar phenomena are observed in crystallographic data for remaining thiocarbamides and gold(I) compounds; details could be retrieved from Publication I.

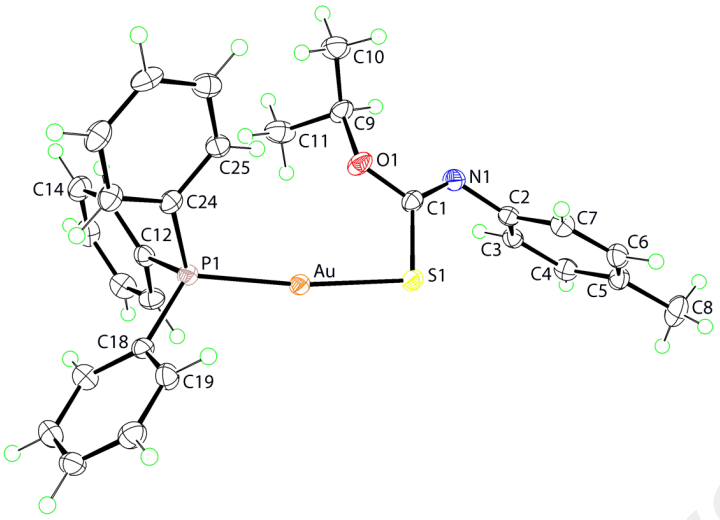

Figure 3.4: Molecular structures of $Ph_3PAu\{SC(OiPr)=NC_6H_4CH_3\text{-}p\}$ (**6**). Displacement ellipsoids are shown at the 50% probability level.

Table 3.2: Selected geometric parameters for **L3**, **L6**, compounds **3** and **6**.

Compound	**Bond (Bond Length (Å))**	
$ROC(=S)NHC_6H_5$ (**L3**)	C1 – S1 1.6748 (16)	C1 – N1 1.3341 (20)
$ROC(=S)NHC_6H_4CH_3\text{-}p$ (**L6**)	C1 – S1 1.6679 (19)	C1 – N1 1.3371 (21)
$Ph_3PAu\{SC(OiPr)=NC_6H_5\}$ (**3**)	C1 – S1 1.7647 (53)	C1 – N1 1.2812 (65)
$Ph_3PAu\{SC(OiPr)=NC_6H_4CH_3\text{-p}\}$ (**6**)	C1 – S1 1.7767 (27)	C1 – N1 1.2687 (38)

Powder X-ray diffraction (PXRD) serves as a platform to determine conformity of bulk materials to that of the crystallographic information file (CIF) obtained from single crystal X-ray crystallography (SCXRD) measurements. The powder X-ray diffraction patterns measured on bulk samples for **1** – **6**, as depicted in Figure 3.5, revealed that they are in close agreement with the patterns stimulated from CIF data.

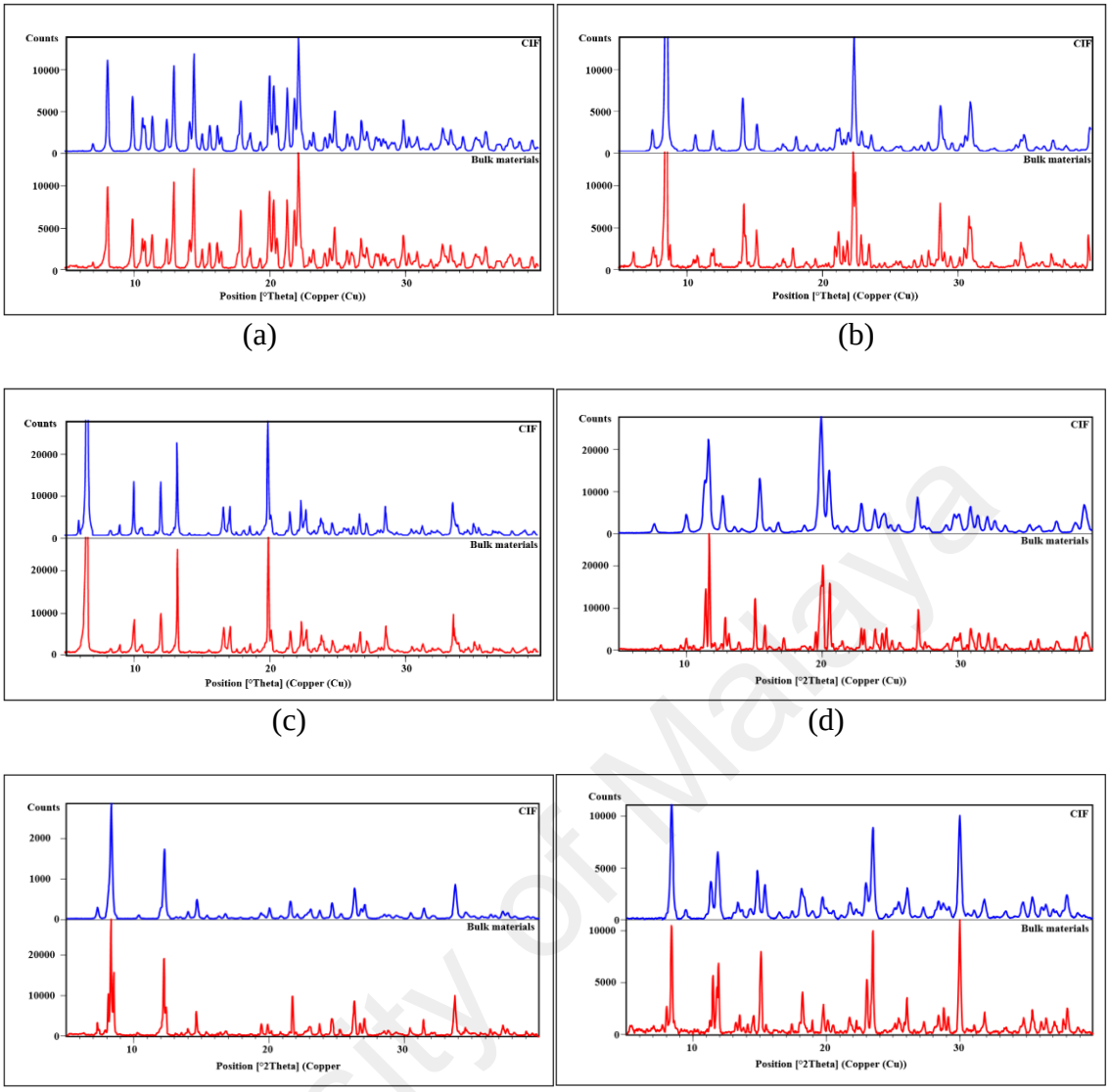

(a) (b)

(c) (d)

(e) (f)

Figure 3.5: Calculated (red trace) and measured (blue trace) PXRD pattern for compounds **1** (a), **2** (b), **3** (c), **4** (d), **5** (e) and **6** (f).

3.1.3 Biological Study

Compounds **1** – **6** were evaluated in vitro against HT-29 human colon cancer cell lines through the inhibition study of cell proliferation activity using the standard procedures as described in Publication I and II. Upon treatment for 24 h, the effects of **1** – **6** on HT-29 cells growth were presented in IC_{50} values, as tabulated in Table 3.3.

Table 3.3: Cytotoxic activities of **1** - **6** against HT-29 colon cancer cell model after 24 h treatment.

Compound	IC_{50} (μM)
1	18.1 ± 0.3
2	11.9 ± 0.4
3	14.2 ± 0.2
4	11.3 ± 0.3
5	17.0 ± 0.3
6	16.8 ± 0.2

Compound **4** demonstrated the highest potency amongst the series of six mononuclear phosphinegold(I) thiocarbamide compounds, whilst compound **1** being the least potent against HT-29 colon cancer cells. Notable that the parent compounds **1** – **3** with different O-bound alkyl group, when arranged according to their cytotoxicity, followed a sequence of **2** > **3** > **1**. Remarkably, incorporation of a methyl group to the thiocarbamides phenyl ring at *para* position however, inverted the sequence into **4** > **6** > **5**. The above suggests that increased hydrophobicity on the phenyl ring enhanced the cytotoxicity for compound with O-bound methyl group, but the inverse is true for ethyl and isopropyl derivatives.

Cell mortality generally driven by apoptotic or necrotic processes. The differences between apoptosis and necrosis include the causing factors that lead to the above; apoptosis is a programmed cell death while necrosis is a cell death triggered by extreme variance from physiological conditions. While necrosis may cause inflammation upon cell swelling and rupture, apoptosis is preferred over the former as the apoptotic bodies formed will be engulfed by white blood cells. The mode of cell death induced by **1** – **6** were assessed from the DNA fragmentation study and membrane permeability study; apoptosis was demonstrated, as discussed below.

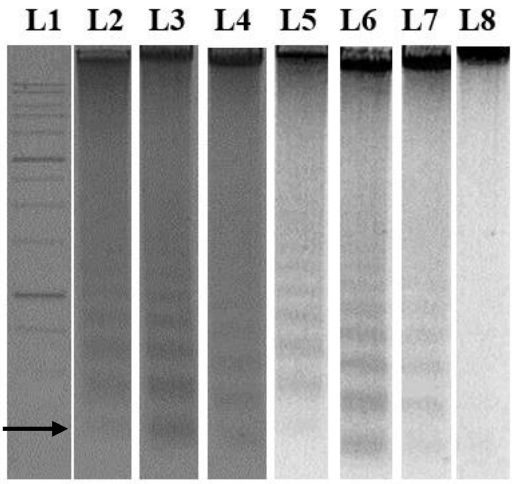

Figure 3.6: Gel images of the DNA fragmentation analysis. The HT-29 cells were cultured for 24 h in DMEM control media, in the presence of 18.1 µM of **1** (L2), 11.9 µM **2** (L3), 14.2 µM **3** (L4), 11.3 µM of **4** (L5), 17.0 µM **5** (L6) and 16.8 µM **6** (L7). DNA was extracted from the cultures and DNA fragmentation was evaluated using electrophoresis with 2% agarose gel. L1 is 1 kb DNA ladder, L8 is negative control (untreated cells). Compounds **1** – **6** showed the presence of fragmented ladders (indicated by arrow) which suggest the cell death by apoptosis.

Apoptotic DNA fragmentation is one of the fundamental characteristic of apoptosis. The confirmation of **1** – **6** induced apoptotic cell death in HT-29 colon cancer cells is as illustrated in Figure 3.6, featured with DNA ladder fragmentation. Owing to the increased sensitivity of apoptotic cells toward certain fluorescent dyes (Kapuscinski *et al.*, 1983; Ormerod *et al.*, 1992), AO/PI staining provides a promising method to evaluate the membrane integrity of HT-29 colon cancer cells after treatment with **1** – **6**. Acridine orange (AO), when in contact with intact membrane, produces a green fluorescent whilst propidium iodide (PI), gives rise to bright-red fluorescent upon its penetration to dead or dying cells that have lost the membrane integrity. As depicted in Figure 3.7, as a representative example, treatment of HT-29 colon cancer cells with compound **1** featured apoptotic cells that were stained green with multiple yellow/green dots of condensed nuclei. Necrotic cells were found present as a minor species, which were stained bright-red due to the influx of PI stain.

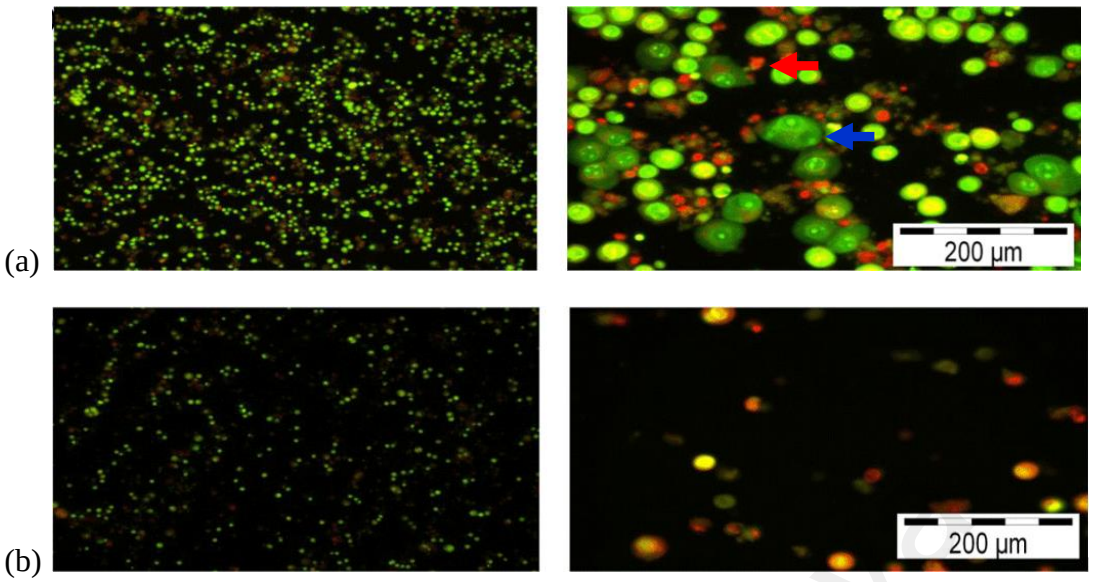

Figure 3.7: Images of AO/PI staining of HT-29 cells (a) after being treated with compound **1** at the IC_{50} dose and (b) untreated cells (negative control). The blue arrow points to an apoptotic cell with a fragmented nucleus and condensed chromatin, and the red arrow points to a necrotic cell.

In summary, compounds **1** – **6** possess significant cytotoxicity to the HT-29 colon cancer cells through the induction of apoptotic cell death, with **4** being the most active. Detailed delineation of the apoptosis pathways demonstrated by compounds **1** - **6** is presented in Publication I and II. Over and above, compounds **4** – **6** were found to exhibit specific action against a broad panel of Gram-positive bacteria (Publication III). The above suggests that compounds **4** – **6** may be potentially developed as bactericidal agents. With the promising biological activity presented, it is therefore worthwhile to explore the above and other related phosphinegold(I) thiocarbamide compounds to uncover their prospective applications for treatment of disease.

3.2 Mono- and Binuclear Phosphinegold(I) Thiocarbamides: Structural Diversity and Chemistry

3.2.1 Synthesis and Spectroscopic Characterisation

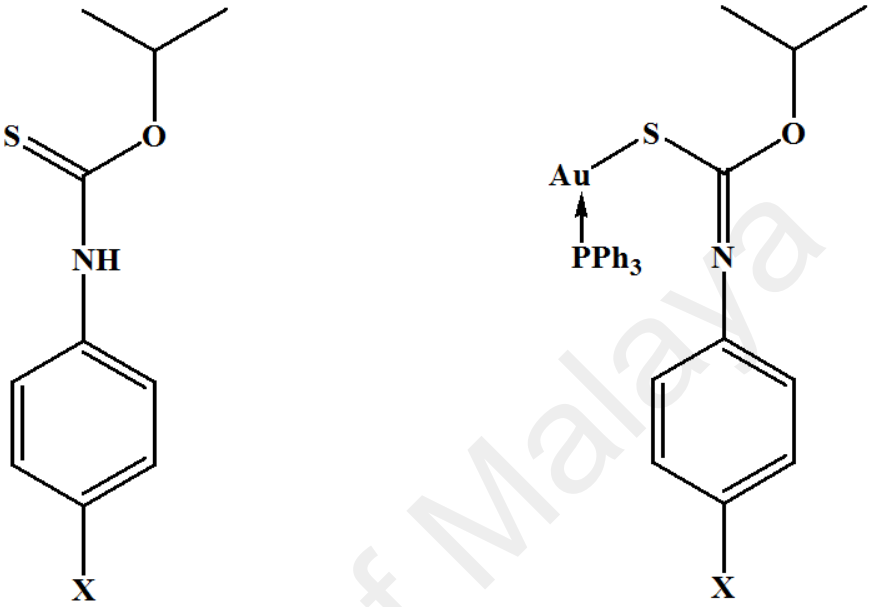

X = H **(L3)**, CH_3 **(L6)**, Cl **(L7)**, NO_2 **(L8)** X = H **(3)**, CH_3 **(6)**, Cl **(7)**, NO_2 **(8)**

Figure 3.8: Chemical structures of thiocarbamides, *i*PrOC(=S)NHC_6H_4X-4 (left) and mononuclear phosphinegold(I) thiocarbamides (right), with X = H, CH_3, Cl and NO_2

The findings of compounds **1** – **6** exhibited promising biological activity prompted the interest of current project, comprising 4 mononuclear Ph_3PAu{SC(OiPr)=NC_6H_4X-4} (Figure 3.8) and 4 binuclear phosphinegold(I) thiocarbamides, (Ph_2P-Fc-PPh_2){AuSC(OiPr)=NC_6H_4X-4}$_2$ (Figure 3.9) with X = H, CH_3 Cl and NO_2. This project serves to provide better insight on the influence exerted by variation of the P-bound and para-substituted thiolate ligands on their chemistry and biological activity. 1,1'-bis(diphenylphosphino)ferrocene was employed in this context in relation to the antitumour ability reported in literature (Bjelosevic *et al.*, 2012; Hill *et al.*, 1989; Pereira *et al.*, 2015).

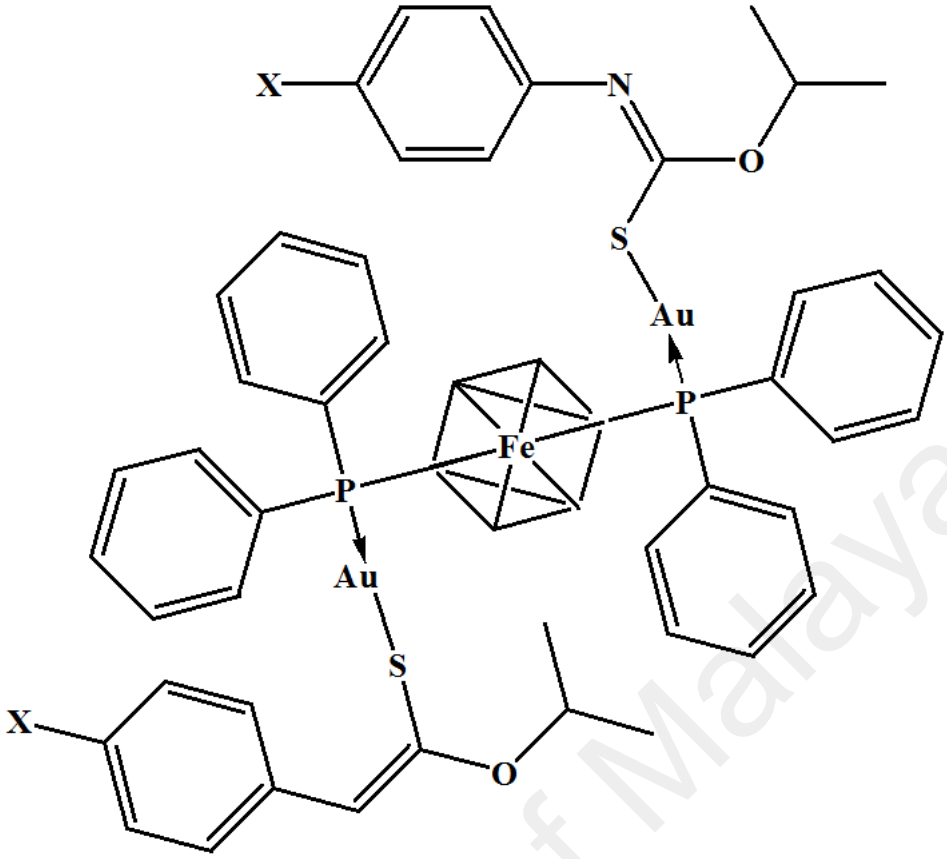

X = H **(9)**, CH_3 **(10)**, Cl **(11)**, NO_2 **(12)**

Figure 3.9: Chemical structures of binuclear phosphinegold(I) thiocarbamide, (Ph_2P-Fc-PPh_2){AuSC(O*i*Pr)=NC_6H_4X-4}$_2$ with X = H, CH_3 Cl and NO_2.

Thiocarbamides, **L3**, **L6** – **L8**, and respective gold(I) compounds were characterised using FT-IR spectroscopy; each of the IR spectrum showed the anticipated absorption bands with notable absence of ν(N-H) in the IR spectra of the gold(I) compounds, as detailed in section 2.2.1 and 2.2.2. Red shift of ν(C=S) to lower wavenumber was observed in compounds **3**, **6** – **12**, indicative of coordination of thiocarbamides as thiolate ligands.

NMR spectroscopy (^{1}H, ^{13}C{^{1}H} and ^{31}P{^{1}H}) also provides evidence for coordination of anionic forms of the ligands. **L3**, **L6** – **L8**, each showed a N-H resonance at approximate δ 8.60 ppm, which was not observed in the ^{1}H NMR spectra of the respective gold(I) compounds. The resonances correspond to thiocarbamides aryl-H were varied with the introduction of the different substituent at the *para* position, *i.e.* H, CH_3,

Cl and NO_2. **L3**, bearing a parent benzene ring at the N-bound position, given rise to three distinct resonances ascribed to *o*-aryl-H, *m*-aryl-H and *p*-aryl-H protons. A broad single resonance was however observed for **L6** N-bound *p*-tolyl group, while ^{1}H NMR spectrum of **L7** showed a doublet and a broad single resonance at δ 7.30 ppm and 7.21 ppm for aryl protons due to the magnetically inequivalency induced by Cl substituent. Likewise, **L8** demonstrated a doublet of triplet (δ 8.22 ppm) and a broad single resonance (δ 7.54 ppm) for aryl protons when a NO_2 group is attached at the *para* position. Despite for **L7** and **L8**, both of their *m*-aryl protons were resolved into a clearly defined doublet and doublet of triplets respectively, there was only a broad single resonance observed for *o*-aryl protons, suggestive of the hydrogen interactions between the *o*-aryl protons and O atom of –OCH(CH_3)$_2$, as observed in the *E*-isomer in –OMe derivative, **L1** (Ho *et al.*, 2005).

Coordination of **L3**, **L6** – **L8** as thiolate ligands resulted in the upfield shift of the resonances correspond to ligand aryl protons as observed in the ^{1}H NMR spectra of the gold(I) compounds. The shifting occurred more prominently in compounds **3**, **6** – **8** with PPh_3 as the P-bound ligand when compared to ferrocene containing binuclear compounds **9** – **12**. In the ^{13}C{^{1}H} NMR spectra of **3**, **6** – **12**, the P-bound aromatic rings experienced coupling effect due to the presence of the P atom as detailed in section 2.2.2. Shifting to lower, higher and higher chemical shifts were also observed for ligand carbons, *i.e.* C_q, C_{ipso} and C_{para}, respectively, while no apparent shifting was indicated for C_{meta}. A single resonance was observed in the ^{31}P{^{1}H} spectra for compounds **3**, **6** – **8** at *ca.* δ 38.0 ppm and **9** – **12** at *ca.* δ 32.5 ppm respectively, with more shielding effect imparted by the ferrocene group.

3.2.2 Thermogravimetric Analysis

Results for thermogravimetric analysis of compounds **3**, **6** – **12** are shown in Table 3.4 and Figure 3.10. Each of the compounds demonstrated different decomposition

pathway with **3** resulted in ½ Au_2S in a single decomposition step from 112.97 – 370.85 °C. In contrast, compounds **6** – **8** yielded elemental Au at endset temperature of 329.03 °C, 426.15 °C and 675.73 °C, respectively. The decomposition pathways of compounds **9** – **12** bearing ferrocene group were found incomplete at temperature up to 800 °C, with $Fe(C_5H_4P)_2$ remained as part of the residue.

Table 3.4: Thermogravimetric analysis results for compounds **3**, **6** – **12**.

Compound	Temp. (°C)	obs., calc'd weight percentage (%)
3	112.97 – 370.85	32.64 *cf*. 32.59 (residue of ½ Au_2S)
6	119.48 – 223.26	11.57 *cf*. 13.65 (loss of *p*-tolyl)
	223.26 – 329.03	27.46 *cf*. 29.51 (residue of Au)
7	145.43 – 426.15	28.76 *cf*. 28.63 (residue of Au)
8	187.59 – 331.54	36.07 *cf*. 37.22 (residue of AuPS)
	331.54 – 675.73	27.90 *cf*. 28.20 (residue of Au)
9	203.97 – 231.24	13.54 *cf*. 13.63 (loss of NPh)
	231.24 – 488.14	25.12 *cf*. 23.07 (Loss of Fc-Ph)
	488.14 – 800.00	46.37 *cf*. 47.87 (Residue of $Fe(C_5H_4P)_2Au_2$)
10	184.67 – 492.00	37.99 *cf*. 38.00 (Loss of NC_6H_4Me-4 and Fc-Ph)
	492.00 – 800.00	47.83 *cf*. 46.88 (residue of $Fe(C_5H_4P)_2Au_2$)
11	204.93 – 371.52	24.47 *cf*. 21.94 (loss of Fc-Ph)
	371.52 – 498.13	16.63 *cf*. 17.86 (loss of NC_6H_4Cl-4)
	498.13 – 800.00	46.75 *cf*. 45.52 (residue of $Fe(C_5H_4P)_2Au_2$)
12	116.96 – 137.62	6.84 *cf*. 6.45 (loss of NO_2)
	137.62 – 248.91	18.60 *cf*. 18.67 (loss of NC_6H_4 and $–CH(CH_3)_2$)
	248.91 – 800.00	47.37 *cf*. 47.10 (residue of $Fe(C_5H_4P)_2$ and Au_2S)

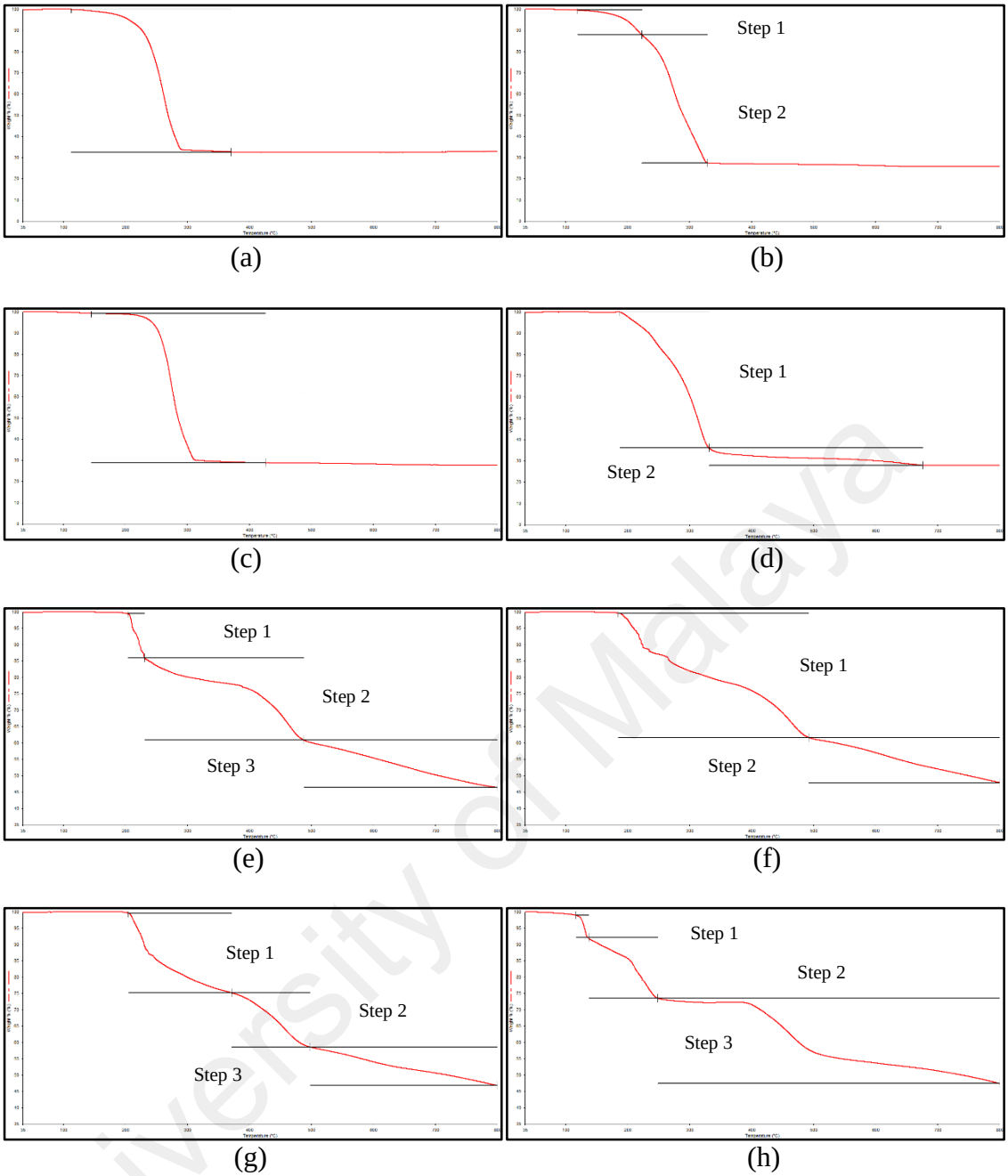

Figure 3.10: Thermograms of **3** (a), **6** (b), **7** (c), **8** (d), **9** (e), **10** (f), **11** (g) and **12** (h)

3.2.3 Molecular Structures

Molecular structures of **L3** (Kuan *et al.*, 2007), compounds **3** (Yeo *et al.*, 2013) and **9** were presented in Figure 3.11, as representative examples for the series. The coordination of thiocarbamide as thiolate ligand was confirmed as indicated by the elongation of S1–C1 bond and contraction of C1–N1 bond in the structures of compound **3** and **9**, as listed in Table 3.5. The gold(I) centre displayed a linear geometry defined by

phosphine-P and thiolate-S, with angle of S1–Au–P1 close to ideal linearity. The slight deviation is attributed to the close proximity of the O atom towards Au centre, giving rise to Au…O interactions.

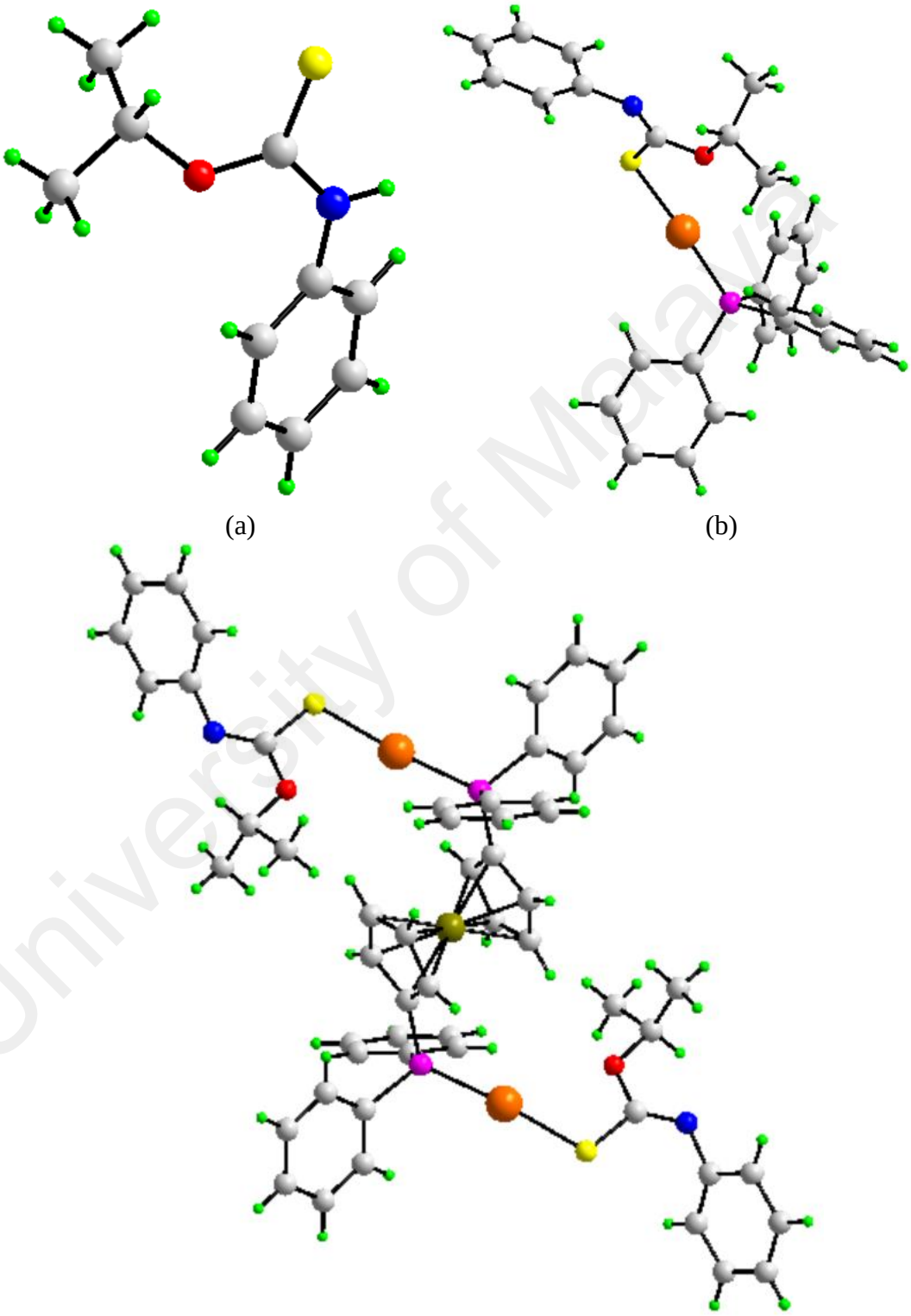

Figure 3.11: Molecular structure of **L3** (a), asymmetric unit of **3** (b) and molecular structure of **9** with solvate molecule eliminated for clarity (c).

Table 3.5: Selected bond lengths (Å) and angles (°) for **L3**, compounds **3** and **9**.

	L3	**3**	**9**
Au–S1	-	2.3137(13)	2.3057(15)
Au–P1	-	2.2643(13)	2.2545(13)
C1–S1	1.6739(13)	1.7647(53)	1.7577(47)
C1–O1	1.3219(16)	1.3470(56)	1.3501(64)
C1–N1	1.3341(21)	1.2812(65)	1.2693(76)
S1–Au–P1	-	176.437(48)	174.477(43)

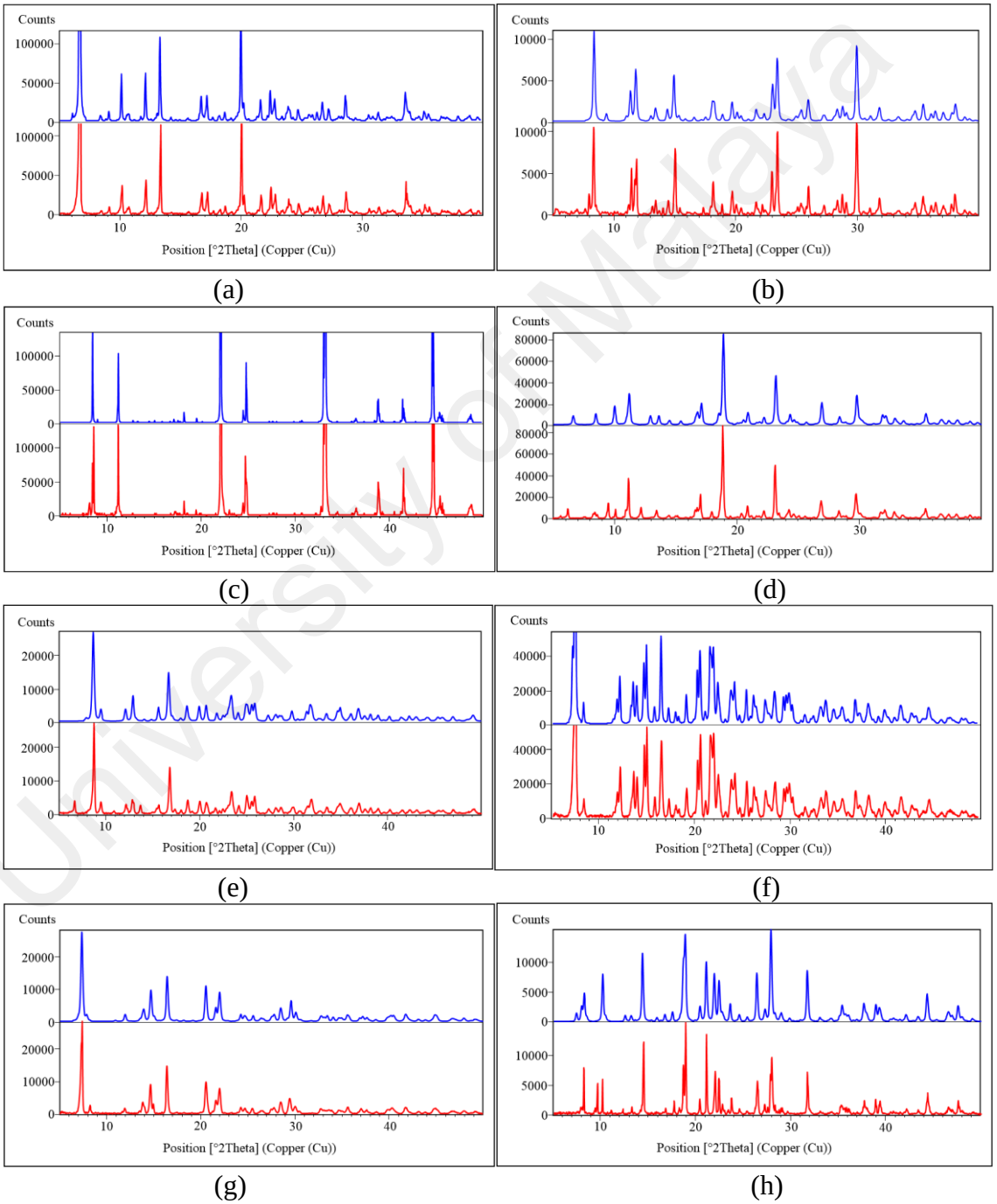

Figure 3.12: PXRD patterns for **3** (a), **6** (b), **7** (c), **8** (d), **9** (e), **10** (f), **11** (g) and **12** (h): Blue trace (generated from CIF), red trace (calculated from bulk material).

The PXRD measurements performed on dried bulk materials for compounds **3**, **6** – **8** (Figure 3.12 (a) – (d)) were consistent with the patterns generated from the single crystal structure. Compounds **9** – **12** each crystallised with the presence of solvate and the sample became opaque when removed from the mother liquor and dried under atmospheric condition. In the absence of solvate molecules, one might expect a collapse in the crystal structure. Insignificant differences in the measured and calculated PXRD patterns were possibly ascribed to the loss of solvate in dried samples, as presented in Figure 3.12 (e) – (f).

3.2.4 Biological Study

Biological properties of **3**, **6** – **12** were evaluated against MCF-7 breast cancer cells and HEK-293 human embryonic kidney cells using the MTT colorimetric assay, employing procedures similar to literature (Ooi *et al.*, 2015), and the results are presented in Table 3.6. Overall, compounds **3**, **6** – **8** exhibited better activity towards MCF-7 as compared to its cytotoxicity against HEK-293 with **6** being the most potent amongst these four mononuclear species. Replacing the P-bound PPh_3 to dppf (1,1'-bis(diphenyphosphino)ferrocene) led to comparable activity for compound **9** (2.58 μM *c.f.* 2.45 μM for **3**) and **10** (1.96 μM *c.f.* 1.71 μM for **6**), respectively, against MCF-7 cell lines. Compounds **11** and **12** were found to reduce in cytotoxicity as compared to the respective mononuclear analogues against MCF-7, and also HEK-293 in the case of **12** where the IC_{50} values against these two cell lines were not determined. HEK-293 cell lines were however more susceptible towards binuclear species, compounds **9** – **11** with IC_{50} of 1.21 μM, 0.28 μM and 0.82 μM respectively, with **10** being the most cytotoxic against HEK-293. In short, compounds with different P-bound ligand exerted a diverse cytotoxic effect towards both of the cancer cell lines. Comparing the activity induced by compounds bearing different ligand, gold(I) compounds with N-bound *p*-tolyl were found to possess remarkable anti-cancer properties in both MCF-7 and HEK-293 cell lines.

Table 3.6: IC_{50} values of **3**, **6** – **12** against MCF-7 and HEK-293 cell lines.

Compounds	IC_{50} ± SD (μM)	
	MCF-7	**HEK-293**
3	2.45 ± 0.02	5.83 ± 0.61
6	1.71 ± 0.09	2.79 ± 0.38
7	3.21 ± 0.01	9.88 ± 0.24
8	2.28 ± 0.36	2.89 ± 0.04
9	2.58 ± 0.13	1.21 ± 0.79
10	1.96 ± 0.13	0.28 ± 0.09
11	5.77 ± 0.79	0.82 ± 0.17
12	ND	ND

ND: not determined as the viability of cells more than 50% across all the tested concentration.

3.3 Bipodal Thiocarbamide and Related Binuclear Phosphinegold(I) Compounds: Importance of Au···π(Aryl) Interactions

3.3.1 Synthesis and Spectroscopic Characterisation

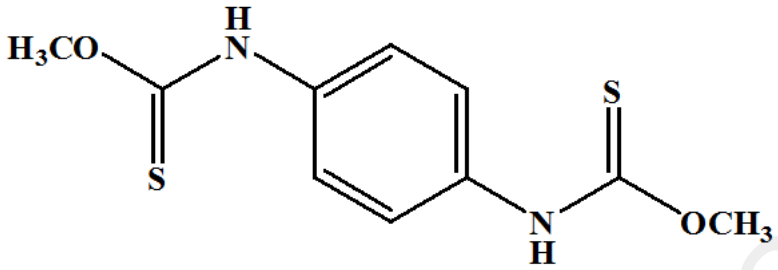

Figure 3.13: Chemical structure of 1,4-[MeOC(=S)N(H)]$_2$C$_6$H$_4$ **(L9)**.

Au···Au interactions that arise from relativistic effects in gold(I) species have garnered the interest of chemists, in addition to their luminescence properties in both the solution and solid states. On the contrary, Au···π interactions that impart comparable stabilisation in crystal structures of gold(I) compounds receive far less attention. This sub-chapter aims to delineate the Au···π interactions afforded from binuclear phosphinegold(I) thiocarbamide compounds. A series of three binuclear phosphinegold(I) thiocarbamide compounds were prepared stemmed from a bipodal thiocarbamide, 1,4-[MeOC(=S)N(H)]$_2$C$_6$H$_4$ prepared. 1,4-[MeOC(=S)N(H)]$_2$C$_6$H$_4$, coded as **L9**, displayed similar characteristic IR bands for thiocarbamides, *e.g.* 3219 cm^{-1}, 1454 cm^{-1}, 1140 cm^{-1} and 1046 cm^{-1} correspond to ν(N–H), ν(C–N), ν(C–O), and ν(C=S), respectively. Remarkably, ^{13}C{^{1}H} NMR spectrum of **L9** showed unpredictable multiple resonances from chemically equivalent sites. In view of the above, variable temperature ^{1}H NMR study was conducted on **L9** in CDCl$_3$ and DMSO-d_6 and the results are discussed and presented below.

Table 3.7: Variable temperature 1H NMR data (δ, ppm; $W_{½}$, bandwidth at half height) for **L9** recorded in DMSO-d_6 solution.

Temp. (°C)	NH	Aryl-H	-OCH_3	$W_{½}$ (Hz)
28	11.08	7.59, 7.29	3.98	29.32
38	11.04	7.57, 7.31	3.98	12.40
48	10.99	7.41	3.98	6.52
58	10.95	7.44	3.99	4.95
68	10.90	7.44	3.99 (sh, 3.98)	3.17
78	10.86	7.44	3.99 (sh, 3.98)	2.29

Table 3.8: Variable temperature 1H NMR data (δ, ppm; $W_{½}$, bandwidth at half height) for **L9** recorded in $CDCl_3$ solution.

Temp. (°C)	NH	Aryl-H	-OCH_3	$W_{½}$ (Hz)
28	8.32	7.56, 7.22	4.12	21.86
35	8.26	N/A	4.12	9.72
45	8.13	7.32	4.12	4.97
55	8.10	7.34	4.12	2.97

Table 3.7 and 3.8 each summarised the ^{1}H NMR data obtained for **L9** in both DMSO-d_6 and $CDCl_3$ solutions. **L9** possesses better solubility in DMSO-d_6; the strong hydrogen interactions of **L9** with DMSO-d_6 as delineated from the δ values correspond to N-H groups at *ca.* 11.0 ppm however restrict a decent study of the solution properties and thus additional experiments were conducted in less interacting $CDCl_3$, with N-H resonances occurred at *ca.* δ 8.30 ppm, as a comparison.

At temperatures below 48 °C, the aryl protons gave rise to two resonances when equivalency might have been expected (Table 3.7 and 3.8 Figure 3.14, 3.15 and 3.16).

The observed two resonances are ascribed to the strong interactions of the –OCH_3 with aryl π-electrons, which led to chemically inequivalency. Upon temperature increment, the two resonances coalesced into a single signal due to the shorten interactions lifetime, so that the chemical shifts of the *ortho*- and *meta*- protons are averaged out. At higher temperatures, ≥ 48 °C, the exchange occurs rapidly and the observed ^1H spectra of the aryl protons are actually the weighted average of the two (Figure 3.16).

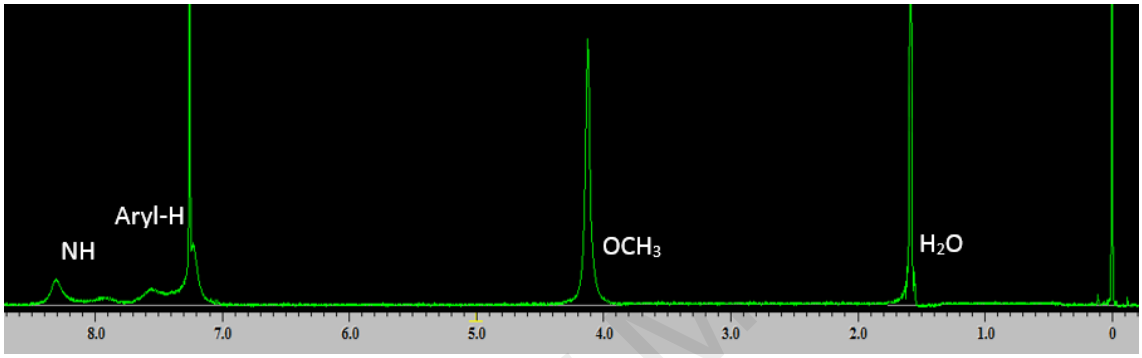

Figure 3.14: ^1H spectrum of **L9** recorded in $CDCl_3$ at room temperature.

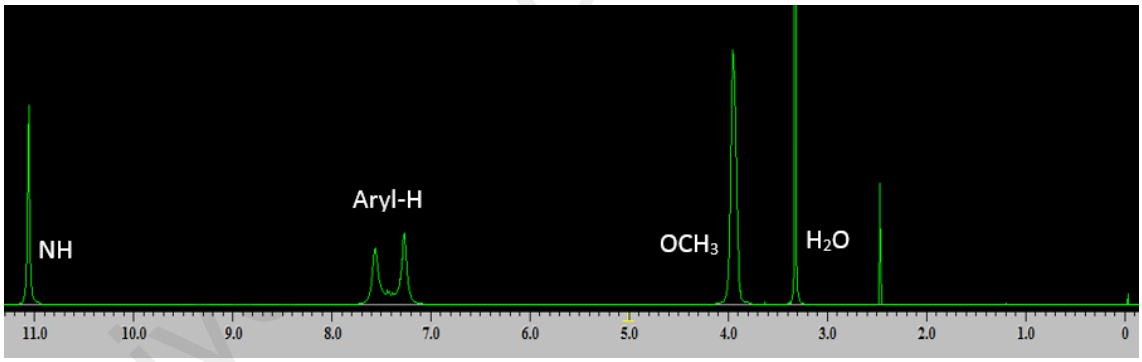

Figure 3.15: ^1H spectrum of **L9** recorded in DMSO-d_6 at room temperature.

While no splitting was observed for –OCH_3 in both DMSO-d_6 and $CDCl_3$ solutions, the consistent marked sharpening of the resonance in the two solutions as manifested in the $W_{½}$ values (Table 3.7 and 3.8), was indicative of a rapid exchange process correspond to –OCH_3···π(aryl) interactions , as in Figure 3.17.

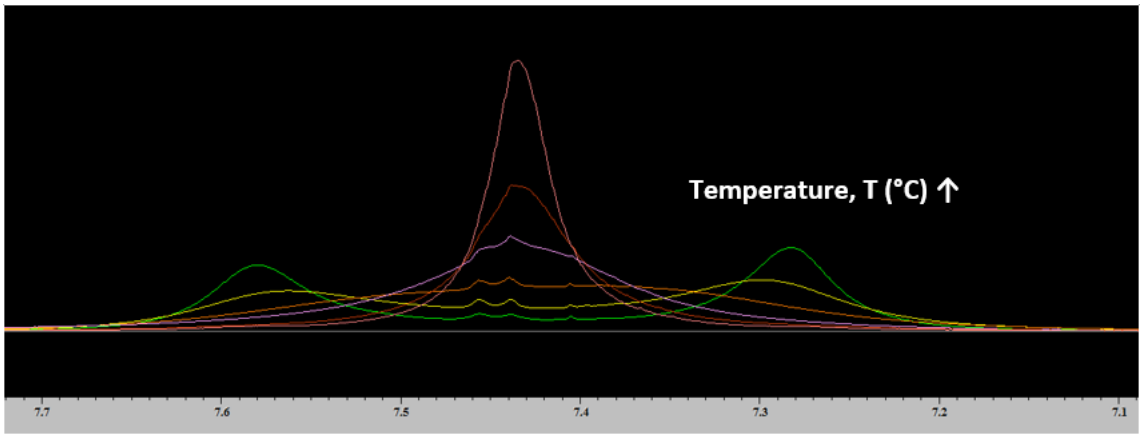

Figure 3.16: Variable temperature ^{1}H resonances responsible for aryl–H of **L9** measured in DMSO-d_6.

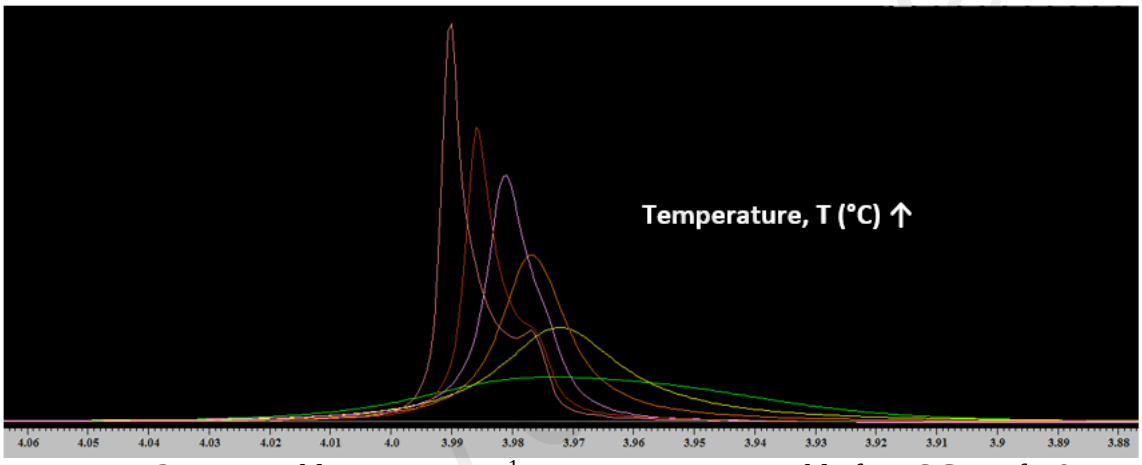

Figure 3.17: Variable temperature ^{1}H resonances responsible for –OCH_3 of **L9** measured in DMSO-d_6.

Notable a slight downfield shift of –OCH_3 resonance was observed when measurements were conducted in DMSO-d_6 but not in the $CDCl_3$ solutions. Complemented by the N-H upfield shift in the DMSO-d_6 and the appearance of a shoulder at 68 °C (Table 3.8 and Figure 3.17), the hydrogen bonding between the N-H and solvent are defined as a two step process and involved a minor species. At lower temperature, the two N-H groups are expected to form strong hydrogen bonding with DMSO-d_6 solvent molecules as a species I, which is expected to exist in rapid equilibrium with single bonded hydrogen-bonded species II (Figure 3.18). At higher temperature, ≥ 68 °C, the lifetime of species II becomes sufficiently long on the NMR time-scale so that a distinct species is observed for the OCH_3 proton.

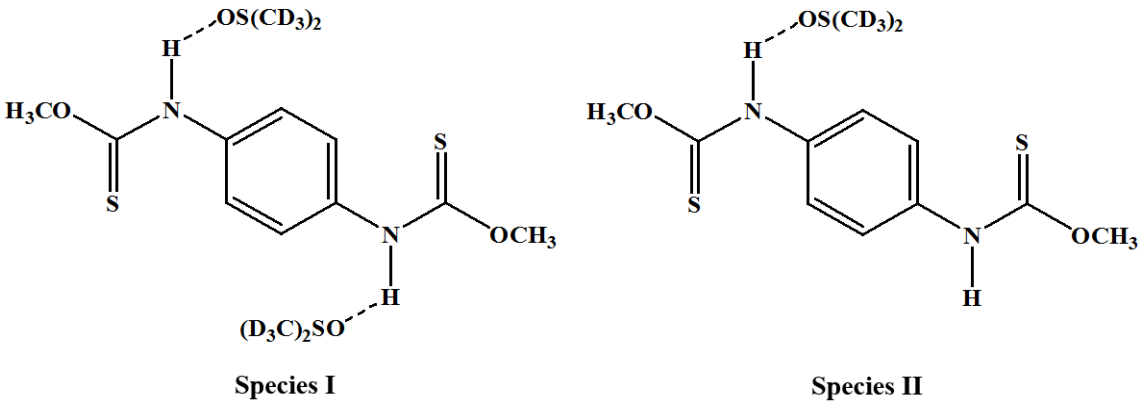

Figure 3.18: Proposed NH···DMSO-d_6 interactions with species I involves both of the N-H groups in the interactions while species II having only one of the N-H groups interacts with DMSO-d_6 solvent molecules.

Upon coordination of **L9** as thiolate ligand, the characteristic ^{1}H NMR resonance corresponds to N-H was no longer observed in the ^{1}H NMR spectra of respective gold(I) compounds **13**, **14** and **15**. Compounds **13**, **14** and **15**, with their chemical structures as illustrated in Figure 3.19, exhibited the expected resonance as detailed in section 2.2.2. In consistent with the crystallographic data obtained, significant upfield shift of the aryl-H resonances of **L9** *i.e.* from δ 7.56 and 7.22 ppm ($CDCl_3$) to δ 6.72, 6.41 and 6.84 ppm for **13**, **14** and **15**, respectively, correlate to the presence of intramolecular Au···π(aryl) interactions.

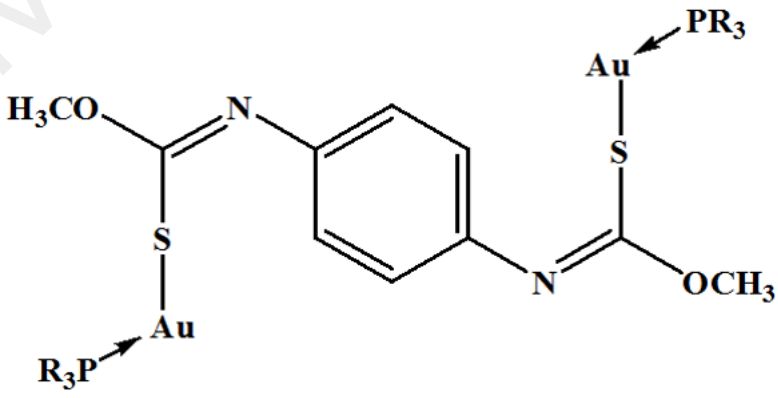

R = Et **(13)**, Ph **(14)** and Cy **(15)**

Figure 3.19: Chemical structures of $(R_3PAu)_2\{1,4\text{-}[SC(OMe)=N]_2C_6H_4\}$, with R = Et, Ph and Cy.

$^{13}C\{^{1}H\}$ NMR spectra of **13**, **14** and **15** revealed that the four aryl-C of the bipodal thiocarbamide, *ortho* and *meta*, all appeared as a single resonance in $CDCl_3$ solutions. $^{13}C\{^{1}H\}$ NMR relaxation study was conducted on **13** as a representative example to assess the rotation motion of this bipodal thiocarbamide phenyl group. At 20 °C, the aryl-C resonated at δ 122.84 ppm; the observed spin–lattice relaxation time (T_1) and the Nuclear Overhauser Effect (NOE) are: T_1 = 0.69 s and NOE = 2.88 (or the NOE enhancement factor η = 1.88) respectively. As this NOE value closes to the maximum value of 2.988 for ^{13}C, it indicates that the dominant relaxation mechanism is the dipole–dipole relaxation mechanism (T_1^{dd}), for which the rate of this dipolar relaxation ($1/ T_1^{dd}$), is proportional to the molecular correlation time (Harris, 1986). The observed relaxation time is therefore a qualitative measure of the motion of the molecule or of a group in the molecule. The observed T_1 value is extremely low for the aryl carbons in **13** in $CDCl_3$ solution. The relaxation data thus indicates that the motion of the phenyl carbons is severely retarded in the solution. There are two motions for the phenyl group in compound **13**: (1) the internal rotation and (2) the reorientational motion which accompanies the tumbling motion of the whole molecule in the solution. The tumbling motion is expected to be normal for this relatively large molecule in solution and hence, the relaxation data imply severe hindrance in the internal rotation of the phenyl group. $^{31}P\{^{1}H\}$ NMR spectra of **13** – **15** each displayed a single resonance at δ 35.6 ppm, 38.1 ppm and 56.5 ppm, respectively, which are shifted downfield compared to uncoordinated Et_3P (-20.0 ppm), Ph_3P (-5.2 ppm) and Cy_3P (9.2 ppm), owing to the loss of electron density upon coordination with gold(I) atom.

3.3.2 Thermogravimetric Analysis

Thermograms of **13** – **15** (Figure 3.20) demonstrate a similar decomposition pathway and the following sequence is proposed. Compound **13** featured a three step decomposition pathway: step 1 – onset temperature 181.9 °C to endset 226.9 °C with observed weight loss of 29.3 % (calcd. 26.7 %) corresponding to the loss of $2Et_3P$. The second step (226.9 – 441.8 °C) attributed to the decomposition of $[MeO(=C)N]_2C_6H_4$ fragment with weight loss 18.0 % *cf*. 21.5 %, leaving 2AuS (obs., calc'd weight remaining 52.7% *cf*. 51.8%) in the intermediate step. The 2AuS eventually reduced to 2Au with the loss of 2S (obs., calc'd weight remaining 45.4% *cf*. 44.5%) from onset temperature 441.8 °C to endset 806.1 °C, with a weight loss of 7.2 % *cf*. 7.3%. The decomposition of compounds **14** and **15** however do not resolve into discernible steps. For compound **14**, the first step was correlated to the loss of $2Ph_3P$ and $[MeO(=C)N]_2C_6H_4$ fragment (obs., calc'd weight loss of 55.2 % *cf*. with 60.9 %) from 163.5 °C to 346.7 °C, giving 2AuS with observed weight remaining 44.7 % *cf*. 39.1 %. The second step involved the loss of 2S (obs., calc'd weight loss of 9.8 % *cf*. 5.5 %), leaving elemental gold (obs., calc'd weight remaining for 2Au 35.0 % *cf*. 33.6 %). Similarly, compound **15** showed a two step decomposition pathway. For step 1, with onset temperature 160.7 °C and endset 422.6 °C, accompanied with 62.7% weight loss *cf*. with calculated 62.1% for concomitant loss of $2Cy_3P$ and $[MeO(=C)N]_2C_6H_4$ fragment (obs., calc'd weight remaining for 2AuS 37.2 % *cf*. 37.8 %), while step 2 with 3.6 % weight loss *cf*. with calculated 5.3 % attributed to the loss of 2S (obs., calc'd weight remaining for 2Au 33.6 % *cf*. 32.6 %) from 422.6 to 815.2 °C.

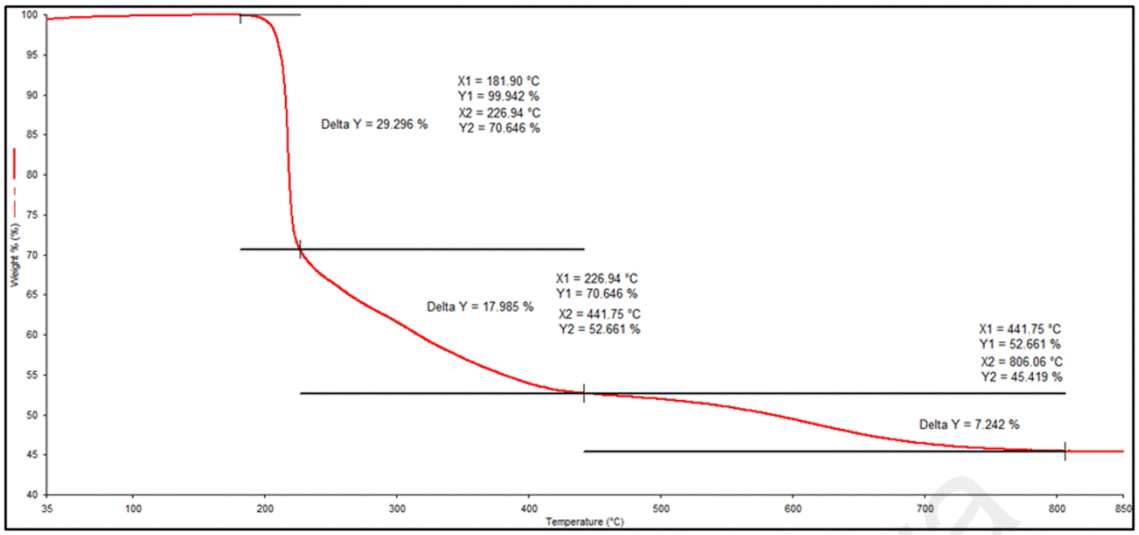

(a)

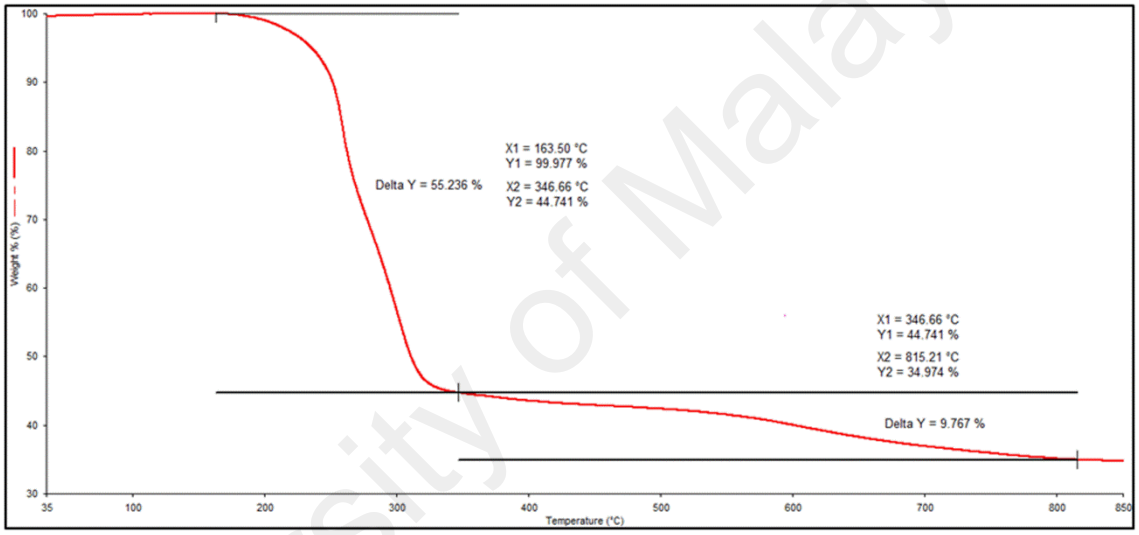

(b)

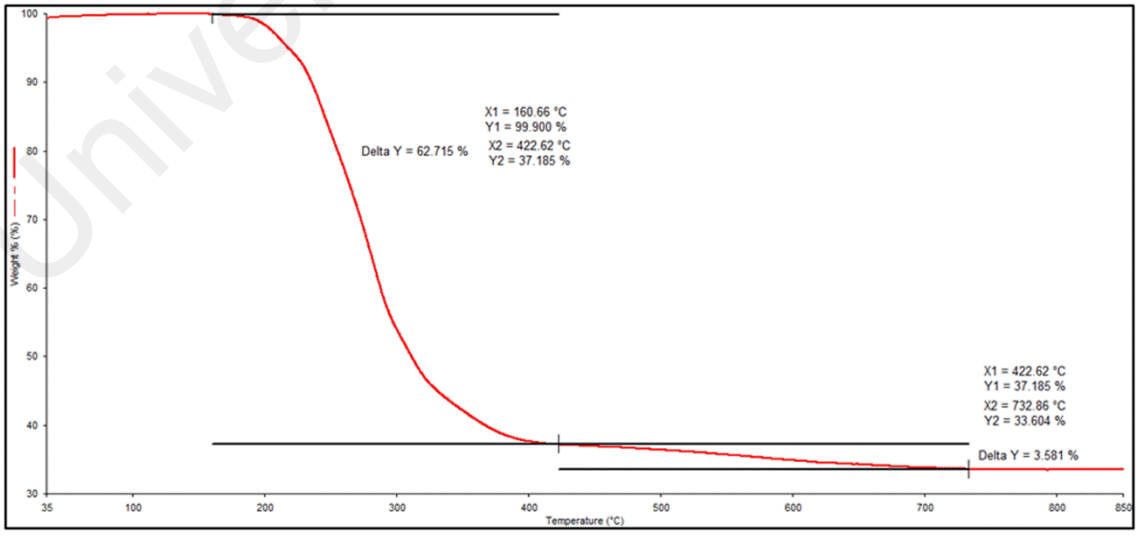

(c)

Figure 3.20: Thermogravimetric traces for **13** (a), **14** (b) and **15** (c).

3.3.3 Molecular Structures

In agreement with general two coordinated gold(I) compounds, molecular structures of **13** – **15** feature linear geometry, with S1–Au–P1 close to ideal linearity, i.e. 172.13(4)°, 167.79(3)° and 168.63(2)°, respectively. The observed deviations are ascribed to the formation of intramolecular Au···π(aryl) interactions. As the crystal structure of **L9** is unavailable, the comparison of the geometric parameters of the gold(I) compounds is made between compounds **13** – **15** with **L1**, $MeOC(=S)NHC_6H_5$, the monopodal analogue of **L9**. As compared to the free thiocarbamide, **L1**, elongation of C1–S1 (1.6708(11) Å) and contraction of C1–N1 (1.3288(15) Å) were observed in compounds **13** – **15**, as listed in Table 3.21, indicative of the coordination mode of **L9** as thiolate ligand.

Table 3.9: Selected bond lengths (Å) and angles (°) for **13** – **15**.

	13	**14**	**15**
Au–S1	2.3152(10)	2.3058(9)	2.3019(6)
Au–P1	2.2663(10)	2.2593(9)	2.2695(6)
C1–S1	1.762(4)	1.761(3)	1.756(3)
C1–O1	1.372(5)	1.356(4)	1.362(3)
C1–N1	1.258(5)	1.268(4)	1.263(3)
S1–Au–P1	172.13(4)	167.79(3)	168.63(2)
Au...Cg[a]	3.26	3.32	3.55
α[a]	22.7	21.6	30.7

[a] is the angle between the normal to the plane through the central ring and the vector passing through the ring centroid (Cg) to the Au atom.

(a)

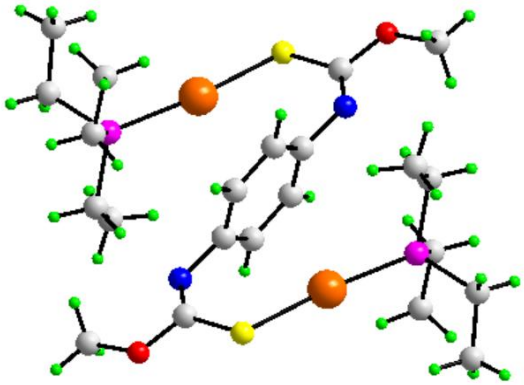

(b)

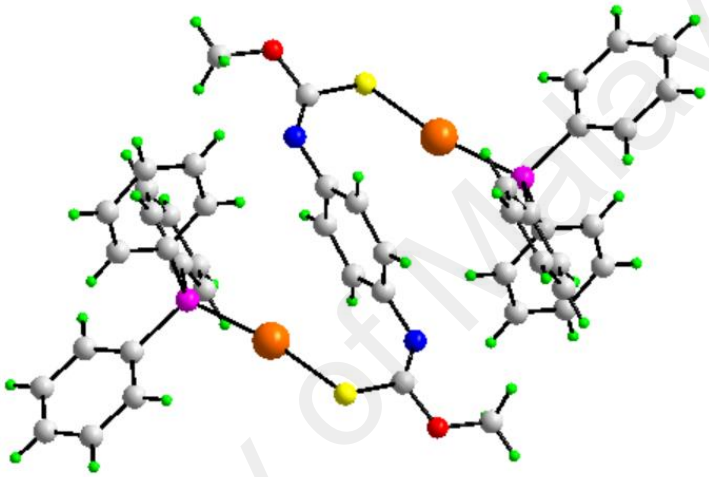

(c)

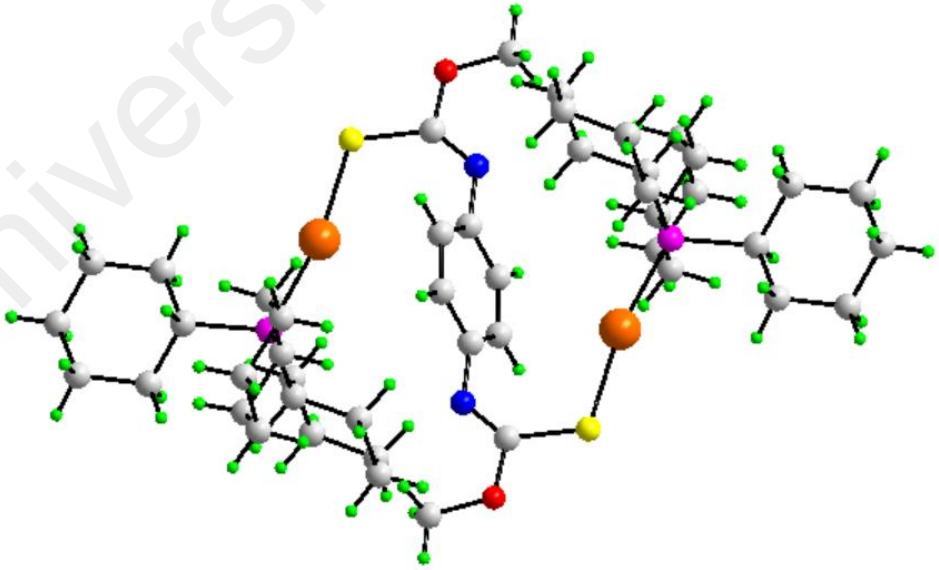

Figure 3.21: Perspective view of molecules of **13** (a), **14** (b) and **15** (c).

While each of **13** – **15** displayed distinctive features in the NMR spectra, their crystal structures demonstrated unexpected Au···π(aryl) interactions; the Au atoms in compounds **13** – **15** are in close proximity to the aryl ring of **L9** (Figure 3.21), with the bond lengths of Au···Cg(aryl) 3.26 Å, 3.32 Å and 3.55 Å, respectively. Crystal structures of **13** – **15** are found unprecedented from a search of the Cambridge Structural Database (CSD) (Groom *et al.*, 2014) for binuclear structures constructed from bipodal thiocarbamides. Out of 31 related structures from CSD (Groom *et al.*, 2014) searches, with general formula of $R_3PAu[SC(OMe)=NR']$ and diphosphine analogues (Ho *et al.*, 2006; Ho *et al.*, 2007; Kuan *et al.*, 2008; Tadbuppa *et al.*, 2007; Tadbuppa *et al.*, 2009; Tadbuppa *et al.*, 2009; Tadbuppa *et al.*, 2009, 2009; Tadbuppa *et al.*, 2010; Tadbuppa *et al.*, 2010), 27 structures feature Au···O interactions while the remaining 4 structures demonstrated Au···π(aryl) interactions. In view of the above, compound **13** was subjected to a computational study for assessment of the stability imparted by Au···π(aryl) interactions.

Figure 3.22 portrayed energy minimised structures with conformation in close agreement with the measured structures. The calculations were performed following procedures detailed in Publication IV. Overall, the calculations revealed that the conformation with two intramolecular Au···π(aryl) interactions, as demonstrated in the molecular structure of compound **13**, possessed higher stability by 12.2 kcal mol^{-1} in comparison with the conformation bearing one Au···π(aryl) interaction and one Au···O interaction. The conformer that featured two Au···O interactions present as the least stable conformation amongst the three with stability 23.6 kcal mol^{-1} lower than that of the first conformer (Figure 3.22 (a)).

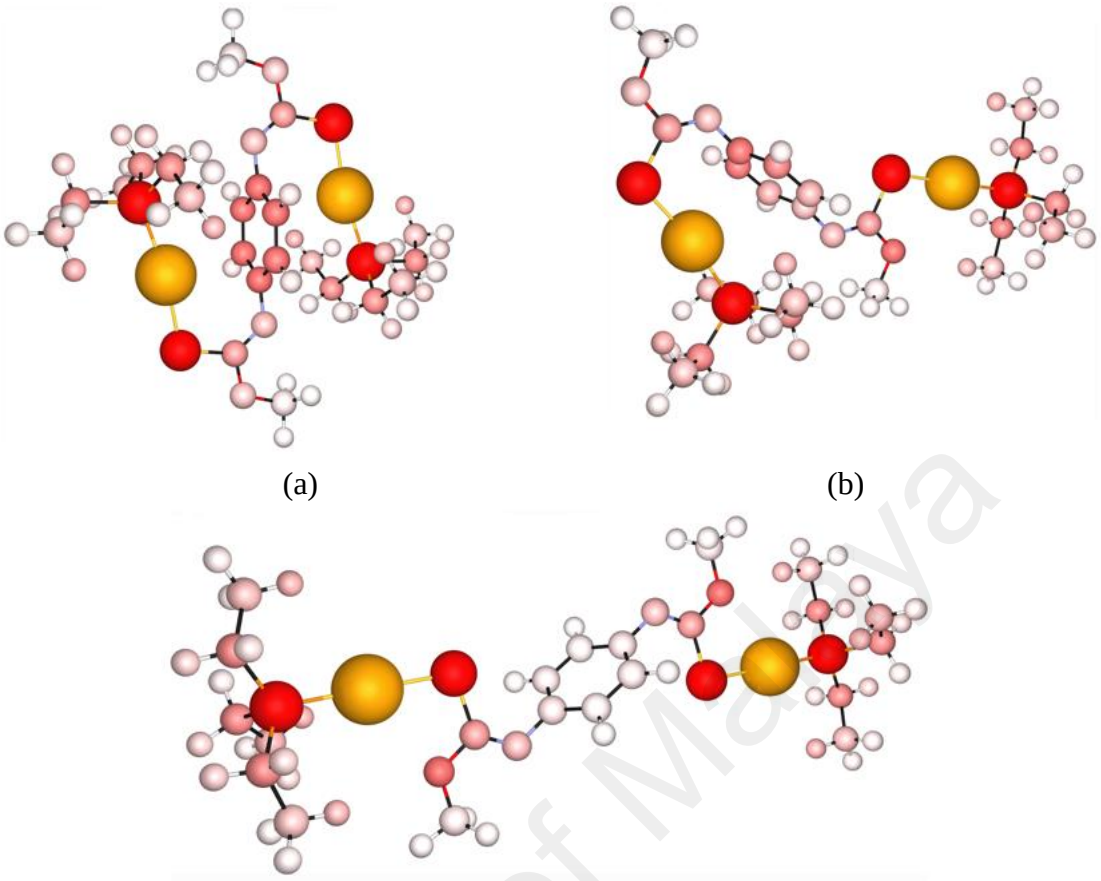

Figure 3.22: Theoretical structure for **13**: (a) the compact, spherical, conformation with two intramolecular Au…π interactions, (b) intermediate structure with one Au…π and one Au…O contact, and (c) the open, rod-like, conformation with two Au…O interactions. Bader' delocalisation indices between gold (in orange) and all other individual atoms are given as a colour scale ranging from zero (white) to 0.30 (red).

Figure 3.22 (a) – (c) are illustrated with atoms of different colour scale as a representation of Bader delocalization indices (DI's), which serves to evaluate the degree of electron deocalisation between interacting moiety (Otero-de-la-Roza *et al.*, 2014). The highest stability exhibited by conformer Figure 3.22 (a) is well elucidated by the orbital interactions between the gold atoms and the π-system.

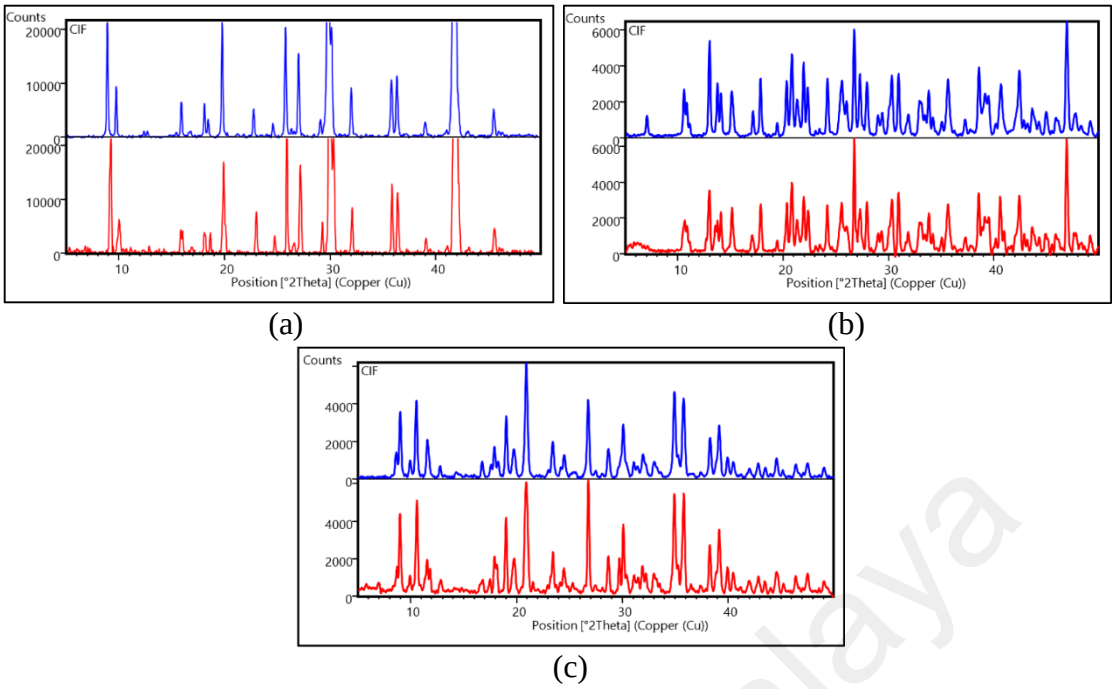

Figure 3.23: Calculated (red trace) and measured (blue trace) PXRD patterns for compounds **13** (a), **14** (b) and **15** (c).

PXRD patterns measured on compounds **13** – **15** are shown in Figure 3.23. The close agreement between the measured and calculated patterns from single crystal data reported herein show that bulk material of **13** – **15** match the crystallographic structure in each case.

3.3.4 Antibacterial Study

Compounds **13** – **15** were screened against a broad panel of Gram-positive and Gram-negative bacteria, with the results of disk diffusion assay reported in Table 3.10. While **L9** possessed no inhibitory effect, compounds **13** – **15** exhibited selective activity toward the 24 strains of pathogen. Of the three compounds, **13** demonstrated promising inhibitory activity against targeted Gram-positive and Gram-negative bacteria, except for pathogen P. *aeruginosa* which was only partially inhibited. As compared to standard antibiotics, tetracycline and chloramphenicol, compound **13** induced better or comparable inhibitory effect against Gram-positive bacteria, with inhibitory zones ranging from 18 to 30 mm. Compounds **14** and **15** however displayed specific inhibitory activity toward

selected Gram-positive bacteria and inactive against all of the Gram-negative pathogens. The three compounds were also subjected to evaluation for their anti-bacterial sensitivity, of which **13** was found to be bactericidal to all of the Gram-positive and Gram-negative bacteria except for E. *faecium* and K. *pheumoniae*. By contrast, the bactericidal activity of **14** and **15** are only limited to Gram-positive pathogens and the detailed outcomes of anti-bacterial evaluation can be accessed from Publication IV. To conclude, a variation of the P-bound groups influences the anti-bacterial activity of the compounds; comprehensive study on related compounds permit the identification of biologically active moiety, which aids in development of highly potent bactericidal agent.

Table 3.10: Anti-bacterial activity measured by zone of inhibition (mm) of **13** – **15**, **L9** and standard anti-biotics.

Microorganism	**13**	**14**	**15**	**L9**	**Standard Anti-biotics**
Gram-positive bacteria					
B. cereus ATCC10876	22	–	–	–	11[a]
B. subtilis ATCC6633	27	10	8	–	24[a]
E. faecalis ATCC29212	20	9	–	–	11[a]
E. faecium ATCC19434	18	9	8	–	16[b]
L. monocytogenes ATCC19117	20	9	8	–	27[a]
S. aureus (MRSA) ATCC43300	23	9	7	–	14[b]
S. aureus ATCC25923	30	9	–	–	18[b]
S. saprophyticus ATCC15305	30	9	8	–	29[a]
Gram-negative bacteria					
A. baumannii ATCC19606	13	–	–	–	16[a]
A. hydrophilla ATCC35654	8	–	–	–	22[a]
C. freundii ATCC8090	8	–	–	–	26[a]
E. aerogenes ATCC13048	7	–	–	–	20[a]
E. cloacae ATCC35030	8	–	–	–	20[a]
E. coli ATCC25922	10	–	–	–	18[a]
K. pneumonia ATCC700603	8	–	–	–	13[a]
P. aeruginosa ATCC27853	14 (T)	–	–	–	14[a]
P. mirabilis ATCC25933	8	–	–	–	14[b]
P. vulgaris ATCC13315	14	–	–	–	19[b]
S. typhimurium ATCC14028	9	–	–	–	24[a]
*S. paratyphi*A ATCC9150	9	–	–	–	22[a]
S. flexneri ATCC12022	12	–	–	–	18[a]
S. sonnei ATCC9290	10	–	–	–	19[a]
S. maltophilia ATCC13637	9	–	–	–	23[b]
V. parahaemolyticus ATCC17802	23	–	–	–	30[a]

The diameter of inhibition zones in millimetres (mm) were measured after 24 h incubation; –, no zone of inhibition; (T), partial zone of inhibition; [a]Tetracycline; [b]Chloramphenicol.

3.4 Bis(triphenylphosphine)copper(I) Thiocarbamides: Putative Arene-C-H···π(Quasi-Chelate Ring) Interactions

3.4.1 Synthesis and Spectroscopic Characterisation

Contemplating the study on phosphinegold(I) thiocarbamides, a series of three bis(triphenylphosphine)copper(I) thiocarbamide compounds, **16** – **18**, as illustrated in Figure 3.24, were prepared. Compounds **16** – **18** were readily prepared in high yield (> 90 %) from the reaction of triphenylphosphine, copper(I) chloride and thiocarbamide **L1** – **L3** respectively, in acetonitrile.

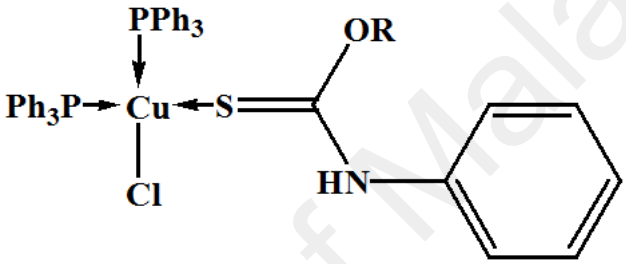

R = Me **(16)**, Et **(17)** and *i*Pr **(18)**

Figure 3.24: Chemical structures of $(Ph_3P)_2CuCl\{ROC(=S)N(H)C_6H_5\}$, with R = Me, Et and *i*Pr.

The characteristic IR bands for **L1** – **L3** were discussed in section 3.1. Compounds **17** – **18** exhibited the similar characteristic bands of thiorcabamides with shifting to lower, lower, higher and higher wavenumber are observed for ν(N–H), ν(C–N), ν(C=S) and ν(C–O) respectively, upon the donation of the sulphur lone pair for complexation.

The ^{1}H NMR resonance corresponds to thiocarbamide N-H was found shifted downfield from *CA.* δ 8.67 ppm to δ 11.86 ppm upon coordination, indicative of the presence of hydrogen interactions, *i.e.* N-H…Cl interactions. Measurements on the 10-folds diluted sample solutions (Figure 3.25) showed a significant highfield shift, attributed to the retention of intramolecular N–H…Cl hydrogen bonds in more concentrated solutions.

(a)

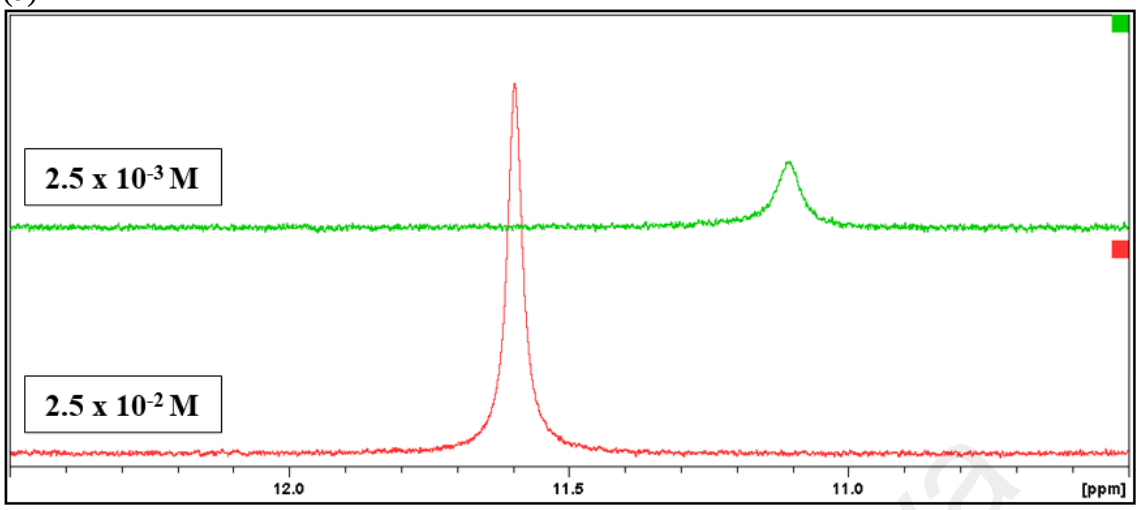

(b)

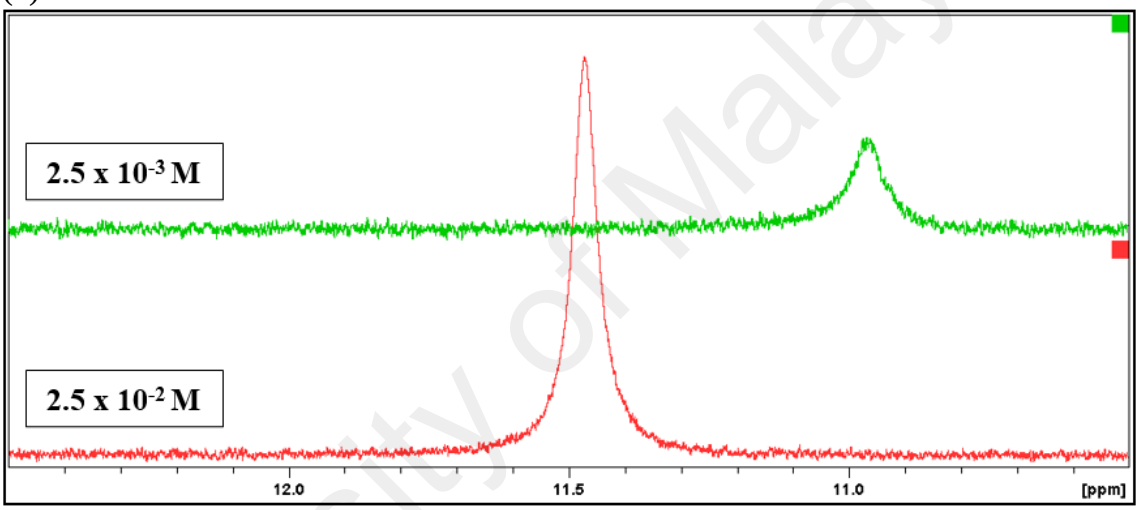

(c)

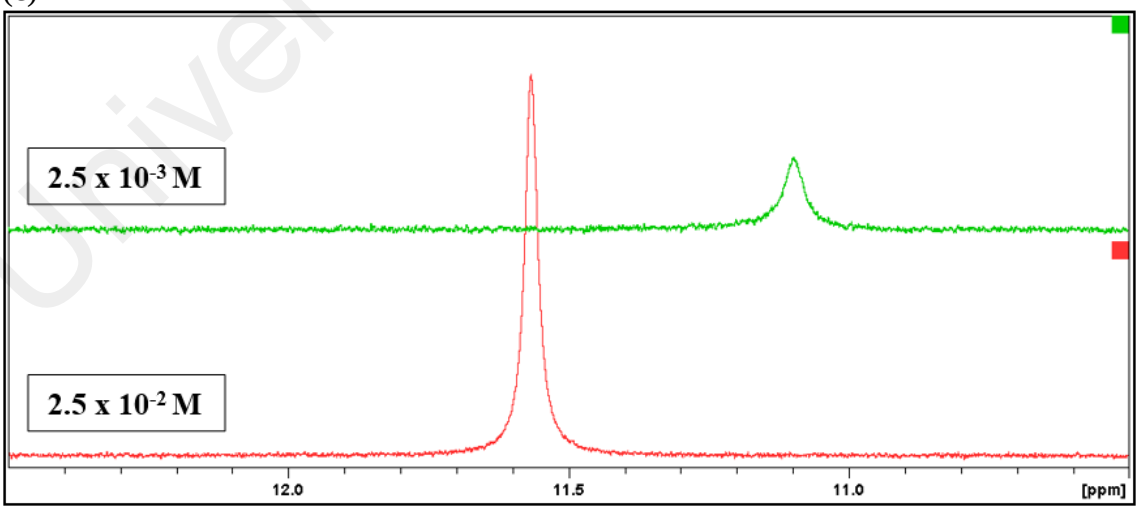

Figure 3.25: ^{1}H NMR spectra for **16** (a), **17** (b) and **18** (c) measured in $CDCl_3$ solution at 2.5 x 10^{-2} M (red spectra) and 2.5 x 10^{-3} M (green spectra).

The formation of N-H…Cl hydrogen bonds is further supported from the ^{1}H NMR of **16** – **18** in the δ 7.48 – 7.11 ppm region; such interactions inflicted changes to the chemical environment of the thiocarbamide aryl-ring protons. Compound **16** displayed indiscernible multiple splitting due to triphenylphosphine and **L1** phenyl rings. Resonances correspond to *o*-aryl and *p*-aryl protons of thiocarbamide were clearly identified in the ^{1}H NMR spectra of **17** and **18**, and their respective positions were found inverted as compared to the uncoordinated thiocarbamides, as illustrated in Figure 3.26. The *m*-aryl protons of thiocarbamide were unable to be identified due to the overlapping with triphenylphosphine protons in the respective region.

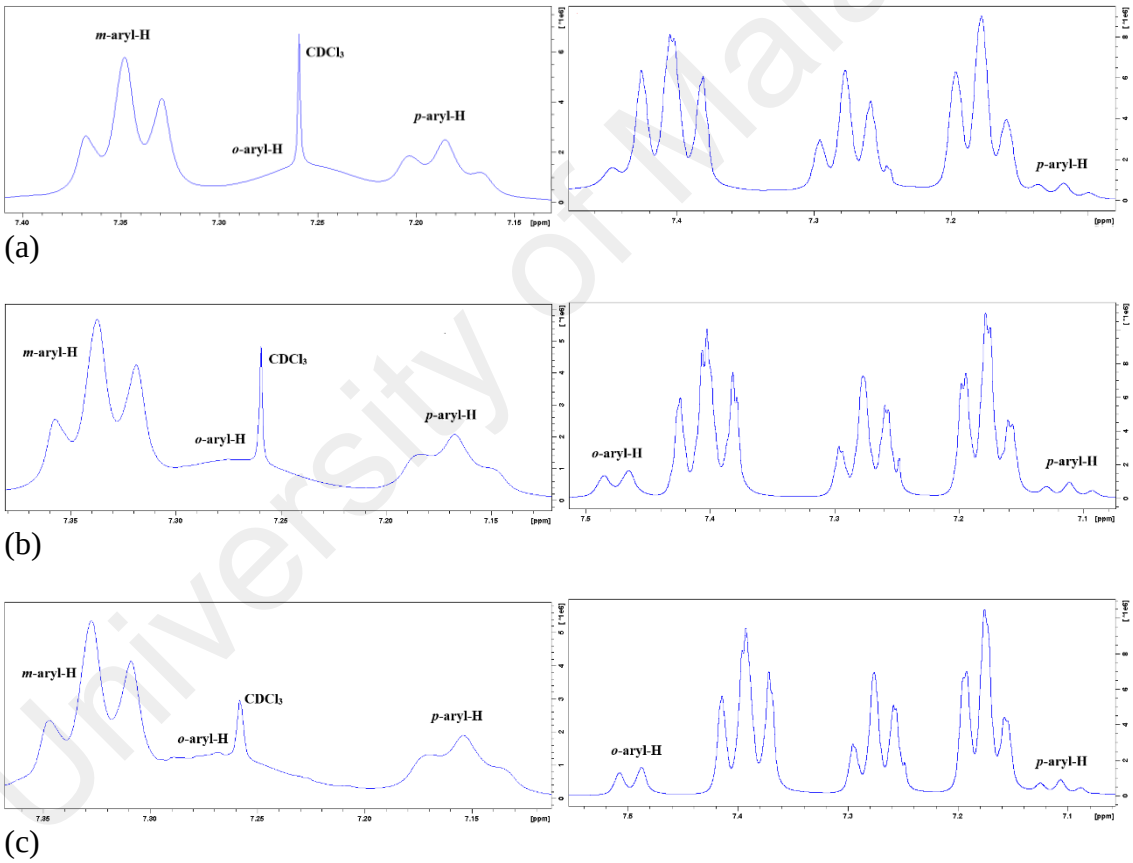

Figure 3.26: ^{1}H NMR spectra (blow up) of **L1** (left), **16** (right) (a), **L2** (left), **17** (right) (b) and **L3** (left), **18** (right) (c).

The ^{13}C{^{1}H} NMR spectra of **16** – **18** exhibited the expected resonances. The phosphorous atom of triphenylphosphine induced coupling effects on the phenyl carbons, *i.e.* doublets were observed for each of the phenyl ring carbon respectively, as reported in

section 2.2.3. $^{31}P\{^{1}H\}$ spectra revealed a single resonance at ca δ -4.1 ppm, indicative of chemically equivalency of the two triphenylphosphine groups.

Photophysical data for **L1** – **L3** and **16** – **18** are presented in Table 3.11. **L1** – **L3** each exhibited λ_{max} at approximate 275 nm in their UV spectra, ascribed to π-π* transitions. Compounds **16** – **18** each showed an intense absorption band at 272 nm, which was slightly blue shifted as compared to the free thiocarbamides. Additional band attributed to triphenylphosphine was not observed in compounds **16** – **18**. With reference to the related phosphinegold(I) analogues, intraligand transitions due to triphenylphosphine occurred at *ca.* 267 nm. It is suspected that the intraligand transitions of triphenylphosphine were masked in the UV spectra of **16** – **18**, this is supported by the blue shift and increased band intensity observed. Photoexcitation of **L1** – **L3** given rise to emission bands in the range of 374 – 825 nm, as listed in Table 3.11. Upon complexation, the fluorescence bands of **16** – **18** were observed in a shorter range, *i.e.* 371 – 532 nm, as compared to the free ligand.

Table 3.11: Photophysical data for **L1** – **L3**, **16** – **18** measured in acetonitrile.

Compound	**λ_{abs} (nm)**	**ε (L cm^{-1}mol^{-1})**	**λ_{em} (nm)**
L1	274	17,800	374, 422, 488, 538, 762 (sh), 788 (sh), 814 (sh)
L2	275	18,270	380, 422, 490, 538, 758(sh), 825(sh)
L3	276	18,450	384, 420, 488, 536, 760(sh), 810(sh)
16	272	36,200	371, 427, 455, 489, 531(sh)
17	272	38,300	374, 428, 458, 486, 532(sh)
18	272	39,500	375, 429, 457, 487, 531(sh)

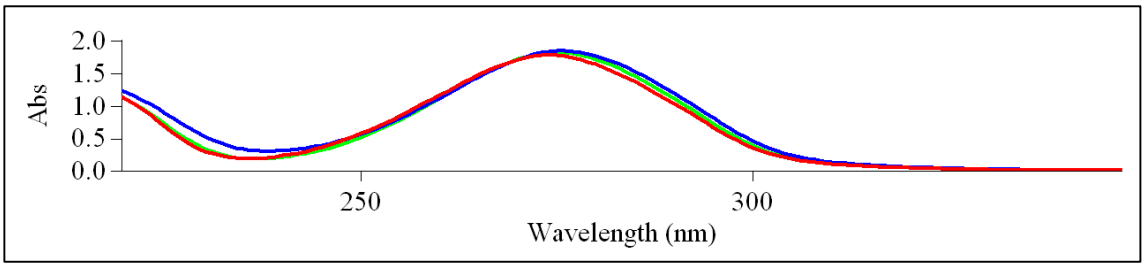

Figure 3.27: UV-Vis spectra of **L1** (red), **L2** (green) and **L3** (blue).

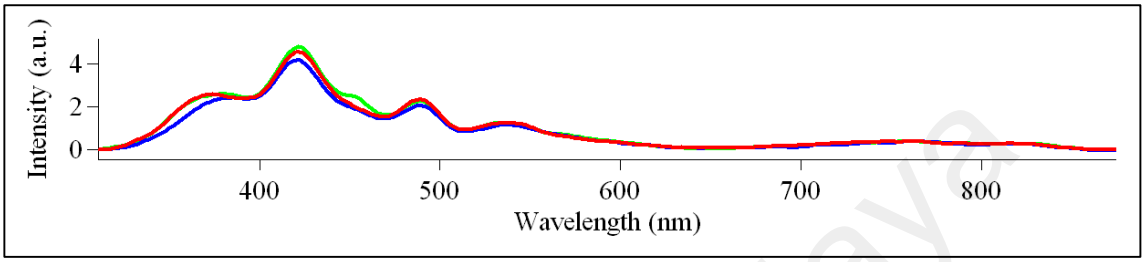

Figure 3.28: Photoluminescent spectra of **L1** at λ_{ex} 274 (red), **L2** at λ_{ex} 275 (green) and **L3** at λ_{ex} 276 (blue).

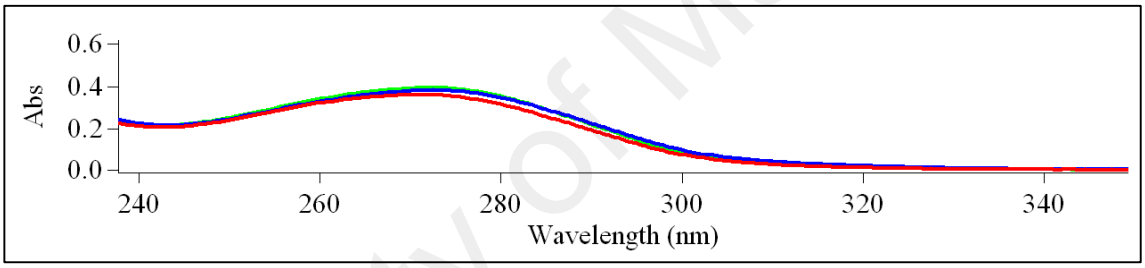

Figure 3.29: UV-Vis spectra of compounds **16** (red), **17** (green) and **18** (blue).

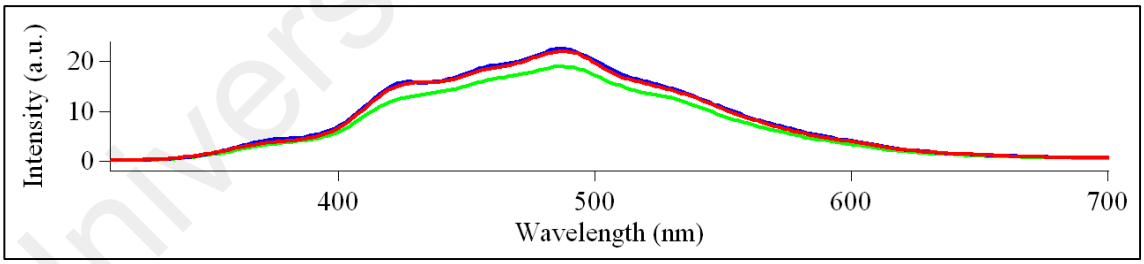

Figure 3.30: Photoluminescent spectra of **16** (red), **17** (green) and **18** (blue) at λ_{ex} 272 nm.

3.4.2 Thermogravimetric Analysis

Compounds **16** – **18** were subjected to thermogravimetric analysis to evaluate their decomposition pathways (Figure 3.31 – 3.33); each of them displayed distinct decomposition pathway as discussed below. For compound **16**, three discernible steps were determined: step 1 (132.79 – 184.67 °C) involved the loss of [$MeOC(NH)C_6H_5$] fragment with observed weight loss of 15.5 % *cf.* 17.1 %. The second step (184.67 – 358.30 °C) resulted in the weight loss of 2 PPh_3 corresponding to a weight loss of 65.9 % *cf.* 66.3 %. The final step attributed to the loss of sulphur (obs., calculated weight loss 5.5 % *cf.* 4.1 %) yielding CuCl (obs., calculated weight remaining 12.8 % *cf.* 12.5 %) from onset temperature 358.30 °C to endset 535.24 °C. A similar three step decomposition was also observed in **17**. For step 1, weight loss of 21.2 % *cf.* 18.5 % was identified between 164.05 – 207.29 °C, ascribed to the loss of [$EtOC(NH)C_6H_5$] fragment. Likewise, step 2 saw a weight loss of 64.9 % *cf.* 65.1 % attributed to the loss of 2 PPh_3 (207.29 – 358.30 °C). Step 3, from onset 358.30 °C to endset temperature 555.20 °C, is accompanied with a weight loss of 4.1 %, leading to ½Cu_2S with weight remaining 9.5 % *cf.* 9.9 %. The decomposition steps were not clearly resolved for **18** however. The step 1 (139.44 – 390.89 °C) was attributed to the loss of 2PPh_3 and L3, *i*$PrOC(=S)NHC_6H_5$ with observed weight loss 87.4 % *cf.* 87.8 %. The final step, from 390.89 °C to 563.85 °C, was having the loss of Cl (obs., calculated weight loss 5.7 % *cf.* 4.3 %), producing elemental Cu with determined weight remaining 5.7 % *cf.* 7.8 %.

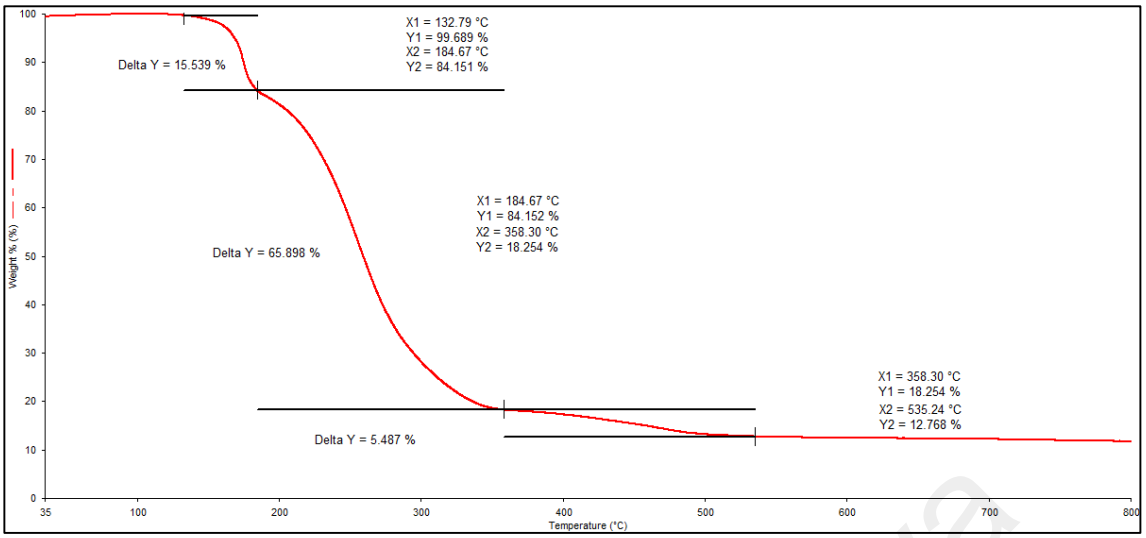

Figure 3.31: Thermogram of **16**.

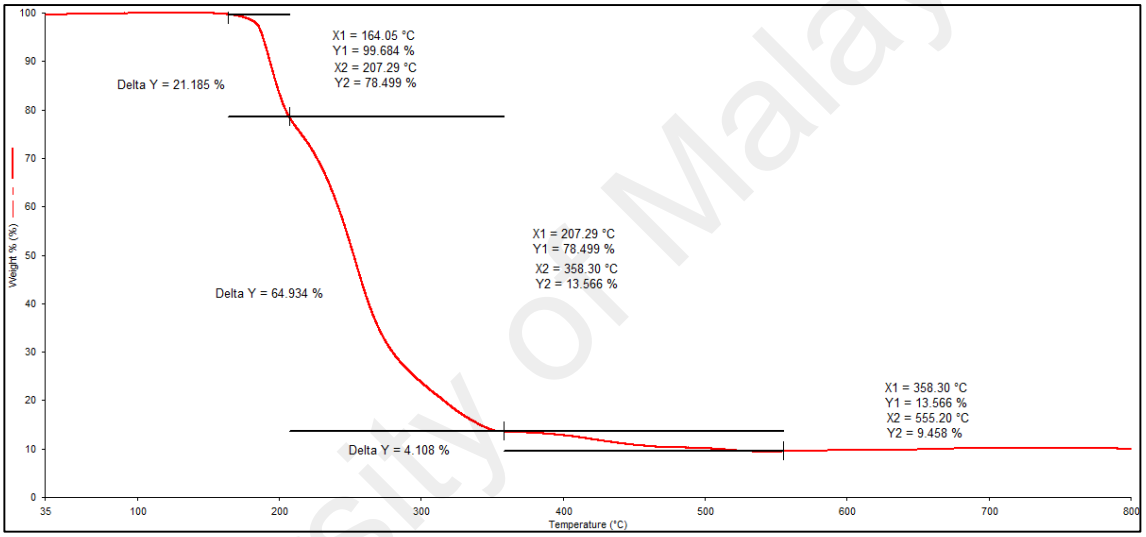

Figure 3.32: Thermogram of **17**.

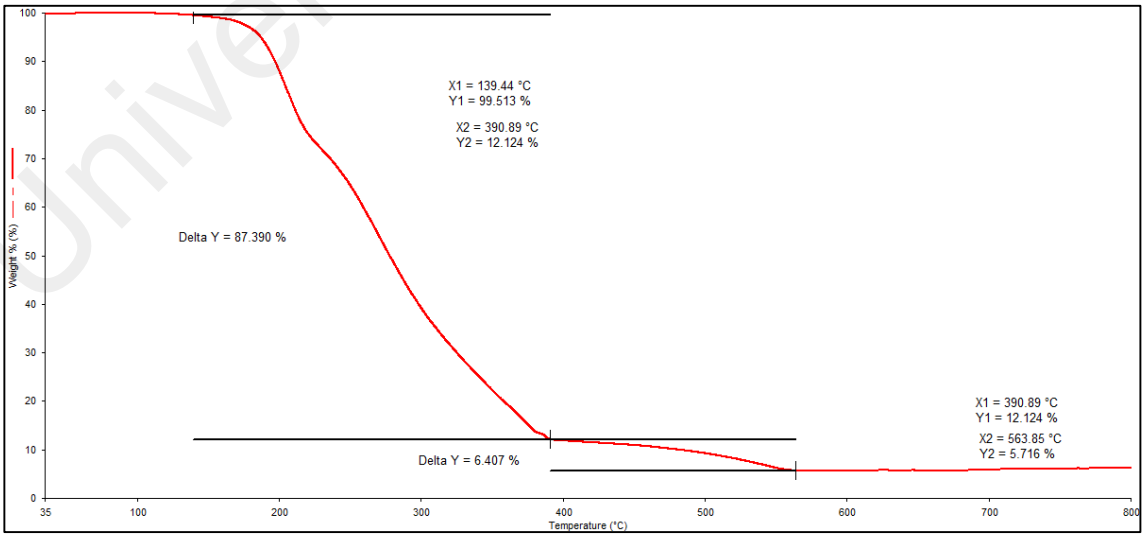

Figure 3.33: Thermogram of **18**.

3.4.3 Molecular Structures

The molecular structures of compounds **17** and **18** (Figure 3.34 (b) and (c)) feature unexpected intramolecular C–H···π(CuCl···HNCS) interactions. Despite its absence in compound **16** (Figure 3.34 (a)), which will be discussed in a later section, the formation of quasi-chelate ring CuCl···HNCS in all three compounds are relevant to the ^{1}H NMR results obtained.

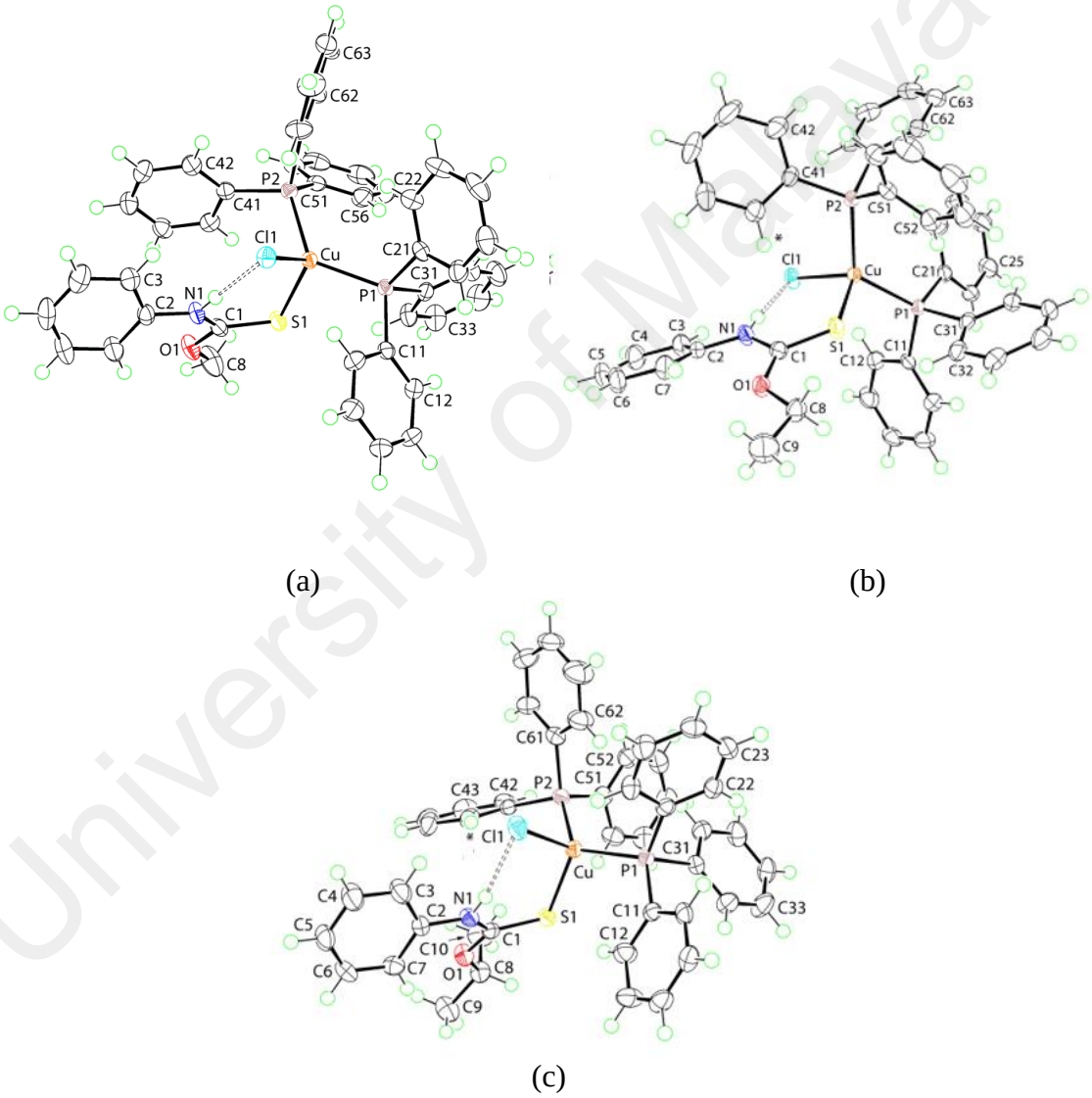

Figure 3.34: Molecular structures of (a) **16**, (b) **17** and (c) **18**, drawn with 70% displacement ellipsoids and showing atom labelling schemes.

Molecular structures of **16** – **18** each demonstrated a tetrahedral geometry defined by two phosphine-P atoms, a chlorido and a sulphur atom. Remarkably, in both **17** and **18**, a phenyl-H of triphenylphosphine ligand appears to orient towards the centre of the quasi-chelate ring, CuCl···HNCS formed. For **17**, the separations between the phenyl-H and each of the constituent atoms of the quasi chelate ring, i.e. C–H*...Cu, Cl1, S1, N1, C1 and H1n are 3.12, 3.41, 2.99, 2.63, 2.88 and 2.48 Å, respectively, while for **18**, the C–H*...Cu, Cl1, S1, N1, C1 and H1n separations are 3.17, 2.87, 3.52, 2.99, 3.17 and 2.78 Å, respectively. The above information on the separations between atoms indicate that the phenyl-H atom is not directed toward any of the constituent atoms of the ring, but to the centroid of the quasi-chelate ring, CuCl···HNCS, with the distance between the phenyl-H and the quasi-chelate ring centroid as 2.31 Å and 2.56 Å for compound **17** and **18**, respectively. In addition to the short distance accounted, the angles of phenyl-H···quasi-chelate ring centroid are 147 ° and 124 ° for **17** and **18**, respectively. The above is termed as C–H···π(CuCl···HNCS) interaction.

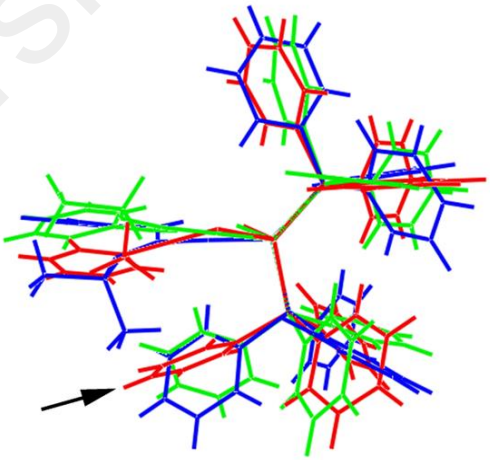

Figure 3.35: Overlay diagram of **16** (red image), **17** (green) and **18** (blue). The molecules have been superimposed so the P1-Cu-P2 atoms are overlapped. In this diagram, the inverted molecule of **17** has been employed for a better fit. The orientation of the overlay diagram has been optimised to highlight the three relevant rings.

Figure 3.35 showed an overlay diagram for **16** – **18**. The arrow points at the relevant rings that involved in putative C–H···π(CuCl···HNCS) interactions. Notable the ring in **16** adopting an almost parallel orientation to the quasi-chelate ring and thus the C–H···π(CuCl···HNCS) interaction is prevented. Over and above, the quasi-chelate ring in 16 exhibits less planarity as compared to **17** and **18**, with r.m.s. deviation of the five non-hydrogen atoms of 0.1902 Å. The above leads to the absence of C–H···π(CuCl···HNCS) interactions in **16**. DFT-D calculations, as detailed in Publication V, were accomplished on a related literature crystal structure (Singh *et al.*, 1995) to study the C–H···π(CuCl···HNCS) interactions where, stabilisation energy of ca. 3.5 kcal mol^{-1}, was found afforded by this interaction.

CHAPTER 4:CONCLUSION

Several series of mononuclear and binuclear phosphinegold(I) thiocarbamide compounds were successfully synthesised. The thiocarbamides coordinated to the gold(I) centre as thiolate ligand, as shown in the IR, ^{1}H NMR and crystallography data. The characteristic N-H stretching at ~3200 cm^{-1} was absent in the metal complex IR spectra. Similar evidence was observed in the ^{1}H NMR of the phosphinegold(I) compounds with the disappearance of N-H resonance at ca. 8.6 ppm. Other than that, deprotonation of ligand was further supported with elongation of S=C bond and shortening of C–N as observed in the crystallographic data of gold(I) compounds. Single crystal X-ray crystallography of the molecules shows that the gold atom is in an essentially linear geometry defined by sulphur and phosphorus atoms.

The six mononuclear compounds, $Ph_3PAu[SC(OR)=NC_6H_4X\text{-}4]$, R = Me, Et and *i*Pr, X = H and CH_3, exhibited significant cytotoxicity to the HT-29 cancer cell line with $Ph_3PAu[SC(OMe)=NC_6H_4CH_3\text{-}4]$ being the most active of the series. $Ph_3PAu[SC(OR)=NC_6H_4Me\text{-}4]$, R = Me, Et and iPr were found to possess promising activity against a broad panel of Gram-positive bacteria. These compounds may be potentially developed as alternative bactericidal agents for use in the treatment of microbial disease especially for recently emerging multidrug resistant strains of methicillin-resistant *S. aureus* (MRSA) and *Enterococcus* spp. which cause life-threatening infections in humans.

A series of four mononuclear $Ph_3PAu\{SC(O$*i*$Pr)=NC_6H_4X\text{-}4\}$ and four binuclear $(Ph_2P\text{-}Fc\text{-}PPh_2)\{AuSC(O$*i*$Pr)=NC_6H_4X\text{-}4\}_2$ with X = H, CH_3 Cl and NO_2 exerted different chemical environment to the molecules as presented by the multi-NMR (^{1}H, $^{13}C\{^{1}H\}$ and $^{31}P\{^{1}H\}$) spectra. $Ph_3PAu\{SC(O$*i*$Pr)=NC_6H_4X\text{-}4\}$ were found to possess greater cytotoxicity against MCF-7 breast cancer cell lines while HEK-293 embryonic kidney cell lines were more susceptible towards $(Ph_2P\text{-}Fc\text{-}PPh_2)\{AuSC(O$*i*$Pr)=NC_6H_4X\text{-}$

4}$_2$. Compounds bearing N-bound *p*-tolyl exhibited more potent activity amongst the series.

X-ray crystallography showed that three novel binuclear phospanegold(I) compounds, $(R_3PAu)_2\{1,4\text{-}[SC(OMe)=N]_2C_6H_4\}$ with R = Et, Ph and Cy, featured unexpected intramolecular Au…π interactions. Theoretical calculation revealed that these interactions to be attractive, with energies of stabilisation to the molecular structure of $(Et_3PAu)_2L$ greater than 12 kcal mol^{-1} compared to putative Au…O interactions. All of the three compounds, with Et_3P, Ph_3P and Cy_3P as the P-bound ligand, each exhibited, bactericidal effect on Gram-positive (**13** – **15**) and Gram-negative (only **13**) pathogens.

Overall, phosphinegold(I) thiocarbamides exhibit promising biological activity as suggested in the literature. By varying the O-bound substituent, as well as the P-bound phosphine ligand, the biological activities are influenced. By increasing the number of gold(I) atoms in the structure, it helps in promoting Au…π interactions which were found to stabilise the molecules in better extend. While effort are channelled to investigate gold(I) compounds, attention is also directed to study the copper analogue. In the copper(I) compounds prepared, unexpected delocalisation is observed in the putative arene system arises from CuCl···HNCS. The hydrogen bonding between the chlorine atom of CuCl and the N-H of thiocarbamides give rise to attractive (ca. 3.5 kcal mol^{-1}) intramolecular C–H···π(CuCl···HNCS) interactions.

In short, thiocarbamides remain as a potential ligand which can be structurally modified for the designing of effective bio-active compounds, in addition to their contribution in the realm of crystal engineering.

REFERENCES

Ahrland, S., Noren, B. & Oskarsson, A. (1985). Crystal-Structure Of Iodo(Tetrahydrothiophene)Gold(I) At 200 K - A Compound With An Infinite Array Of Gold-Gold Bonds. *Inorganic Chemistry, 24*(9), 1330-1333.

Al-Omary, F. A. M., Karakaya, M., Sert, Y., Haress, N. G., El-Emam, A. A. & Çırak, Ç. (2014). Structural And Spectroscopic Analysis Of 3-[(4-Phenylpiperazin-1-yl)Methyl]-5-(Thiophen-2-yl)-2,3-Dihydro-1,3,4-Oxadiazole-2-Thione With Experimental (FT-IR, Laser-Raman) Techniques And Ab Initio Calculations. *Journal of Molecular Structure, 1076*(0), 664-672.

Alajarin, M., Marin-Luna, M., Ortin, M. M., Sanchez-Andrada, P. & Vidal, A. (2009). Benzylic Newman-Kwart Rearrangement Of *O*-Azidobenzyl Thiocarbamates Triggered By Phosphines: Pseudopericyclic [1,3] Shifts *via* Uncoupled Concerted Mechanisms. *Tetrahedron, 65*(12), 2579-2590.

Albores-Velasco, M., Thorne, J. & Wain, R. L. (1995). Fungicidal Activity Of Phenyl *N*-(4-Substituted-Phenyl)Thionocarbamates. *Journal of Agricultural and Food Chemistry, 43*(8), 2260-2261.

Arora, V., Salunkhe, M. M., Sinha, N., Sinha, R. K. & Jain, S. (2004). Synthesis And Antibacterial Activity Of Some Aryloxy/Thioaryloxy Oxazolidinone Derivatives. *Bioorganic and Medicinal Chemistry Letters, 14*(18), 4647-4650.

Arslan, H., Floerke, U. & Kulcu, N. (2007). Theoretical Studies Of Molecular Structure And Vibrational Spectra of *O*-Ethyl Benzoylthiocarbamate. *Spectrochimica Acta Part a-Molecular and Biomolecular Spectroscopy, 67*(3-4), 936-943.

Aslanidis, P., Cox, P. J., Divanidis, S. & Karagiannidis, P. (2004). Copper(I) Halide Complexes From Cis-1,2-Bis(diphenylphosphino)ethylene And Some Heterocyclic Thiones. *Inorganica Chimica Acta, 357*(4), 1063-1076.

Aslanidis, P., Cox, P. J., Divanidis, S. & Karagiannidis, P. (2004). *Trans*-1,2-Bis(Diphenylphosphino)Ethene As Bridging Ligand In Thione-S-Ligated Dimeric Copper(I) Chloride Complexes. *Inorganica Chimica Acta, 357*(14), 4231-4239.

Aslanidis, P., Cox, P. J., Divanidis, S. & Tsipis, A. C. (2002). Copper(I) Halide Complexes With 1,3-Propanebis(Diphenylphosphine) And Heterocyclic Thione Ligands: Crystal And Electronic Structures (DFT) Of [CuCl(pymtH)(dppp)], [CuBr(pymtH)(dppp)], And $[Cu(\mu\text{-}I)(dppp)]_2$. *Inorganic Chemistry, 41*(25), 6875-6886.

Aslanidis, P., Divanidis, S., Cox, P. J. & Karagiannidis, P. (2005). Polymer And Cage-Type Structures In Silver(I) Complexes With Heterocyclic Thiones And Bridging Diphosphine Ligands. Crystal Structures Of $[Ag(\mu\text{-dpppent})(tHpymtH)(ONO_2)]_n$ And $[Ag_2(\mu\text{-}Trans\text{-dppen})_3(pymtH)_2](NO_3)_2 \bullet CH_3CN$. *Polyhedron, 24*(7), 853-863.

Bardi, R., Delpra, A., Piazzesi, A. M., Sindellari, L. & Zarli, B. (1981). Crystal And Molecular-Structure Of *Trans*-Dithiocyanatobis(*N*-Methyl *O*-Ethylthiocarbamate)Palladium(II). *Inorganica Chimica Acta-Articles, 47*(2), 231-234.

Batsanov, A. S., Kunishige, J. A., Jensen, C. M. & Takara, S. (2009). Crystal Structure Of $[(AuCl)_2\{m_2\text{-}1,2\text{-Bis(Diisopropoxy)Phosphano-1,2-Dimethylhydrazine-P,P'}\}]$. *X-ray Structure Analysis Online, 25*, 113-114.

Beers, W. H. & Reich, E. (1970). Structure And Activity Of Acetylcholine. *Nature, 228*(5275), 917-922.

Berners-Price, S. J. & Filipovska, A. (2011). Gold Compounds As Therapeutic Agents For Human Diseases. *Metallomics, 3*(9), 863-873.

Berners-Price, S. J., Johnson, R. K., Giovenella, A. J., Faucette, L. F., Mirabelli, C. K. & Sadler, P. J. (1988). Antimicrobial And Anticancer Activity Of Tetrahedral, Chelated, Diphosphine Silver(I) Complexes - Comparison With Copper And Gold. *Journal of Inorganic Biochemistry, 33*(4), 285-295.

Berners-Price, S. J., Mirabelli, C. K., Johnson, R. K., Mattern, M. R., McCabe, F. L., Faucette, L. F., Sung, C. M., Mong, S. M., Sadler, P. J. & Crooke, S. T. (1986). Invivo Antitumor-Activity And In Vitro Cytotoxic Properties Of Bis-1,2-Bis(Diphenylphosphino)Ethane Gold(I) Chloride. *Cancer Research, 46*(11), 5486-5493.

Bhabak, K. P., Bhuyan, B. J. & Mugesh, G. (2011). Bioinorganic And Medicinal Chemistry: Aspects Of Gold(I)-Protein Complexes. *Dalton Transactions, 40*(10), 2099-2111.

Bjelosevic, H., Guzei, I. A., Spencer, L. C., Persson, T., Kriel, F. H., Hewer, R., Nell, M. J., Gut, J., van Rensburg, C. E. J., Rosenthal, P. J., Coates, J., Darkwa, J. & Elmroth, S. K. C. (2012). Platinum(II) And Gold(I) Complexes Based On 1,1′-Bis(diphenylphosphino)metallocene Derivatives: Synthesis, Characterization And Biological Activity Of the gold Complexes. *Journal of Organometallic Chemistry, 720*, 52-59.

Bost, R. W. & Andrews, E. R. (1943). Sulfur Studies. XIX. Alkyl Esters Of Phenylthiocarbamic Acid1. *Journal of the American Chemical Society, 65*(5), 900-901.

Bott, R. C., Healy, P. C. & Smith, G. (2004). Evidence For Au(I)···Au(I) Interactions In A Sterically Congested Environment: Two-Coordinate Gold(I) Halide Phosphine Complexes. *Australian Journal of Chemistry, 57*(3), 213-218.

Brandenburg, K. (2006). DIAMOND *Crystal Impact GbR, Bonn, Germany*.

Breiter, W. A., Baker, J. M. & Koskinen, W. C. (1998). Direct Measurement Of Henry's Constant For *S*-Ethyl *N*,*N*-Di-n-Propylthiocarbamate. *Journal of Agricultural and Food Chemistry, 46*(4), 1624-1629.

Breme, K., Fernandez, X., Meierhenrich, U. J., Brevard, H. & Joulain, D. (2007). Identification Of New, Odor-Active Thiocarbamates In Cress Extracts And Structure-Activity Studies On Synthesized Homologues. *Journal of Agricultural and Food Chemistry, 55*(5), 1932-1938.

Brown, C. L., Bushell, G., Whitehouse, M. W., Agrawal, D. S., Tupe, S. G., Paknikar, K. M. & Tiekink, E. R. T. (2007). Nanogold-Pharmaceutics - (I) The Use Of Colloidal Gold To Treat Experimentally-Induced Arthritis In Rat Models; (II) Characterization Of The Gold In Swarna Bhasma, A Micro Particulate Used In Traditional Indian Medicine. *Gold Bulletin, 40*(3), 245-250.

Buckley, R. G., Elsome, A. M., Fricker, S. P., Henderson, G. R., Theobald, B. R. C., Parish, R. V., Howe, B. P. & Kelland, L. R. (1996). Antitumor Properties Of Some 2-[(Dimethylamino)Methyl]Phenylgold(III) Complexes. *Journal of Medicinal Chemistry, 39*(26), 5208-5214.

Carlucci, L., Ciani, G., Moret, M., Proserpio, D. M. & Rizzato, S. (2000). Polymeric Layers Catenated By Ribbons Of Rings In A Three-Dimensional Self-Assembled Architecture: A Nanoporous Network With Spongelike Behavior. *Angewandte Chemie International Edition, 39*(8), 1506-1510.

Casellato, U., Fracasso, G., Graziani, R., Sindellari, L., Gonzalez, A. S. & Nicolini, M. (1990). Gold(I) Complexes Of Thiocarbamate And Dithiocarbamate Esters - The Structure Of Bis(*N*-Methyl-*O*-Ethyl-Thiocarbamate)Gold(I) Chloride. *Inorganica Chimica Acta, 167*(1), 21-24.

Casini, A., Cinellu, M. A., Minghetti, G., Gabbiani, C., Coronnello, M., Mini, E. & Messori, L. (2006). Structural And Solution Chemistry, Antiproliferative Effects, And DNA And Protein Binding Properties Of A Series Of Dinuclear Gold(III) Compounds With Bipyridyl Ligands. *Journal of Medicinal Chemistry, 49*(18), 5524-5531.

Cesarini, S., Spallarossa, A., Ranise, A., Fossa, P., La Colla, P., Sanna, G., Collu, G. & Loddo, R. (2008). Thiocarbamates As Non-Nucleoside HIV-1 Reverse Transcriptase Inhibitors. Part 1: Parallel Synthesis, Molecular Modelling And Structure-Activity Relationship Studies On *O*-2-(Hetero)Arylethyl-*N*-Phenylthiocarbamates. *Bioorganic & Medicinal Chemistry, 16*(7), 4160-4172.

Chao, H. Y., Lu, W., Li, Y. Q., Chan, M. C. W., Che, C. M., Cheung, K. K. & Zhu, N. Y. (2002). Organic Triplet Emissions Of Arylacetylide Moieties Harnessed Through Coordination To $Au(PCy_3)^+$. Effect Of Molecular Structure Upon Photoluminescent Properties. *Journal of the American Chemical Society, 124*(49), 14696-14706.

Che, C. M., Kwong, H. L., Poon, C. K. & Yam, V. W. W. (1990). Spectroscopy And Redox Properties Of The Luminescent Excited-State Of $Au_2(DPPM)_2^{2+}$ (DPPM = PH_2PCH_2PPH2). *Journal of the Chemical Society-Dalton Transactions*(11), 3215-3219.

Che, C. M., Kwong, H. L., Yam, V. W. W. & Cho, K. C. (1989). Spectroscopic Properties And Redox Chemistry Of The Phosphorescent Excited-State Of Au_2Bis(Diphenylphosphino)Methane$)_2^{2+}$. *Journal of the Chemical Society-Chemical Communications*(13), 885-886.

Coker, N. L., Bauer, J. A. K. & Elder, R. C. (2004). Emission Energy Correlates With Inverse Of Gold-Gold Distance For Various $Au(SCN)_2^-$ Salts. *Journal of the American Chemical Society, 126*(1), 12-13.

Cookson, P. D. & Tiekink, E. R. T. (1994). Chloro Tri(*p*-Tolyl)Phosphine Gold(I). *Acta Crystallographica Section C-Crystal Structure Communications, 50*, 1896-1898.

CrysAlisPro. (2010). Agilent Technologies *Yarnton, Oxfordshire, England*.

Daniel, K., Chen, D., Orlu, S., Cui, Q., Miller, F. & Dou, Q. P. (2005). Clioquinol And Pyrrolidine Dithiocarbamate Complex With Copper To Form Proteasome Inhibitors And Apoptosis Inducers In Human Breast Cancer Cells. *Breast Cancer Research, 7*(6), R897 - R908.

De Wall, S. L., Painter, C., Stone, J. D., Bandaranayake, R., Wiley, D. C., Mitchison, T. J., Stern, L. J. & Dedecker, B. S. (2006). Noble Metals Strip Peptides From Class II MHC Proteins. *Nature Chemical Biology, 2*(4), 197-201.

Divanidis, S., Cox, P. J., Karagiannidis, P. & Aslanidis, P. (2005). Linking Thione-Ligated Copper(I) Centres With *Trans*-1,2- Bis(Diphenylphosphino)Ethene (*Trans*-dppen): Crystal Structures Of The Pyrimidine-2-Thione Derivatives $[CuBr(\mu_2$-*Trans*-dppen)(pymtH)$]_2$ And $[CuI(\mu_2$-*Trans*-dppen)(pymtH)$]_2$. *Polyhedron, 24*(2), 351-358.

Dixit, P. P., Nair, P. S., Patil, V. J., Jain, S., Arora, S. K. & Sinha, N. (2005). Synthesis And Antibacterial Activity Of Novel (Un)Substituted Benzotriazolyl Oxazolidinone Derivatives. *Bioorganic and Medicinal Chemistry Letters*, *15*(12), 3002-3005.

Du, W. & Curran, D. P. (2003). Synthesis Of Carbocyclic And Heterocyclic Fused Quinolines By Cascade Radical Annulations Of Unsaturated *N*-Aryl Thiocarbamates, Thioamides, And Thioureas. *Organic Letters*, *5*(10), 1765-1768.

El-Adasy, A. B. A. A. M. (2007). Some Nucleophilic Reactions With Isothiocyanatoazobenzene. *Phosphorus, Sulfur and Silicon and the Related Elements*, *182*(11), 2625-2635.

Elbjeirami, O. & Omary, M. A. (2007). Photochemistry Of Neutral Isonitrile Gold(I) Complexes: Modulation Of Photoreactivity By Aurophilicity And p-Acceptance Ability. *Journal of the American Chemical Society*, *129*(37), 11384-11393.

Elderfield, R. C. & Short, F. W. (1953). Synthesis And Reactions Of Certain Benzothiazoles. *Journal of Organic Chemistry*, *18*(9), 1092-1103.

Ellis, C. A., Miller, M. A., Spencer, J., Zukerman-Schpector, J. & Tiekink, E. R. T. (2009). Co-Crystallization Experiments Of Thiocarbamides With Bipyridine-Type Molecules. *CrystEngComm, 11*(7), 1352-1361.

Faizi, S., Siddiqui, B. S., Saleem, R., Siddiqui, S., Aftab, K. & Gilani, A. (1992). Isolation And Structure Elucidation Of Novel Hypotensive Agents, Niazinin-A, Niazinin-B, Niazimicin And Niaziminin-A+B From Moringa-Oleifera - The 1st Naturally-Occurring Thiocarbamates. *Journal of the Chemical Society-Perkin Transactions 1*(23), 3237-3241.

Faizi, S., Siddiqui, B. S., Saleem, R., Siddiqui, S., Aftab, K. & Gilani, A. U. H. (1994). Novel Hypotensive Agents, Niazimin-A, Niazimin-B, Niazicin-A And Niazicin-B From Moringa-Oleifera - Isolation Of First Naturally-Occurring Carbamates. *Journal of the Chemical Society-Perkin Transactions 1*(20), 3035-3040.

Farrugia, L. (2012). WinGX And ORTEP For Windows: An Update. *Journal of Applied Crystallography, 45*(4), 849-854.

Fortman, G. C. & Nolan, S. P. (2010). Solution Calorimetric Study Of Ligand Exchange Reactions In The Au(L)Cl System (L = Phosphine And Phosphite). *Organometallics, 29*(20), 4579-4583.

Furlani, C., Tarantelli, T., Gastaldi, L. & Porta, P. (1971). Complexing Behaviour Of Thiocarbamic Esters: Crystal And Molecular Structure Of Bis-(*O*-Methyl Phenylthiocarbamato)(Triphenylphosphine)-Palladium(II). *Journal of the Chemical Society A: Inorganic, Physical, Theoretical*(0), 3778-3783.

Gais, H. J. & Böhme, A. (2002). Palladium(0)-Catalyzed Enantioselective *O,S*-Rearrangement Of Racemic *O*-Allylic Thiocarbamates: A New Entry To Enantioenriched Allylic Sulfur Compounds. *Journal of Organic Chemistry, 67*(4), 1153-1161.

Gans, J. D. & Shalloway, D. (2001). Qmol: A Program For Molecular Visualization On Windows-Based PCs. *Journal of Molecular Graphics and Modelling, 19*(6), 557-559.

Ghorab, M. M., Taha, N. M. H., Radwan, M. A. A., Amin, N. E., Shehab, M. A. & Faker, I. M. I. (2008). Dapson In Heterocyclic Chemistry, Part I: Novel Synthesis Of Sulfone Biscompounds For Antimicrobial And Antitumor Activities. *Phosphorus, Sulfur and Silicon and the Related Elements, 183*(12), 2891-2905.

Giannini, E. H., Brewer, E. J., Kuzmina, N., Shaikov, A. & Wallin, B. (1990). Auranofin In The Treatment Of Juvenile Rheumatoid Arthritis. *Arthritis & Rheumatism, 33*(4), 466-476.

Gielen, M. & Tiekink, E. R. T. (2005). *Metallotherapeutic Drugs And Metal-Based Diagnostic Agents: The Use Of Metals In Medicine*: Wiley.

Glisic, B. D. & Djuran, M. I. (2014). Gold Complexes As Antimicrobial Agents: An Overview Of Different Biological Activities In Relation To The Oxidation State Of The Gold Ion And The Ligand Structure. *Dalton Transactions, 43*(16), 5950-5969.

Goel, A., Mazur, S. J., Fattah, R. J., Hartman, T. L., Turpin, J. A., Huang, M., Rice, W. G., Appella, E. & Inman, J. K. (2002). Benzamide-Based Thiolcarbamates: A New Class Of HIV-1 NCp7 Inhibitors. *Bioorganic & Medicinal Chemistry Letters, 12*(5), 767-770.

Gomes, L. R., Low, J. N., Quesada, A., Santos, L. M. N. B. F., Rocha, M. A. A. & Schröder, B. (2009). Synthesis, Structural Characterization And Conformational Aspects Of Thenoylthiocarbamic-*O*-Alkylesters. *Journal of Molecular Structure, 936*(1-3), 37-45.

Gomes, L. R., Low, J. N., Rocha, M. A. A., Santos, L. M. N. B. F., Schröder, B., Brandão, P., Matos, C. & Neves, J. (2011). Nickel(II) Complexes Of *N*′-(2-Thienylcarbonyl)Thiocarbamates *O*-Alkyl-Esters: Structural And Spectroscopic Characterization And Evaluation Of Their Microbiological Activities. *Journal of Molecular Structure, 990*(1-3), 86-94.

Greenwood, N. N. & Earnshaw, A. (2012). *Chemistry Of The Elements* (2 ed.): Elsevier Science.

Groom, C. R. & Allen, F. H. (2014). The Cambridge Structural Database In Retrospect And Prospect. *Angewandte Chemie International Edition, 53*(3), 662-671.

Hadjikakou, S. K., Aslanidis, P., Karagiannidis, P., Mentzafos, D. & Terzis, A. (1991). Synthesis And Photolysis Of Mixed Copper(I) Complexes With Thiones And Tri-*p*-Tolylphosphine Or Triphenylphosphine; X-Ray Crystal Structure Of Bis[Copper(I)(1,3-Thiazolidine-2-Thione)(Tri-*p*-Tolylphosphine)Chloride]. *Polyhedron, 10*(9), 935-940.

Harris, G. H. & Fischback, B. C. (1954). U.S. Patent No. 2691635.

Harris, R. K. (1986). *Nuclear Magnetic Resonance Spectroscopy*. Harlow: Longman.

Hashmi, A. S. K., Hengst, T., Lothschuetz, C. & Rominger, F. (2010). New And Easily Accessible Nitrogen Acyclic Gold(I) Carbenes: Structure And Application In The Gold-Catalyzed Phenol Synthesis As Well As The Hydration Of Alkynes. *Advanced Synthesis & Catalysis, 352*(8), 1315-1337.

Healy, P. (2003). A New Polymorph Of m-Bis(Diphenylphosphino)Methane-k^{2}P:P'-Bis[Chlorogold(I)]. *Acta Crystallographica Section E, 59*(12), m1112-m1114.

Hill, D. T., Girard, G. R., McCabe, F. L., Johnson, R. K., Stupik, P. D., Zhang, J. H., Reiff, W. M. & Eggleston, D. S. (1989). [μ-1,1'-Bis(diphenylphosphino)ferrocene]bis(chlorogold): Synthesis, Iron-57 And Gold-197 Moessbauer Spectroscopy, X-Ray Crystal Structure, And Antitumor Activity. *Inorganic Chemistry, 28*(18), 3529-3533.

Ho, S. Y., Bettens, R. P. A., Dakternieks, D., Duthie, A. & Tiekink, E. R. T. (2005). Prevalence Of The Thioamide $\{\cdots H\text{-}N\text{-}C{=}S\}_2$ Synthon-Solid-State (X-Ray Crystallography), Solution (NMR) And Gas-Phase (Theoretical) Structures Of *O*-Methyl-*N*-Aryl-Thiocarbamides. *CrystEngComm, 7*(113), 682-689.

Ho, S. Y., Cheng, E. C. C., Tiekink, E. R. T. & Yam, V. W. W. (2006). Luminescent Phosphine Gold(I) Thiolates: Correlation Between Crystal Structure And Photoluminescent Properties In $[R_3PAu\{SC(OMe){=}NC_6H_4NO_2\text{-}4\}]$ (R = Et, Cy, Ph) And $[(Ph_2P\text{-}R\text{-}PPh_2)\{AuSC(OMe){=}NC_6H_4NO_2\text{-}4\}_2]$ (R = CH_2, $(CH_2)_2$, $(CH_2)_3$, $(CH_2)_4$, Fc). *Inorganic Chemistry, 45*(20), 8165-8174.

Ho, S. Y. & Tiekink, E. R. T. (2007). Supramolecular Aggregation Patterns In The Crystal Structures Of The Dinuclear Phosphinegold(I) Thiolates, $[(Ph_2P(CH_2)_4PPh_2)\{AuSC(OR){=}NC_6H_4Y\text{-}4\}_2]$ For R = Me, Et Or *i*Pr And Y = H, NO_2 Or Me: The Influence On Intermolecular Interactions Exerted By R And Y. *CrystEngComm, 9*(5), 368-378.

Jemal, A., Bray, F., Center, M. M., Ferlay, J., Ward, E. & Forman, D. (2011). Global Cancer Statistics. *CA: A Cancer Journal for Clinicians, 61*(2), 69-90.

Jian, F. F., Wang, K. F., Zhao, P. S., Zhuang, R. R. & Zheng, J. (2006). Synthesis, Crystal Structure And Density Functional Theoretical Studies On Phenyl-Thiocarbamic Acid-*O*-Pyridin-4-ylmethyl Ester. *Structural Chemistry, 17*(5), 539-545.

Jones, P. G. & Ahrens, B. (1998). Gold(I) Complexes With Amine Ligands, II. Methylpyridine Complexes Of Gold(I). *Zeitschrift Fur Naturforschung Section B-a Journal of Chemical Sciences, 53*(7), 653-662.

Jones, W. B., Yuan, J., Narayanaswamy, R., Young, M. A., Elder, R. C., Bruce, A. E. & Bruce, M. R. M. (1995). Solid-State Exafs And Luminescence Studies Of Neutral, Dinuclear Gold(I) Complexes - Gold(I)-Gold(I) Interactions In The Solid-State. *Inorganic Chemistry, 34*(8), 1996-2001.

Kapuscinski, J., Darzynkiewicz, Z. & Melamed, M. R. (1983). Interactions Of Acridine Orange With Nucleic Acids: Properties Of Complexes Of Acridine Orange With Single Stranded Ribonucleic Acid. *Biochemical Pharmacology, 32*(24), 3679-3694.

Karagiannidis, P., Hadjikakou, S. K., Aslanidis, P. & Hountas, A. (1990). Synthesis And Photochemical Study Of Cu(I) Complexes With Tri-*p*-Tolylphosphine And Heterocyclic Thiones. The Crystal Structure Of [CuCl(pymtH)(*p*-$CH_3C_6H_4)_3P]_2$. *Inorganica Chimica Acta, 178*(1), 27-34.

Katz, M. J., Sakai, K. & Leznoff, D. B. (2008). The Use Of Aurophilic And Other Metal-Metal Interactions As Crystal Engineering Design Elements To Increase Structural Dimensionality. *Chemical Society Reviews, 37*(9), 1884-1895.

Kaur, D., Sharma, P. & Bharatam, P. V. (2005). Amide Resonance In Thio- And Seleno-Carbamates: A Theoretical Study. *Journal of Molecular Structure-Theochem, 757*(1-3), 149-153.

Kean, W. F., Forestier, F., Kassam, Y., Buchanan, W. W. & Rooney, P. J. (1985). The History Of Gold Therapy In Rheumatoid Disease. *Seminars in Arthritis and Rheumatism, 14*(3), 180-186.

King, C., Wang, J. C., Khan, M. N. I. & Fackler, J. P. (1989). Luminescence And Metal-Metal Interactions In Binuclear Gold(I) Compounds. *Inorganic Chemistry, 28*(11), 2145-2149.

Krishna, P. M. & Reddy, K. H. (2009). Synthesis, Single Crystal Structure And DNA Cleavage Studies On First ^{4}N-Ethyl Substituted Three Coordinate Copper(I) Complex Of Thiosemicarbazone. *Inorganica Chimica Acta, 362*(11), 4185-4190.

Kuan, F. S., Ho, S. Y., Tadbuppa, P. P. & Tiekink, E. R. T. (2008). Electronic And Steric Control Over Au···Au, C-H···O And C-H···p Interactions In The Crystal Structures Of Mononuclear Triarylphosphinegold(I) Carbonimidothioates: R_3PAu[SC(OMe)=NR'] For R = Ph, *o*-Tol, *m*-Tol or *p*-Tol, And R' = Ph, *o*-Tol, *m*-Tol, *p*-Tol Or $C_6H_4NO_2$-4. *CrystEngComm, 10*(5), 548-564.

Kuan, F. S., Mohr, F., Tadbuppa, P. P. & Tiekink, E. R. T. (2007). Principles Of Crystal Packing In *O*-Isopropyl-*N*-Aryl-Thiocarbamides: *i*PrO(C=S)N(H)C_6H_4-4-Y: Y = H, Cl, And Me. *CrystEngComm, 9*(7), 574-581.

Kutschy, P., Suchý, M., Andreani, A., Dzurilla, M., Kováčik, V., Alföldi, J., Rossi, M. & Gramatová, M. (2002). A New Approach To The Synthesis Of Rare Thiazino[6,5-b]Indol-4-one Derivatives. First Total Synthesis Of The Indole Phytoalexin Cyclobrassinon. *Tetrahedron, 58*(44), 9029-9039.

Kutschy, P., Suchý, M., Andreani, A., Dzurilla, M. & Rossi, M. (2001). A New Photocyclization Approach To The Rare 1,3-Thiazino[6,5-B]Indol-4-one Derivatives. *Tetrahedron Letters, 42*(52), 9281-9283.

Langdon-Jones, E. E. & Pope, S. J. A. (2014). Recent Developments In Gold(I) Coordination Chemistry: Luminescence Properties And Bioimaging Opportunities. *Chemical Communications, 50*(72), 10343-10354.

Larson, L. J., McCauley, E. M., Weissbart, B. & Tinti, D. S. (1995). Luminescent Gold(I) Complexes - Optical And ODMR Studies Of Mononuclear Halo(Triphenylphosphine)Gold(I) And Halo(Triphenylarsine)Gold(I) Complexes. *Journal of Physical Chemistry, 99*(19), 7218-7226.

Lee, D., Donkers, R. L., Wang, G. L., Harper, A. S. & Murray, R. W. (2004). Electrochemistry And Optical Absorbance And Luminescence Of Molecule-Like Au-38 Nanoparticles. *Journal of the American Chemical Society, 126*(19), 6193-6199.

Lee, J., Kang, S. U., Choi, H. K., Lim, J. O., Kil, M. J., Jin, M. K., Kim, K. P., Sung, J. H., Chung, S. J., Ha, H. J., Kim, Y. H., Pearce, L. V., Tran, R., Lundberg, D. J., Wang, Y., Toth, A. & Blumberg, P. M. (2004). Analysis Of Structure-Activity Relationships For The 'B-Region' Of *N*-(3-Acyloxy-2-Benzylpropyl)-*N*′-[4-(Methylsulfonylamino)Benzyl]Thiourea Analogues As Vanilloid Receptor Antagonists: Discovery Of An *N*-Hydroxythiourea Analogue With Potent Analgesic Activity. *Bioorganic and Medicinal Chemistry Letters, 14*(9), 2291-2297.

Lee, Y. A. & Eisenberg, R. (2003). Luminescence Tribochromism And Bright Emission In Gold(I) Thiouracilate Complexes. *Journal of the American Chemical Society, 125*(26), 7778-7779.

Lee, Y. A., McGarrah, J. E., Lachicotte, R. J. & Eisenberg, R. (2002). Multiple Emissions And Brilliant White Luminescence From Gold(I) *O*,*O*'-Di(Alkyl)Dithiophosphate Dimers. *Journal of the American Chemical Society, 124*(36), 10662-10663.

Li, C. K., Cheng, E. C. C., Zhu, N. Y. & Yam, V. W. W. (2005). Luminescent Phosphinocrown-Containing Gold(I) Complexes: Their Syntheses, Spectroscopic Studies And Host-Guest Chemistry. *Inorganica Chimica Acta, 358*(14), 4191-4200.

Li, C. K., Lu, X. X., Wong, K. M. C., Chan, C. L., Zhu, N. Y. & Yam, V. W. W. (2004). Molecular design of luminescence ion probes for various cations based on weak gold(I)center dot center dot center dot gold(I) interactions in dinuclear gold(I) complexes. *Inorganic Chemistry, 43*(23), 7421-7430.

Linder, M. C. (1991). *Biochemistry of Copper*: Plenum Press, New York.

Lobana, T. S., Sharma, R., Hundal, G. & Butcher, R. J. (2006). Synthesis Of 1D $\{Cu_6(\mu_3\text{-}SC_3H_6N_2)_4(\mu\text{-}SC_3H_6N_2)_2(\mu\text{-}I)_2I_4\}_n$ and 3D $\{Cu_2(\mu\text{-}SC_3H_6N_2)_2(\mu\text{-}SCN)_2\}_n$ Polymers With 1,3-Imidazolidine-2-thione: Bond Isomerism In Polymers. *Inorganic Chemistry, 45*(23), 9402-9409.

McKeage, M. J., Maharaj, L. & Berners-Price, S. J. (2002). Mechanisms Of Cytotoxicity And Antitumor Activity Of Gold(I) Phosphine Complexes: The Possible Role Of Mitochondria. *Coordination Chemistry Reviews, 232*(1–2), 127-135.

Merchant, B. (1998). Gold, The Noble Metal And The Paradoxes Of Its Toxicology. *Biologicals, 26*(1), 49-59.

Min, K. H., Lee, S., Kim, H. S. & Suh, Y. G. (2010). Discovery Of Novel TRPV1 Ligands Through Rational Approach Based On Its Putative Endogenous Ligand, 12(5)-HPETE. *Bulletin of the Korean Chemical Society, 31*(6), 1501-1505.

Mirabelli, C. K., Jensen, B. D., Mattern, M. R., Sung, C. M., Mong, S. M., Hill, D. T., Dean, S. W., Schein, P. S., Johnson, R. K. & Crooke, S. T. (1986). Cellular Pharmacology Of m-1,2-Bis(Diphenylphosphino)Ethane Bis (1-Thio-b-D-Glucopyranosato-S)Gold(I) - A Novel Antitumor Agent. *Anti-Cancer Drug Design, 1*(3), 223-234.

Mirabelli, C. K., Johnson, R. K., Sung, C. M., Faucette, L., Muirhead, K. & Crooke, S. T. (1985). Evaluation Of The In Vivo Antitumor Activity And In Vitro Cytotoxic Properties Of Auranofin, A Coordinated Gold Compound, In Murine Tumor Models. *Cancer Research, 45*(1), 32-39.

Mizuno, T., Takahashi, J. & Ogawa, A. (2003). Facile *S*-Alkyl Thiocarbamate Synthesis By A Novel DBU-Assisted Carbonylation Of Amines With Carbon Monoxide And Sulfur. *Tetrahedron, 59*(8), 1327-1331.

Montiel-Ortega, L. A., Rojas-Lima, S., Otazo-Sanchez, E. & Villagómez-Ibarra, R. (2004). *O*-Benzyl-*N*-(2-Furoyl)Thiocarbamate. *Journal of Chemical Crystallography, 34*(2), 89-93.

Narayanaswamy, R., Young, M. A., Parkhurst, E., Ouellette, M., Kerr, M. E., Ho, D. M., Elder, R. C., Bruce, A. E. & Bruce, M. R. M. (1993). Synthesis, Structure, And Electronic Spectroscopy Of Neutral, Dinuclear Gold(I) Complexes - Gold(I)-Gold(I) Interactions In Solution And In The Solid-State. *Inorganic Chemistry, 32*(11), 2506-2517.

Nelson, J. H. (2003). *Nuclear Magnetic Resonance Spectroscopy*: Prentice Hall.

Nobili, S., Mini, E., Landini, I., Gabbiani, C., Casini, A. & Messori, L. (2010). Gold Compounds As Anticancer Agents: Chemistry, Cellular Pharmacology, And Preclinical Studies. *Medicinal Research Reviews, 30*(3), 550-580.

Okada, T., Patterson, B. K., Ye, S.-Q. & Gurney, M. E. (1993). Aurothiolates Inhibit HIV-1 Infectivity By Gold(I) Ligand Exchange With A Component Of The Virion Surface. *Virology, 192*(2), 631-642.

Ooi, K., Yeo, C., Ang, K.-P., Akim, A., Cheah, Y.-K., Halim, S., Seng, H.-L. & Tiekink, E. T. (2015). Phosphanegold(I) thiolates, $Ph_3PAu[SC(OR)=NC_6H_4Me\text{-}4]$ for R = Me, Et and *i*Pr, Induce Apoptosis, Cell Cycle Arrest And Inhibit Cell Invasion Of HT-29 Colon Cancer Cells Through Modulation Of The Nuclear Factor-κB Activation Pathway And Ubiquitination. *JBIC Journal of Biological Inorganic Chemistry, 20*(5), 855-873.

Ormerod, M. G., Collins, M. K. L., Rodriguez-Tarduchy, G. & Robertson, D. (1992). Apoptosis In Interleukin-3-Dependent Haemopoietic Cells: Quantification By Two Flow Cytometric Methods. *Journal of Immunological Methods, 153*(1–2), 57-65.

Otero-de-la-Roza, A., Johnson, E. R. & DiLabio, G. A. (2014). Halogen Bonding From Dispersion-Corrected Density-Functional Theory: The Role Of Delocalization Error. *Journal of Chemical Theory and Computation, 10*(12), 5436-5447.

Ott, I. (2009). On The Medicinal Chemistry Of Gold Complexes As Anticancer Drugs. *Coordination Chemistry Reviews, 253*(11–12), 1670-1681.

Partyka, D. V., Robilotto, T. J., Zeller, M., Hunter, A. D. & Gray, T. G. (2007). Dialkylbiarylphosphine Complexes Of Gold(I) Halides. Gold−Aryl π-Interactions In The Solid State. *Organometallics, 27*(1), 28-32.

Pereira, F. d. C., Lima, B. A. V., de Lima, A. P., Pires, W. C., Monteiro, T., Magalhães, L. F., Costa, W., Graminha, A. E., Batista, A. A., Ellena, J. & Siveira-Lacerda, E. d. P. (2015). Cis-$[RuCl(BzCN)(N–N)(P–P)]PF_6$ Complexes: Synthesis And In Vitro Antitumor Activity: (BzCN = Benzonitrile; N–N = 2,2′-Bipyridine; 1,10-Phenanthroline; P–P = 1,4-Bis(diphenylphosphino)butane, 1,2-Bis(diphenylphosphino)ethane, Or 1,1′-(Diphenylphosphino)ferrocene). *Journal of Inorganic Biochemistry, 149*, 91-101.

Perez-Galan, P., Delpont, N., Herrero-Gomez, E., Maseras, F. & Echavarren, A. M. (2010). Metal-Arene Interactions In Dialkylbiarylphosphane Complexes Of Copper, Silver, And Gold. *Chemistry – A European Journal, 16*(18), 5324-5332.

Pissuwan, D., Niidome, T. & Cortie, M. B. (2011). The Forthcoming Applications Of Gold Nanoparticles In Drug And Gene Delivery Systems. *Journal of Controlled Release, 149*(1), 65-71.

Plutín, A. M., Suárez, M., Machado, T., Àlvarez, A., Rodríguez, A., Martínez, R., Duque, J., Martínez-Àlvarez, R. & Martín, N. (2010). On The Selective Methylation Of Benzoyl And Furoylthiocarbamates. *Arkivoc, 2010*(10), 276-290.

Plutín, A. M., Suárez, M., Ochoa, E., Machado, T., Mocelo, R., Concellón, J. M. & Rodríguez-Solla, H. (2005). Synthesis Of New Acyl, Furoyl, And Benzoylthiocarbamates As Polydentate Systems. Structural Study Of Isopropyl *N*-(2-Furoyl)Thiocarbamate. *Tetrahedron, 61*(24), 5812-5817.

Pyykko, P., Runeberg, N. & Mendizabal, F. (1997). Theory Of The d^{10}-d^{10} Closed-Shell Attraction. 1. Dimers Near Equilibrium. *Chemistry – A European Journal, 3*(9), 1451-1457.

Quas, L., Schroder, U., Schroder, B., Dietze, F. & Beyer, L. (2000). Heavy Metal Extraction With Thiocarbamic-*O*-Alkylesters. *Solvent Extraction and Ion Exchange, 18*(6), 1167-1177.

Ranise, A., Spallarossa, A., Cesarini, S., Bondavalli, F., Schenone, S., Bruno, O., Menozzi, G., Fossa, P., Mosti, L., La Colla, M., Sanna, G., Murreddu, M., Collu, G., Busonera, B., Marongiu, M. E., Pani, A., La Colla, P. & Loddo, R. (2005). Structure-Based Design, Parallel Synthesis, Structure-Activity Relationship, And Molecular Modeling Studies Of Thiocarbamates, New Potent Non-Nucleoside HIV-1 Reverse Transcriptase Inhibitor Isosteres Of Phenethylthiazolylthiourea Derivatives. *Journal of Medicinal Chemistry, 48*(11), 3858-3873.

Ribeiro da Silva, M. A. V., Monteiro, I. M. M., Santos, L. M. N. B. F. & Schröder, B. (2007). Thermochemical Studies On Five *N*-Thenoylthiocarbamic-*O*-*n*-Alkylesters. *Journal of Chemical Thermodynamics, 39*(5), 767-772.

Ribeiro Da Silva, M. A. V., Santos, L. M. N. B. F., Schröder, B., Dietze, F. & Beyer, L. (2004). Thermochemical Studies Of Three Bis(*O*-Alkyl-*N*-Benzoylthiocarbamato) Nickel(II) Complexes. *Journal of Chemical Thermodynamics, 36*(8), 627-631.

Rodríguez-Argüelles, M. C., Tourón-Touceda, P., Cao, R., García-Deibe, A. M., Pelagatti, P., Pelizzi, C. & Zani, F. (2009). Complexes Of 2-Acetyl-γ-butyrolactone And 2-Furancarbaldehyde Thiosemicarbazones: Antibacterial And Antifungal Activity. *Journal of Inorganic Biochemistry, 103*(1), 35-42.

Romankiw, L. T. & Division, E. S. E. (2000). *Electrochemical Technology Applications In Electronics: Proceedings Of The Third International Symposium*: Electrochemical Society.

Rudra, S., Sangita, F., Gujrati, A., Pandya, M., Bhateja, P., Mathur, T., Singhal, S., Rattan, A., Salman, M. & Das, B. (2007). Synthesis And Antibacterial Activity Of Novel Oxazolidinones With Methylene Oxygen- And Methylene Sulfur-Linked Substituents At C5-Position. *Bioorganic and Medicinal Chemistry Letters, 17*(17), 4778-4783.

Ryder, N. S., Frank, I. & Dupont, M. C. (1986). Ergosterol Biosynthesis Inhibition By The Thiocarbamate Antifungal Agents Tolnaftate And Tolciclate. *Antimicrobial Agents and Chemotherapy, 29*(5), 858-860.

Sadler, P. J. & Guo, Z. J. (1998). Metal Complexes In Medicine: Design And Mechanism Of Action. *Pure and Applied Chemistry, 70*(4), 863-871.

Santini, C., Pellei, M., Papini, G., Morresi, B., Galassi, R., Ricci, S., Tisato, F., Porchia, M., Rigobello, M. P., Gandin, V. & Marzano, C. (2011). In Vitro Antitumour Activity Of Water Soluble Cu(I), Ag(I) And Au(I) Complexes Supported By Hydrophilic Alkyl Phosphine Ligands. *Journal of Inorganic Biochemistry, 105*(2), 232-240.

Schmidbaur, H. (2001). Supramolecular Chemistry: Going For Gold. *Nature, 413*(6851), 31-33.

Schmidbaur, H. & Schier, A. (2012). Aurophilic Interactions As A Subject Of Current Research: An Update. *Chemical Society Reviews, 41*(1), 370-412.

Schmidbaur, H., Weidenhiller, G., Steigelmann, O. & Muller, G. (1990). (2-Methylphenyl)Phosphine Gold(I) Bromide - A New Type Of Structure For Au-Au Contacts In (Phosphine)Gold(I) Halides. *Zeitschrift Fur Naturforschung Section B-a Journal of Chemical Sciences, 45*(6), 747-752.

Schmidbaur, H., Wohlleben, A., Wagner, F., Orama, O. & Huttner, G. (1977). Gold-Komplexe Von Diphosphinomethanen, I. Synthese Und Kristallstruktur Zweikerniger Gold(I)-Verbindungen. *Chemische Berichte, 110*(5), 1748-1754.

Schroder, U., Beyer, L., Dietze, F., Richter, R., Schmidt, S. & Hoyer, E. (1995). Ligand Properties Of *N*-Acyl-Thiocarbamic-*O*-Alkylesters - A New Class Of Aza-Analogous 1,3-Thioxoketones. *Journal Fur Praktische Chemie-Chemiker-Zeitung, 337*(3), 184-188.

Sekiyama, Y., Mizukami, Y., Takada, Y. & Numata, Y. (1994). Vapor Pressure And Stability Of Allyl Isothiocyanate. *J. Food Hyg. Soc. Japan, 35*(4), 365-370.

Selvakumar, N., Raheem, M. A., Khera, M. K., Rajale, T. V., Kumar, M. S., Kandepu, S., Das, J., Rajagopalan, R., Iqbal, J. & Trehan, S. (2003). Influence Of Ethylene-Oxy Spacer Group On The Activity Of Linezolid: Synthesis Of Potent Antibacterials Possessing A Thiocarbonyl Group. *Bioorganic and Medicinal Chemistry Letters, 13*(23), 4169-4172.

Selvakumar, N., Yadi Reddy, B., Sunil Kumar, G., Khera, M. K., Srinivas, D., Sitaram Kumar, M., Das, J., Iqbal, J. & Trehan, S. (2006). Synthesis Of Novel Tricyclic Oxazolidinones By A Tandem SN_2 And SNAr Reaction: SAR Studies On Conformationally Constrained Analogues Of Linezolid. *Bioorganic and Medicinal Chemistry Letters, 16*(16), 4416-4419.

Seryakova, I. V., Vorobiova, G. A., Glembotsky, A. V. & Zolotov, Y. A. (1975). Extraction Of Metals By Neutral Sulfur-Containing Extractants: Part I. *O*-Isopropyl-*N*-Ethylthiocarbamate. *Analytica Chimica Acta, 77*(0), 183-190.

Shagun, V. A., Smirnov, V. I., Shagun, L. G., Shevchenko, S. G. & Frolov, Y. L. (2006). Mechanism Of Mercury Monomethyl Cation Detoxication In The Interaction With 1-Chloro-2,2-Propane Dithiol. *Journal of Structural Chemistry, 47*(5), 831-838.

Shaw, C. F. (1999). Gold-Based Therapeutic Agents. *Chemical Reviews, 99*(9), 2589-2600.

Sheldrick, G. (2008). A Short History Of SHELX. *Acta Crystallographica Section A, 64*(1), 112-122.

Sigel, H., Rheinberger, V. M. & Fischer, B. E. (1979). Stability Of Metal Ion/Alkyl Thioether Complexes In Solution. Ligating Properties Of "Isolated" Sulfur Atoms. *Inorganic Chemistry, 18*(12), 3334-3339.

Singh, R. & Dikshit, S. K. (1995). Synthesis And Characterization Of Mixed Ligand Copper(I) Complexes Containing Halides, Triphenylarsine And *N*,*N*-Dimethyl-*N′*-Phenylthiourea (dmptH), *N*,*N*-Dibutyl-*N′*-Phenylthiourea (dbptH) Or 1,3-Thiazolidine-2-Thione (tzdtH). The X-Ray Crystal Structure Of $[Cu(PPh_3)_2(dmptH)Cl]$. *Polyhedron, 14*(13–14), 1799-1807.

Skinner, G. S. & Vogt, H. C. (1955). Benzoylcyanamide From Ethyl Benzoylthioncarbamate. *Journal of the American Chemical Society, 77*(20), 5440-5441.

Snyder, R. M., Mirabelli, C. K., Johnson, R. K., Sung, C. M., Faucette, L. F., McCabe, F. L., Zimmerman, J. P., Whitman, M., Hempel, J. C. & Crooke, S. T. (1986). Modulation Of The Antitumor And Biochemical-Properties Of Bis(Diphenylphosphine)Ethane With Metals. *Cancer Research, 46*(10), 5054-5060.

Soung, M.-G., Jang, S.-C. & Sung, N.-D. (2010). Minimum Structural Requirements For Fungicidal Evaluation Of *N*-Phenyl-*O*-Phenylthionocarbamates Against The Capsicum Phytophthora Blight (Phyophthora Capsici) Based On The 3D-QSARs. *Bulletin of the Korean Chemical Society, 31*(11), 3297-3300.

Spallarossa, A., Cesarini, S., Ranise, A., Bruno, O., Schenone, S., La Colla, P., Collu, G., Sanna, G., Secci, B. & Loddo, R. (2009). Novel Modifications In The Series Of *O*-(2-Phthalimidoethyl)-*N*-Substituted Thiocarbamates And Their Ring-Opened Congeners As Non-Nucleoside HIV-1 Reverse Transcriptase Inhibitors. *European Journal of Medicinal Chemistry, 44*(4), 1650-1663.

Spek, A. L. (2003). Single-Crystal Structure Validation With The Program PLATON. *Journal of Applied Crystallography, 36*(1), 7-13.

Stanetty, P. & Krumpak, B. (1996). Novel Synthesis Of Benzothiazole Derivatives *Via* Directed Lithiation And Aryne-Mediated Cyclization Followed By Quenching With Electrophiles. *Journal of Organic Chemistry, 61*(15), 5130-5133.

Stott, T. L., Wolf, M. O. & Patrick, B. O. (2005). Structural And Electronic Properties Of Phosphino(Oligothiophene) Gold(I) Complexes. *Inorganic Chemistry, 44*(3), 620-627.

Sutton, B. M. (1986). Gold Compounds For Rheumatoid Arthritis. *Gold Bulletin, 19*(1), 15-16.

Sutton, B. M., McGusty, E., Walz, D. T. & DiMartino, M. J. (1972). Oral Gold. Antiarthritic Properties Of Alkylphosphinegold Coordination Complexes. *Journal of Medicinal Chemistry, 15*(11), 1095-1098.

Tadbuppa, P. P. & Tiekink, E. R. T. (2007). [*O*-Methyl *N*-(4-Chlorophenyl)Thiocarbamato-kS](Triethylphosphine-kP)Gold(I). *Acta Crystallographica Section E, 63*(4), m1101-m1102.

Tadbuppa, P. P. & Tiekink, E. R. T. (2009). [(Z)-*N*-(2-Chlorophenyl)-*O*-Methylthiocarbamato-kS](Triphenylphosphine-kP)Gold(I). *Acta Crystallographica Section E, 65*(12), m1646.

Tadbuppa, P. P. & Tiekink, E. R. T. (2009). [(Z)-*N*-(4-Chlorophenyl)-*O*-Methylthiocarbamato-kS](Triphenylphosphine-kP)Gold(I). *Acta Crystallographica Section E, 65*(12), m1700.

Tadbuppa, P. P. & Tiekink, E. R. T. (2009). [(Z)-*N*-Isopropyl-*O*-Methylthiocarbamato-kS](Tri-*p*-Tolylphosphine-kP)Gold(I). *Acta Crystallographica Section E, 65*(12), m1557.

Tadbuppa, P. P. & Tiekink, E. R. T. (2009). [(Z)-*O*-Methyl-*N*-Propylthiocarbamato-kS](Triphenylphosphine-kP)Gold(I). *Acta Crystallographica Section E, 65*(12), m1558.

Tadbuppa, P. P. & Tiekink, E. R. T. (2010). [(Z)-*O*-Methyl *N*-(3-Chlorophenyl)Thiocarbamato-kS](Tricyclohexylphosphine-kP)Gold(I). *Acta Crystallographica Section E, 66*(4), m450.

Tadbuppa, P. P. & Tiekink, E. R. T. (2010). [(Z)-*O*-Methyl *N*-(3-Chlorophenyl)Thiocarbamato-kS](Triphenylphosphine-kP)Gold(I). *Acta Crystallographica Section E, 66*(6), m664.

Taguchi, M., Goda, K. I., Sugimoto, K., Akama, T., Yamamoto, K., Suzuki, T., Tomishima, Y., Nishiguchi, M., Arai, K., Takahashi, K. & Kobori, T. (2003). Biological Evaluation Of Sphingomyelin Analogues As Inhibitors Of Sphingomyelinase. *Bioorganic and Medicinal Chemistry Letters, 13*(21), 3681-3684.

Takhi, M., Singh, G., Murugan, C., Thaplyyal, N., Maitra, S., Bhaskarreddy, K. M., Amarnath, P. V. S., Mallik, A., Harisudan, T., Trivedi, R. K., Sreenivas, K., Selvakumar, N. & Iqbal, J. (2008). Novel And Potent Oxazolidinone Antibacterials Featuring 3-Indolylglyoxamide Substituents. *Bioorganic and Medicinal Chemistry Letters, 18*(18), 5150-5155.

Tamaru, Y., Hojo, M., Kawamura, S. I., Sawada, S. & Yoshida, Z. I. (1987). Stereoselective Intramolecular Iodoetherification of 4-Pentene-1,3-Diols: Synthesis Of *Cis*-2-(Iodomethyl)-3-Hydroxytetrahydrofurans. *Journal of Organic Chemistry, 52*(18), 4062-4072.

Tan, C. K., Chen, F. & Yeung, Y.-Y. (2011). Studies Toward Lewis Basic Thiocarbamate And Thiourea Mediated Bromolactonization: The Effect Of A Trace Amount Of Water On The Reactivity And Enantioselectivity. *Tetrahedron Letters, 52*(38), 4892-4895.

Tan, C. K., Le, C. & Yeung, Y.-Y. (2012). Enantioselective Bromolactonization Of *Cis*-1,2-Disubstituted Olefinic Acids Using An Amino-Thiocarbamate Catalyst. *Chemical Communications, 48*(46), 5793-5795.

Tarantelli, T. & Furlani, C. (1971). Palladium(II) And Platinum(II) Complexes Of Thiocarbamic Esters. *Journal of the Chemical Society A: Inorganic, Physical, Theoretical*(0), 1213-1217.

Tiekink, E. R. T. (2002). Gold Derivatives For The Treatment Of Cancer. *Critical Reviews in Oncology / Hematology, 42*(3), 225-248.

Tiekink, E. R. T. (2003). Gold Compounds In Medicine: Potential Anti-Tumour Agents. *Gold Bulletin, 36*(4), 117-124.

Tiekink, E. R. T. & Kang, J.-G. (2009). Luminescence Properties Of Phosphinegold(I) Halides And Thiolates. *Coordination Chemistry Reviews, 253*(11–12), 1627-1648.

Tiekink, E. R. T. & Zukerman-Schpector, J. (2009). Gold···p Aryl Interactions As Supramolecular Synthons. *CrystEngComm, 11*(7), 1176-1186.

Tokuyama, R., Takahashi, Y., Tomita, Y., Tsubouchi, M., Iwasaki, N., Kado, N., Okezaki, E. & Nagata, O. (2001). Structure-Activity Relationship (SAR) Studies On Oxazolidinone Antibacterial Agents. 3. Synthesis And Evaluation Of 5-Thiocarbamate Oxazolidinones. *Chemical and Pharmaceutical Bulletin, 49*(4), 361-367.

Tsukamoto, G., Yoshino, K., Kohno, T., Ohtaka, H., Kagaya, H. & Ito, K. (1980). Synthesis And Anti-Inflammatory Activity Of Some 2-(Substituted-Pyridinyl)Benzimidazoles. *Journal of Medicinal Chemistry, 23*(7), 734-738.

Tzeng, B. C., Huang, Y. C., Wu, W. M., Lee, S. Y., Lee, G. H. & Peng, S. M. (2004). Crystal Engineering Of Luminescent Gold(I) Compounds Of 2-Amino-5-Mercapto-1,3,4-Thiadiazolate And 6-Amino-2-Mercaptobenzothiazolate. *Crystal Growth & Design, 4*(1), 63-70.

Vallejos, S. T., Erben, M. F., Piro, O. E., Castellano, E. E. & Della Védova, C. O. (2009). N-H···S=C Hydrogen Bond In *O*-Alkyl *N*-Methoxycarbonyl Thiocarbamates, $ROC(S)N(H)C(O)OCH_3$ (R = CH_3-, CH_3CH_2-). *Polyhedron, 28*(5), 937-946.

van Zyl, W. E., Lopez-de-Luzuriaga, J. M. & Fackler, J. P. (2000). Luminescence Studies Of Dinuclear Gold(I) Phosphor-1,1-Dithiolate Complexes. *Journal of Molecular Structure, 516*(1), 99-106.

Varma, R. S. & Nobles, W. L. (1968). Synthesis And Antibacterial Activity Of Certain 3-Substituted Benzoxazolinones. *Journal of Pharmaceutical Sciences, 57*(1), 39-44.

Vogler, A. & Kunkely, H. (2001). Photoreactivity Of Gold Complexes. *Coordination Chemistry Reviews, 219–221*(0), 489-507.

Xiong, L., Shen, S., Liu, L. & Zhang, l. (2014). Selective And Effective Reduction OOf Gold Ions From Acidic HCl–$NaClO_3$ Leachate With Oxalic Acid. *Industrial & Engineering Chemistry Research, 53*(43), 16672-16677.

Yam, V. W. W. & Cheng, E. C. C. (2001). Design Of Luminescent Sulfur-Containing Polynuclear Gold(I) Complexes For Advanced Nanomaterials And Chemosensors. *Gold Bulletin, 34*(1), 20-23.

Yam, V. W. W., Lai, T. F. & Che, C. M. (1990). Novel Luminescent Polynuclear Gold(I) Phosphine Complexes - Synthesis, Spectroscopy, And X-Ray Crystal-Structure Of $Au_3(Dmmp)_2^{3+}$ Dmmp = Bis(Dimethylphosphinomethyl)Methylphosphine. *Journal of the Chemical Society-Dalton Transactions*(12), 3747-3752.

Yam, V. W. W., Li, C. K. & Chan, C. L. (1998). Proof Of Potassium Ions By Luminescence Signaling Based On Weak Gold - Gold Interactions In Dinuclear Gold(I) Complexes. *Angewandte Chemie-International Edition, 37*(20), 2857-2859.

Yamashita, S., Iso, K., Kitajima, K., Himuro, M. & Hirama, M. (2011). Total Synthesis Of Cortistatins A And J. *The Journal of Organic Chemistry, 76*(8), 2408-2425.

Yamashita, S., Kitajima, K., Iso, K. & Hirama, M. (2009). Efficient And Stereoselective Installation Of Isoquinoline: Formal Total Synthesis Of Cortistatin A. *Tetrahedron Letters, 50*(26), 3277-3279.

Yeo, C. I., Ooi, K. K., Akim, A. M., Ang, K. P., Fairuz, Z. A., Halim, S. N. B. A., Ng, S. W., Seng, H.-L. & Tiekink, E. R. T. (2013). The Influence Of R Substituents In Triphenylphosphinegold(I) Carbonimidothioates, $Ph_3PAu[SC(OR)=NPh]$ (R = Me, Et And *i*Pr), Upon In Vitro Cytotoxicity Against The HT-29 Colon Cancer Cell Line And Upon Apoptotic Pathways. *Journal of Inorganic Biochemistry, 127*(0), 24-38.

Yoon, J., Choi, H., Lee, H. J., Ryu, C. H., Park, H. G., Suh, Y. G., Oh, U., Jeong, Y. S., Choi, J. K., Park, Y. H. & Kim, H. D. (2003). Chain-Branched Acyclic Phenethylthiocarbamates As Vanilloid Receptor Antagonists. *Bioorganic and Medicinal Chemistry Letters, 13*(9), 1549-1552.

Yun, S. S., Kim, J. K., Jung, J. S., Park, C., Kang, J. G., Smyth, D. R. & Tiekink, E. R. T. (2006). Pseudo-Polymorphism In The Tri(*O*-Tolyl)Phosphinegoid(I) 2-Mercaptobenzoates: Crystallographic, Thermal Decomposition, And Luminescence Studies. *Crystal Growth & Design, 6*(4), 899-909.

Zhang, G. (2008). Design, Synthesis, And Evaluation Of Bisubstrate Analog Inhibitors Of Cholera Toxin. *Bioorganic and Medicinal Chemistry Letters, 18*(13), 3724-3727.

Zhang, H. X. & Che, C. M. (2001). Aurophilic Attraction And Luminescence Of Binuclear Gold(I) Complexes With Bridging Phosphine Ligands: Ab Initio Study. *Chemistry – A European Journal, 7*(22), 4887-4893.

Zhou, Y., Wang, L., Han, L., Meng, F. & Yang, C. (2009). Synthesis, Antifungal Activities, And Potential Detoxification Of *N*-(2,3,4,6-Tetra-*O*-Acetyl-β-D-Glucopyranosyl)Thiocarbamates. *Carbohydrate Research, 344*(11), 1289-1296.

Zhu, B., Marinelli, B. A., Abbanat, D., Foleno, B. D., Bush, K. & Macielag, M. J. (2007). Synthesis And Antibacterial Activity Of 3-Keto-6-*O*-Carbamoyl-11,12-Cyclic Thiocarbamate Erythromycin A Derivatives. *Bioorganic & Medicinal Chemistry Letters, 17*(14), 3900-3904.

CONFERENCES AND PRESENTATIONS

Oral Presentations:

4th Asian Conference on Coordination Chemistry (ACCC4) in Jeju Island, Korea (4th – 7th August 2013)

Presentation Title: Potential alternative bactericidal agents: Triphenylphosphanegold(O-alkylthiocarbamates), $Ph_3PAu[SC(OR)=N(p\text{-tolyl})]$ (R = Me, Et and *i*Pr).

University Of Malaya Pharmaceutical Co-Crystal Symposium 2014 (19th July 2014)

Presentation Title: Phosphanegold(I) thiocarbamides: Biological study and crystal engineering.

Poster Presentation:

15th Asian Chemical Congress (15ACC) In Singapore (19th – 23th August 2013)

Poster Title: Triphenylphosphinegold(I) Carbonimidothioates, $Ph_3PAu[SC(OR)=NPh]$ (R = Me, Et And *i*Pr) and their in vitro cytotoxicity againts HT-29 colon cancer cell line.

LIST OF PUBLICATIONS AND PAPERS PRESENTED

I

Yeo, C. I., Ooi, K. K., Akim, A. M., Ang, K. P., Fairuz, Z. A., Halim, S. N. B. A., Ng, S. W., Seng, H.-L. & Tiekink, E. R. T. (2013). The Influence Of R Substituents In Triphenylphosphinegold(I) Carbonimidothioates, $Ph_3PAu[SC(OR)=NPh]$ (R = Me, Et And *i*Pr), Upon In Vitro Cytotoxicity Against The HT-29 Colon Cancer Cell Line And Upon Apoptotic Pathways. *Journal of Inorganic Biochemistry, 127*(0), 24-38.

II

Ooi, K. K., Yeo, C. I., Ang, K.-P., Akim, A., Cheah, Y.-K., Halim, S., Seng, H.-L. & Tiekink, E. R. T. (2015). Phosphanegold(I) thiolates, $Ph_3PAu[SC(OR)=NC_6H_4Me\text{-}4]$ for R = Me, Et and *i*Pr, Induce Apoptosis, Cell Cycle Arrest And Inhibit Cell Invasion Of HT-29 Colon Cancer Cells Through Modulation Of The Nuclear Factor-κB Activation Pathway And Ubiquitination. *JBIC Journal of Biological Inorganic Chemistry, 20*(5), 855-873.

III

Yeo, C. I., Sim, J.-H., Khoo, C.-H., Goh, Z.-J., Ang, K.-P., Cheah, Y.-K., Fairuz, Z., Halim, S., Ng, S., Seng, H.-L. & Tiekink, E. R. T. (2013). Pathogenic Gram-Positive Bacteria Are Highly Sensitive To Triphenylphosphanegold(*O*-Alkylthiocarbamates), $Ph_3PAu[SC(OR)=N(p\text{-tolyl})]$ (R = Me, Et And *i*Pr). *Gold Bulletin, 46*(3), 145-152.

IV

Yeo, C. I., Khoo, C.-H., Chu, W.-C., Chen, B.-J., Chu, P.-L., Sim, J.-H., Cheah, Y.-K., Ahmad, J., Abdul Halim, S. N., Seng, H.-L., Ng, S., Otero-de-la-Roza, A. & Tiekink, E. R. T. (2015). The Importance Of Au···π(Aryl) Interactions In The Formation Of Spherical Aggregates In Binuclear Phosphane Gold(I) Complexes Of A Bipodal Thiocarbamate Dianion: A Combined Crystallographic And Computational Study, And Anti-microbial Activity. *RSC Advances, 5*(52), 41401-41411.

V

Yeo, C. I., Halim, S. N. A., Ng, S. W., Tan, S. L., Zukerman-Schpector, J., Ferreira, M. A. B. & Tiekink, E. R. T. (2014). Investigation Of Putative Arene-C-H···π(Quasi-Chelate Ring) Interactions In Copper(I) Crystal Structures. *Chemical Communications, 50*(45), 5984-5986.